# Discovery of Novel Human Biomarkers Using Variable Lymphocyte Receptor Antibodies of the Sea Lamprey

by

Tze Ho (Justin) Chan

A thesis submitted in conformity with the requirements
for the degree of Doctor of Philosophy

Department of Immunology
University of Toronto

# Discovery of Novel Human Biomarkers Using Variable Lymphocyte Receptor Antibodies of the Sea Lamprey

Tze Ho (Justin) Chan

Doctor of Philosophy

Department of Immunology
University of Toronto

2019

## Abstract

Diversity, specificity, and memory are the fundamentals of vertebrate immunity – an intricate system that arose in response to the necessary cohabitation of vertebrates with the most ancient forms of life as we know it, namely microbial life.

Although microorganisms are a cause of disease, another critical postulate or determinant is the capacity or capability of one's immune system. In other words, the same pathogen will not be harmful to all individuals and disease can arise from the immune system itself. Notably, cancer, autoimmunity, and viral infection expose the limitations of human immunity. Not unlike how we observe interindividual variation in disease susceptibility and immune capacity, differences are amplified when we compare different species. Can the strengths of an alternate immune system address the restrictions of ours?

Recently, immunologists have acknowledged that organisms as evolutionarily distant as jawless vertebrates are also endowed with adaptive immunity. Pancer and colleagues were the first to elucidate the molecular origins of adaptive immunity in a lamprey. Adaptive immunity in this jawless fish functions through cells and mechanisms of shared ancestry with those of other vertebrates. In stark contrast however, lampreys rely upon distinct antigen receptors analogous but not homologous to T cell receptors and immunoglobulins.

For research and therapeutic purposes, lamprey antibodies are potentially novel tools that may target markers of disease not readily recognized by mammalian immune systems and to which immunoglobulin antibodies are not easily elicited. We hypothesize that the evolutionary distance separating sea lampreys and humans, as well as the unique architecture of lamprey variable lymphocyte receptor *antibodies* can address tolerogenic constraints of mammalian immune systems, and structural constraints of immunoglobulins.

Here, we detail strategies for isolating serum biomarker-specific variable lymphocyte receptor antibodies that may detect, diagnose, or prognose disease. Additionally, we characterize the variable lymphocyte receptor VLRB N8 antibody whose binding specifically to antigen-experienced human B cells is unlike that of any known antibody. Thus, we have described a potential plasma and memory B cell-specific modification of human leukocyte antigen class I, the antigen bound by VLRB N8, and gained insight into B cell biology.

# Dedication

*To my family, Althea, Wesley, and Antony*

*who are the archetypes of unconditional compassion.*

*In memory of* 公公。

# Acknowledgements

Thank you to Dr. Götz Ehrhardt whose mentorship and education guided me through my own differentiation to maturity, and (although he would be appalled at being compared to a helper T cell) from naïve to experience. Despite my subpar academic credentials, being a liability, my daily breakdowns, and the everyday upheavals at every level of academia, he took a chance and welcomed me into his lab, his world, in 2012 – a non-negligible risk for an at-the-time new professor. All his undergraduate, graduate, and post-graduate students would agree that he is an exemplary and omnipresent mentor as his door is literally always open (against all fire safety regulations) and who has always prioritized education and other's wellbeing above his own. Although, this relationship was not without contretemps, and schmerz, I am grateful that opposites can bond towards discoveries both microscopic and macroscopic.

To my lab mates past and present including Shabab Ali and Ksenia Bezverbnaya, I'm sorry I was not the lab mate they deserved but I am sincerely grateful for their warm welcome, mentorship and support, despite lacking the words to express it. I knew this was meant to be when I first met Dr. Srijit Khan in 2015. He is wise beyond his years and this thesis could not have been completed without him devising experiments and laying the foundations upon which it lies. I wish I could show as much eternal optimism, patience and compassion Dr. Yanling Liu has shown to her child and to children such as myself in the lab. Miranda Shi inspired me to become the architect of the future I want for this planet. To the future Dr. Leslie Leung, 加油。

When I was in disarray about where the future was going, I have my supervisory committee to thank for convincing me in 2013 to pursue and persevere through this degree. I have Dr. Michele Anderson to thank for her belief in me and supporting my class-switch or reclassification into the program. She has helped shape this thesis and me into what they are today. I'll never forget the exam question Dr. Michael Ratcliffe posed to me in 2014 that has led me to consider all scientific problems rationally and with the utmost scrutiny. Dr. Naoto Hirano really is the omniscient figure everybody looks up to in the Department. Every second of every conversation with him is beyond fruitful and insightful whether it was about academia, society, or science.

Thank you to Dr. Alexander Palazzo and his laboratory, including Mathew Truong, Eliza Lee, Hui Zhang, and Nevraj Kejiou, for accommodating me with open arms into their department for a most pivotal experiment and breakthrough for this thesis.

To peers, notably the residents of the 7th floor of the Medical Sciences Building, this was truly an open institution where help is openly offered and where even a pariah like me felt at home. Thank you Elisabeth (Lis) Förster for guiding me to give back to the community through SciChat or our student association. These activities kept me sane. Alex Ling was a bottomless well of wisdom and truly an enlightened one. He is the Department's true social representative, feeding us food and thought. Thank you Dr. Clare So, for listening and helping me exorcise my deepest neuroses.

To the administrative staff, past and present, thank you for making the Department the most seamless of bureaucracies and for valuing every single student.

To my family, I can't imagine what they have suffered through as I spent over a fifth of my life at this institution. they created the space I needed to fulfill my scientific responsibilities, and unconditionally accepted all of my irresponsible and selfish decisions taken on a whim. I know these were harrowing years and they deserve more than I could ever provide. I am grateful to my uncle and aunt for helping me transition to life in Toronto. Thank you for helping me see that Ontario is also une belle province.

To my dearest friends Michael Alex Leney-Greene and Todd Mitchell Douglas, my copains in the commiseration over some of the pains of science, it is the warmest of comforts knowing that 'even with the distance, our hearts still beat the same.'

Andria, Astraea, and Ana(stasia) freely gave me rides to school almost every single day, gliding through and uplifted by the summer breeze or weathering winter's furor, and truly made graduate school life possible in this city. I'm sorry I could not always reciprocate by fixing what ails them.

I am grateful and thankful for these friends, family, and those I call both who helped me see through this crucible. Je me souviendrai.

Dear readers, thank you for laying eyes upon this work. May it offer that which you seek.

# Table of contents

# List of Figures and Table

**Chapter 1 | Introduction**



**Chapter 2 | Discovery of Human Serum Biomarkers of Disease Using Lamprey VLR Antibodies**

**Chapter 3 | A Tyrosine Sulfation-Dependent HLA Class I Modification Identifies Memory B Cells and Plasma Cells**

**Chapter 4 | Discussion**

# Abbreviations

| | |
|---|---|
| aa | Amino acid |
| AID | Activation-induced cytidine deaminase |
| ANOVA | Analysis of variance |
| APOBEC | Apolipoprotein B mRNA editing enzyme, catalytic polypeptide-like |
| BCR | B cell receptor |
| β2m | Beta-2 microglobulin |
| (k)bp | (kilo)base pair |
| BSA | Bovine serum albumin |
| CAR | Chimeric antigen receptor |
| CDA | Cytidine deaminase |
| cDNA | Complementary DNA |
| CDR | Complementarity-determining region |
| CRISPR-Cas | Clustered regularly interspersed short palindromic repeats and Cas protein |
| DTT | Dithiothreitol |
| ELISA | Enzyme-linked immunosorbent assay |
| FACS | Fluorescence-activated cell sorting |
| FBS | Fetal bovine serum |
| Fc | Fragment crystallizable |
| FCRL4 | Fc receptor-like 4 |
| GC | Germinal center |
| GFP | Green fluorescent protein |
| GPI | Glycosylphosphatidylinositol |
| HA | Hemagglutinin |
| HEL | Hen egg lysozyme |
| HER2/Neu | Human epidermal growth factor receptor 2/proto-oncogene Neu |
| HLA | Human leukocyte antigen |

| | |
|---|---|
| HRP | Horseradish peroxidase |
| IFN | Interferon |
| Ig | Immunoglobulin |
| IP | Immunoprecipitation |
| LRR | Leucine-rich repeat |
| MHC | Major histocompatibility complex |
| MS | Multiple sclerosis |
| PAPS | 3'-phosphoadenosine 5'-phosphosulfate |
| PBMC | Peripheral blood mononuclear cell |
| PBS | Phosphate-buffered saline |
| PCR | Polymerase chain reaction |
| PE | Phycoerythrin |
| PEI | Polyethylenimine |
| PMA-I | Phorbol 12-myristate 13-acetate and ionomycin |
| PSGL-1 | P-selectin glycoprotein ligand-1 |
| qPCR | Quantitative polymerase chain reaction |
| RAG | Recombination-activating gene |
| SDS-PAGE | Sodium dodecyl sulfate polyacrylamide gel electrophoresis |
| SD | Standard deviation |
| S(D/G)CAA | Synthetic dextrose/galactose plus casein amino acids |
| shRNA | Short hairpin RNA |
| siRNA | Small interfering RNA |
| SLE | Systemic lupus erythematosus |
| TAP | Transporter associated with antigen processing |
| TCR | T cell receptor |
| TPST | Tyrosylprotein sulfotransferase |
| TLR | Toll-like receptor |
| V(D)J | Variable (diversity) joining |
| VLR | Variable lymphocyte receptor |
| YPD | Yeast extract-peptone-dextrose |
| YSD | Yeast surface display |

# Chapter 1 | Introduction

## *1.1 Adaptive immunity*

All forms of life as we know it face a common challenge: coexisting with the most primordial, ubiquitous, and successful life forms on Earth, namely microorganisms. Bacterial, viral, and parasite diversity is limitless – a result of horizontal gene transfer, rapid mutation rate, and innovative life cycles. Although the human genome encodes over 20,000 genes that each express at least one representative protein (1), this number is insufficient to match the variety of microbial life (2) and their products – this remains true when forms, variants and modifications of human proteins are factored in (3). In contrast to passive and active mechanisms at the population level such as genetic drift or natural selection, diversity in organisms must be driven within one's lifespan at the cellular level, all while maintaining tolerance to not only ourselves, but microorganisms deemed symbiotic. Ancestors to modern vertebrates addressed this need with a boundless and robust immune system (4).

From an antigen receptor gene, somatic diversification gives rise to a plethora of antigen receptor proteins that are not germline-encoded. From a primary response, select T lymphocytes, and B lymphocytes are maintained. Compared to naïve cells, these memory lymphocytes may be proportionately more abundant, have a metabolic advantage, or, specifically in B cells, carry affinity-matured and functionally specialized antigen receptors (5).

Unlike innate immunity which is possessed in some form by all animals and all phyla of life, adaptive immunity was thought to be an innovation of jawed vertebrates. However, our characterization of immunity is incomplete and everchanging – for example, the description of immunological memory was recently redefined by the appreciation of the CRISPR-Cas system in bacteria and archaea, whereby phage infection initiates host genome editing and provides prophylaxis against reinfection (6). Focusing on vertebrates, our understanding of immunology is largely founded on observations in humans, birds, and common laboratory animals such as rodents. We now appreciate the diversity amongst immunoglobulin (Ig)-based systems and that these

systems were not the sole solution devised 500 million years ago by cold-blooded fishes (7). The recent discovery of an alternative immune system in jawless fishes has uncovered antigen receptors that are most unconventional.

## *1.2 The evolutionarily distant sea lamprey (*Petromyzon marinus*)*

The sea lamprey, specifically *Petromyzon marinus*, is a member of one of two surviving orders of jawless fishes – lampreys and hagfishes. Though phylogenetically classified as vertebrates, the eel-like lampreys, and the hagfishes are fishes that do not possess vertebral columns but do share features with true vertebrates such as having (cartilaginous) skulls (8).

Sea lampreys follow an anadromous[1] life cycle. To spawn, this jawless fish migrates upstream, from oceanic waters to freshwater, or from lakes into tributaries. Lamprey larvae burrow and can filter feed for years before metamorphosing into the parasitic adults who feed on the bodily fluids of other fishes. Sea lamprey are infamously associated with being invaders of the Great Laurentian Lakes where adults partake of 'fisheries'. However, access to the Great Lakes is entirely anthropogenic and the lamprey can benefit aquatic systems by the cycling of nutrients (9). As demonstrated in teleost fishes, both an anadromous life cycle (10) and Antarctic environment (11) have been demonstrated to mold physiology and immune capacity. Therefore, the immunity of jawless sea lampreys is likewise impacted by their own distinct life stages and ecological niche.

A common ancestor to extant jawless and jawed vertebrates diverged approximately 550 to 450 million years ago (12, 13). Thus, lampreys and hagfishes hold unique evolutionary positions as textbook examples in phylogenetics. For instance, they have shared, preserved, derived, or lost traits compared to the descendants of jawed vertebrates, and vice-versa. Specifically, we are interested in the ancient variable lymphocyte receptor (VLR)-based adaptive immunity of jawless vertebrates and its contrast to Ig-based adaptive immunity derived by jawed vertebrates.

[1]*Anadromous* Describing migratory fish whose adult stages transit from saltwater to freshwater for spawning.

## *1.3 Alternative adaptive immunity in the sea lamprey*

Along with paired appendages, bone (in the non-cartilaginous species), and jaws, it was long hypothesized that adaptive immunity is also a trait derived by gnathostomes[1] after their divergence from the agnathans[2]. However, observations of accelerated rejection of a second allograft (14) and, in response to immunization, secretion of agglutinins specific to *Brucella* bacteria (15) suggested memory and, at the very least, a diverse repertoire of secreted antigen receptors. The source of these prototypical adaptive responses remained a mystery due to the absence of recombination-activating gene (RAG), major histocompatibility complex (MHC), Ig, and T cell receptor (TCR) orthologues (16), and the lack of thymus and spleen in jawless vertebrates (7). This, despite sharks and rays (the cartilaginous jawed vertebrates most evolutionarily distant from humans) possessing these select lymphoid organs along with orthologues of all these defining immune components (7).

In a classic study, Pancer et al. elucidated the molecular nature of lamprey adaptive immune responses and antigen receptors, redefining immunity as we knew it (17). Transcripts specifically enriched in large lymphocytes from mitogen- and xenogeneic cell-stimulated lamprey larvae were analyzed. Among these genes, hundreds of homologous yet non-identical sequences were identified, their protein sequences being organized into leucine-rich repeat (LRR) modules. Furthermore, over 100 *VLR* clones unique in protein sequence were identified and no two animals shared an identical transcript. Together, these observations suggest that the diversity cannot be accounted for by a finite few homologues/paralogues of innate receptors such as toll-like receptors (TLRs) but are characteristic of a germline gene amenable to somatic diversification and assembly into a mature coding sequence. We now know that initially non-functional genes are rearranged as is the case for *TCRα*/*β* and *IgH*/*L*, albeit through a distinct mechanism (18, 19). Designated 'variable lymphocyte receptors', complete rearranged genes are absent in myeloid cells and erythrocytes (17, 20), and diversity is attributed to LRR inserts variable in number and sequence.

[1] *Gnathostomes* Jawed vertebrates
[2] *Agnathans* Jawless vertebrates

By further examining the similarities and dissimilarities between VLR- and Ig-based adaptive immune systems, we will rationalize the application of VLRs for basic and clinical research.

## *1.4 Somatic rearrangement and diversification of the variable lymphocyte receptor gene*

Beginning at the N-terminus, following a conserved signal peptide, mature VLR proteins are successively composed of six types of sequence-variable modules and an invariant stalk (**Fig. 1.1**):

a. A N-terminal-capping LRR (LRRNT)
b. An atypical shorter 18-aa module (LRR1)
c. Zero to nine variable LRR modules (LRRVs) with each unit bearing the 24-residue consensus XLXXLXXLXLXXNXLXXLPXXXFX ('X' representing any amino acid)
d. LRRVe, a C-terminal LRRV-like module not conforming to the above consensus sequence
e. A 13-residue connecting peptide (CP)
f. A variable-length C-terminal-capping LRR (LRRCT)
g. A threonine- and proline-rich stalk

A mended *VLR* results in a variable region bookended by the 3' end of LRRNT and the 5' end of LRRCT. Individual loci can span over 2 Mbp and include hundreds of germline LRR cassettes upstream and downstream of the incomplete germline *VLR* (18). Cassettes are defined as donor recombination units bearing either partial modules, complete modules, or both; in other words, cassettes do not necessarily provide a full-length module. Furthermore, available cassettes can encode a combination of the same or different types of modules. **Fig. 1.1** illustrates 3'-LRRNT-LRR1-5'-LRRV, 3'-LRRV-5'-LRRV, 3'-LRRV-5'-LRRVe, and 3'-LRRVe-CP-5'-LRRCT that are annotated, among other cassettes.

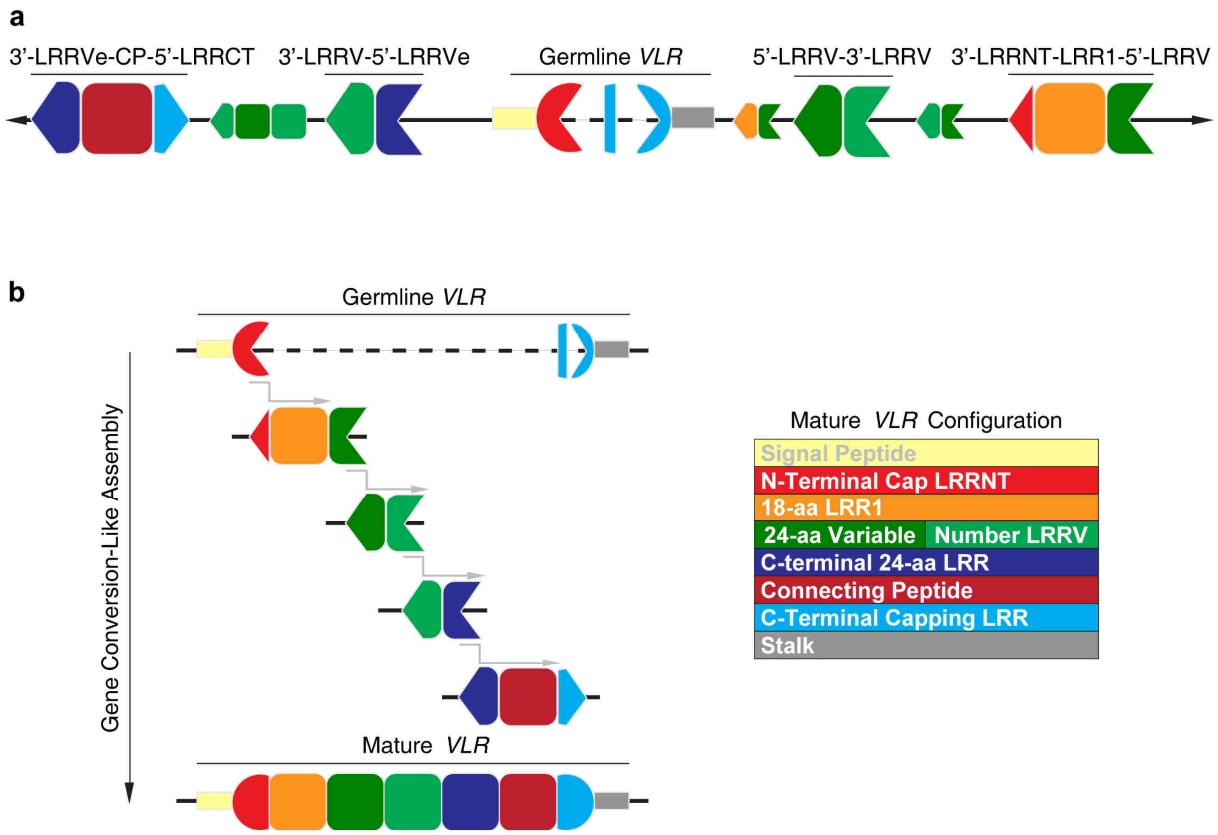


**Figure 1.1 | Assembly of a mature *VLR* from an incomplete germline gene into a mature protein-coding configuration.** *VLR* rearrangement involves replacement of non-coding germline sequences using coding (but partial/incomplete) cassettes that flank this core germline gene. **a |** An example of a germline *VLR* locus (dashed lines) is shown. In reality, hundreds of incomplete cassettes that vary in composition and number of LRRV (if applicable) flank the germline gene. Cassettes encode complete (squares) or incomplete (partially hollowed squares) LRR modules of every type (distinguished by color, see 'Mature *VLR* Configuration' table in **b**). Incomplete LRR cassettes encode only a 3' portion or 5' portion of a module. Cassettes that are used in this hypothetical assembly are the ones annotated whereas unused germline cassettes are depicted with smaller shapes. **b |** A hypothetical assembly is depicted and is mediated by step-wise homologous recombination (grey arrowed lines) using the four donor germline cassettes introduced in **a**. Shown is a 5' to 3' assembly though the reverse is also possible. Distances between germline and surrounding sequences are not to scale. Figure adapted from Boehm et al. (22).

For the somatic diversification of a *VLR* repertoire, studies support a DNA gene conversion-like mechanism termed 'copy-choice' rather than classical rearrangement (19). In this model of non-reciprocal recombination, donor sequences replace those of the acceptor, but the former remains unaltered. Gene conversion diversifies *Ig* in animals such as birds and this process may inform us of that in jawless vertebrates. We know that chickens employ gene conversion for the generation of their primary *Ig* repertoire. Unlike mammals, the core chicken *IgH* and *IgL* loci are limited with no choice of V and J segments, and few $D_H$ segments to select from (21). However, additional $V_L$ and $V_H$ segments lie upstream. These are incompatible with gene rearrangement but are used via gene conversion to diversify the primary *Ig* repertoire. As in the chicken, the lamprey gene conversion-like mechanism is thought to be initiated by cytidine deaminases (CDAs, members of the AID-APOBEC family) (18): a CDA gains access to single stranded DNA and deaminates dC into dU; repairing the mismatch may involve nicks, breaks, and intermediates which are mended with pseudogenes as templates. Sequences of homology ranging from 10 to 30 bp allow recombination between germline *VLR* and donor pseudogenes (19), the latter being the germline LRR cassettes flanking the *VLR* locus. During assembly, inserted sequences then act as recipient sites for subsequent cassettes.

Similar to combinatorial *TCR* and *Ig*, *VLR*s are somatically varied by the choice of exons incorporated into the mature gene. However, absent in agnathans are mechanisms conferring non-templated junctional diversity – random P nucleotides, and N-nucleotide addition. Additionally, being single-chain receptors, VLR diversity is not enhanced by heterodimerization with a second chain. Nonetheless, a variable distinct to *VLR* assembly is the stochastic non-discrete stitching of LRR cassettes in the assembly of a module, a process Boehm et al. have termed 'fusional diversity' (22). Through the gene conversion-like mechanism, hybrid non-germline-encoded LRR modules can be formed whereas in classical somatic rearrangement, V, D, or J segments themselves are germline-encoded and there is no fusion among their respective segments to form hybrid exons. With up to 820 modules encoded by 454 cassettes flanking a single *VLR* locus (18), between 0 to 9 *LRRV* modules inserted [the insertion of two

*LRRV*s being the most frequent (23)], and the selection of LRR cassettes being compounded by the stochastic factor of fusional diversity, the theoretical VLR repertoire is estimated to encode $10^{14}$ to $10^{17}$ possible unique antigen receptors (18).

Regarding any mutagenic contribution of the *CDA1* and *CDA2* paralogues to *VLR* diversity, whether primary or secondary, CDA activity has only been demonstrated in the former (18). Interestingly, when comparing mature *VLR*s and their germline C:G mismatch sites significantly correlated with a mutable motif of CDA1 (18). However, these mutations do not affect antigen contact sites unlike the activity of mammalian AID which preferentially targets complementarity-determining regions (CDRs). Additionally, *CDA* expression does not change with antigen or mitogen challenge and *CDA1* expression is rare outside sites of lymphocyte development (24). Thus, it is unlikely that either CDA is implicated in secondary diversification as observed in somatic hypermutation of *Ig*. Perhaps assembled mature genes are instead further diversified by the gene conversion-like mechanism in a manner such as the gene conversion of the primary semi-invariant chicken *Ig* genes. Although opting for a system independent of RAG-mediated gene rearrangement, this CDA-led mechanism can generate an assorted antigen receptor repertoire that is theoretically comparable to that of the TCR and B cell receptor (BCR) in diversity (25).

## *1.5 The duality and reciprocity of cellular and humoral immunity in lampreys*

We now know that the initial *VLR* identified by Pancer and colleagues (*VLRB*) is one of three paralogues, *VLRA*, *VLRB*, and *VLRC*. These receptors accompany a trinity of lymphocyte lineages (22, 26), reminiscent of jawed vertebrate αβ T lymphocytes, B lymphocytes, and γδ T lymphocytes (27), respectively. The germline *VLRA*, *VLRB*, and *VLRC* loci can be distinguished by the degree of coding sequence completion but all three loci invariably lack sequences between LRR1 and CP (22). They can also be distinguished by the recombination cassettes at their disposal. *VLRA* and *VLRC* are proximal within the genome and share cassettes (28), a situation not unlike the *trans*-rearrangement of IgM V segments to TCRδ D and J segments in the nurse shark (29); or the unity of the *TCRα* and *TCRδ* loci and their sharing of V segments

(30, 31). However, *VLRB* is isolated and does not partake of this pool of elements. Unlike TCRαβ, TCRγδ, or IgH-IgL, VLRs are single chain antigen receptors. Akin to the Ig-based adaptive immune system, mechanisms of allelic exclusion and lineage-specification result in individual lymphocytes expressing either functional VLRA, VLRB, or VLRC, of a single specificity (20, 26).

Lymphocyte lineages can also be compartmentalized phenotypically and spatially, whether during development or after maturation. Unlike the expression of *RAG1/2* that does not selectively accompany that of *TCR* or *Ig,* it is hypothesized that during development, *CDA1* and *CDA2* are inseparable from *VLRA*-expressing and *VLRB*-expressing lymphocytes, respectively. From hematopoietic tissues and blood, cells sorted by VLRA or VLRB surface expression exclusively express *CDA1*, and *CDA2*, respectively (20). Through RNA *in situ* hybridization, Bajoghli et al. observed that the thymoid, located at the ends of the larval gill filaments, is a thymus equivalent where *CDA1*, *VLRA*, and a homologue of the *Foxn1* thymopoietic marker are expressed in the absence of *CDA2* and *VLRB* (24). For the latter, we define the reciprocal developmental site as containing VLRB$^+$ lymphocytes along with *CDA2* and it is thought to be in the hematopoietic tissues of the typhlosole, located within the concave folds of the intestine. In support of its status as a primary lymphoid organ, the typhlosole houses mature VLRB-positive cells that are relatively non-reactive to antigen unlike those of blood and kidney (32). However, surgical procedures analogous to bursectomy in chickens need to be performed to demonstrate these organs as sites of hematopoiesis. Regarding mature VLR-expressing lymphocytes, expression of both VLRA and VLRB isotypes is found in vasculature as well as in kidney, typhlosole, and the gills (24, 32) but only in the latter do VLRA$^+$ cells significantly outnumber their VLRB$^+$ counterparts. Secondary lymphoid organs have yet to be identified.

After translation, VLRB is covalently linked to a glycosylphosphatidylinositol (GPI) anchor for membrane tethering (17) whereas VLRA and VLRC are transmembrane proteins (22). In response to immunization with bacteria, VLRA$^+$ and VLRB$^+$ lymphocytes undergo lymphoblastoid differentiation (17, 24). VLRA$^+$ lymphocytes proliferate in response to the T cell phytohemagglutinin mitogen (20) whereas VLRB$^+$

lymphocytes react to immunization by differentiation into plasma cells possessing characteristic extended rough endoplasmic reticuli (32). Subsequently, specific antibody titers are measurable in a matter of weeks. Thus, circulating VLRB rather than VLRA were the agglutinins observed in initial studies of lamprey immune responses. It remains unclear how cell surface VLR initiates signal transduction. Since VLRB is not strictly transmembrane but rather anchored, interactions with adaptor proteins are necessary. Being GPI-anchored proteins, perhaps localization in lipid rafts facilitates formation of a VLR immunological synapse upon antigen binding.

The restriction of *VLR* and *CDA* gene expression to certain cell subpopulations suggests lineage-specific transcriptional regulation. Indeed, VLRA$^+$ lymphocytes express orthologues of T cell genes implicated in thymus homing (*CCR9*), development (*CD45* and *Notch 1*), and differentiation (*GATA2/3*) (20). On the other hand, VLRB$^+$ cells express B lymphocyte genes of hematopoietic tissue homing (*CXCR4*), BCR signal transduction (*Syk*), and various innate immune receptors (*TLR2*, *TLR7*, and *TLR10*). Furthermore, inter-lineage communication is likely preserved by the complementary expression of ligand-receptor pairs such as the *IL-17* cytokine and *IL-17R* receptor orthologues in VLRA$^+$ and VLRB$^+$ lymphocytes, respectively.

Overall, the duality and reciprocity of humoral and cell-mediated immunity observed in both gnathostomes and agnathans suggests that, unlike adoption of either Ig or VLR antigen receptors, adaptive immunity did not arise independently in these vertebrate clades. Rather, the hypothesis is that lymphocyte lineages, their function, and their crosstalk were established prior to separation of jawed and jawless vertebrates. A common predecessor to all extant vertebrates likely had primordial Ig- and LRR-based antigen receptors as well as CDAs. Several non-vertebrate and vertebrate genes are speculated to be the primordial Ig receptor – analysis of the transcriptome of lamprey lymphocytes yielded an immunoreceptor tyrosine-based inhibitory motif-containing invariant *TCR* orthologue, as well as a *CD4* orthologue in the lamprey (16). From the alignment of LRR receptors, Rogozin et al. hypothesize that modern *VLR* shares a common ancestor with the platelet glycoprotein receptor, GP1bα (18). Although LRR-based receptors such as *TLR*s are also organized much like *VLR*s with

N-terminal and C-terminal caps flanking various LRR modules, only pan-vertebrate GP1bα shares a stretch of 5 to 14 aa residues with VLRA and VLRB corresponding to inserts within LRRCT. In gene organization, the former remarkably resembles a *VLR* with eight LRRV modules capped by LRRNT and LRRCT. What followed, from these *Ig* and *VLR* precursors was independent evolution – the watershed event in jawed vertebrates is hypothesized to be insertion of a transposon encoding *RAG* and recombination signal sequences into an *Ig* superfamily locus leading to complete devotion to Ig-based immunity (4, 33). However, at the marrow, lymphocytes and their predecessors always bore the potential for or were the bearers of somatic diversification, hence the homology between T cells and B cells with VLRA/C$^+$ and VLRB$^+$ lymphocytes, respectively. This is also supported by the maintenance and sharing of orthologous transcription factors orchestrating the development and function of the trinity of lymphocyte lineages. Lampreys and hagfishes diverged 470 to 390 million years ago (34), shortly after the separation of jawed and jawless fishes. Thus, because modern hagfishes also maintain a VLRA/B/C compartmentalization, it is unlikely that hagfishes and lampreys independently evolved a VLRA/B/C system and, by extension, that gnathostomes independently developed the duality of a T-B lineage system. Overall, somatic diversification and lymphocyte lineage specification are evolutionarily adaptive for survival in all vertebrate species.

## *1.6 Antigen binding by variable lymphocyte receptors*

In biology, function follows form. We can speculate on VLR binding characteristics by comparing them to similar and dissimilar structures as well as extrapolating from the crystal structures of VLR-antigen complexes.

Akin to other LRR proteins, VLRs form solenoid structures that curve into a crescent-like shape (**Fig. 1.2a**) with the inner concave face of the molecule folding into a parallel β-sheet. The capping LRRs shelter the hydrophobic core of the molecule. At the C-terminus, the flexible stalk region is glycosylated, and is necessary for disulfide bond-mediated multimerization of VLRBs. Based on the antigen-binding modes of other LRR proteins, such as GP1bα (the nearest homologue to VLRs) in complex with the von Willebrand factor (35) (**Fig. 1.2b**), all modules spanning LRRNT to

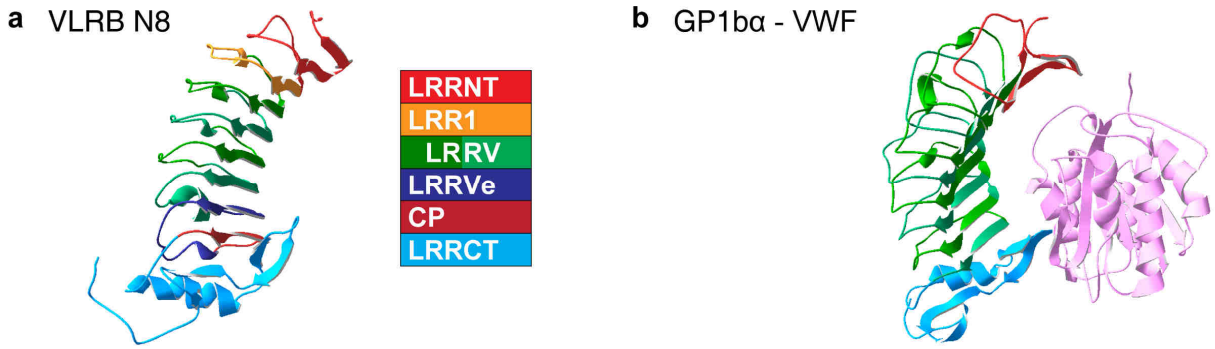


**Figure 1.2 | Structure of LRR receptors VLRB N8 and GP1bα. a |** The predicted structure of VLRB clone N8 (**Chapter 3**) as modelled by SWISS-MODEL (ExPASy). The hydrophobic core of the molecule is shielded by capping LRRNT and LRRCT modules. LRR modules form a parallel β-sheet, the extent of which is determined by the variable number of LRRV inserts that each contribute one beta strand (four LRRV inserts are incorporated into VLRB N8). **b |** As a result of shared ancestry and structural features, the solved crystal structure of GP1bα in complex with the von Willebrand Factor (PDB ID: 1m10) suggests that VLRB can bind antigen with the concave surface of the croissant-like receptor with a contribution from all modules spanning LRRNT to LRRCT inclusive. The ribbon models were created with Swiss-PdbViewer 4.1 (ExPASy).

LRRCT together form a pocket where antigen can be lodged; not only do β strands contribute to antigen binding but sizeable LRRCT protruding loops can insert into antigen (36) or help round out the pocket and enclose antigen (37).

Being found in all gnathostomes, IgM is the most ancient Ig isotype which suggests that, as introduced in *1.5*, an ancient lymphocyte lineage employed multimeric adaptive immune receptors that evolutionarily converged into VLRB and IgM. However, evidence suggests that VLRBs share only certain characteristics with conventional antibodies of the IgM isotype (38) – specializing in natural immunity against viruses and bacteria; low affinity of individual binding sites compensated for by multimerization; and binding to iterative epitopes such as microbial cell surface molecules. Immunization with bacterial components such as *Bacillus* exosporium (39), whole bacteria (15), or UV-inactivated virus (40) readily raises VLRBs against repetitive structures while lampreys are unable to readily produce antibodies against nor clear soluble antigen (32). However, unlike IgM, there is no evidence of the general polyreactivity nor the restricted gene usage that are observed in B1 cells (38). The majority of antigen-specific VLRs that have been isolated are low in affinity. Despite immunization, the affinity of elicited VLRBs remain within the lower μM to upper nM range also exhibited by IgM antibodies (36). Reducing multimeric monoclonal VLRBs such as the anti-CD5 VLR32 completely eliminates binding (41). However, other studies demonstrate that specific VLRBs with dissociation constants in the nM to pM range can be derived from lamprey immunized with *β*-galactosidase (42), from *in vitro* affinity-matured VLRB clones (36), or from the repertoire of naïve animals after application of display technology and enrichment techniques such as FACS (fluorescence-activated cell sorting) and magnetic-activated cell sorting (43). These studies prove that no inherent structural limitations preclude somatic assembly of and selection of high affinity VLR antibodies. Despite the variability in binding strength between VLRB antibodies, they are nonetheless highly specific receptors as exemplified by clone VLR4 which distinguishes between *Bacillus anthracis* and *Bacillus cereus* exosporium coat glycoproteins despite 90% amino acid identity (39) and by an idiotype-specific VLRB isolated in the context of chronic lymphocytic leukemia (44).

The structures of monoclonal VLRBs in complex with protein [hen egg lysozyme (HEL)] (36) and carbohydrate antigen (human O erythrocyte H-trisaccharide type II) (45) have been crystallized and solved. The concave surface formed predominantly by 24-aa LRRV modules, as well as the LRRCT module are necessary for antigen binding, as determined by site-directed mutagenesis (36, 39). With analysis of 588 unique VLRB sequences plus the crystal structure of a VLRB-HEL complex (clone VLRB.2D, **Fig. 1.3a**), Velikovsky et al. observed that sequence diversity between LRRNT and CP inclusive was concentrated in 20 amino acid residues, 19 of which in VLRB.2D made contact with HEL (36). All successful *in vitro* affinity-matured clones conserved these residues to maintain antibody specificity and the authors concluded that these amino acids likely compose the general antigen-binding sites of VLRBs. Although the LRRNT module was not implicated in binding in the VLRB.2D-HEL complex, the most diverse residues in LRRNT together with analogous residues of downstream modules, form three antigen-binding ridges – perpendicular to the β-strands, with each strand contributing identically positioned residues to these ridges. Overall, the involvement of any module to binding is dependent on the size of the target antigen and the number of LRRV inserts in a VLR receptor in question: although both the tetrasaccharide LNnT and the type II H-trisaccharide are bound by VLRB clone O13, Collins et al. demonstrated that the LRRNT module of clone O13 only interacted with the larger LNnT sugar (37); in the same study examining two highly homologous anti-H-trisaccharide VLRB clones, binding to the acetamide group of the trisaccharide was shifted one LRRV (24 aa) between O13 and RBC36 because they vary by the insertion of an extra LRRV in clone O13.

One structural feature that does not fall in line with other LRR receptors is the distinct characteristic of the C-terminal LRRCT module: only VLRA and VLRB form a flexible hypervariable protruding loop akin to that of GP1bα and CDR3 of atypical BCRs (46, 47) but absent in LRR receptors such as TLRs. As such, LRRCT does not contribute to the parallel ridges, the loop it encodes may lend itself to antibody binding modalities that do not overlap with those of conventional IgH-IgL immunoglobulin antibodies.

## *1.7 Structural and evolutionary divergence of variable lymphocyte receptors may lead to unique binding specificities*

Like Igs, VLRs have been co-opted as adaptive immune receptors. However, VLRs originate from a divergent immune system and are structurally unrelated to Ig. This may lead to binding properties distinct from those of conventional Igs.

The difficulty of eliciting broadly neutralizing Ig antibodies against HIV highlights constraints of conventional Igs twofold: tolerogenic and structural. Current efforts in vaccine development target the HIV envelope and the challenge arises from not only the breadth of virus but also the harrowing path of repeated and fortuitous Ig somatic mutations required, explaining why only 20% of all patients eventually develop broadly neutralizing antibodies after prolonged infection (48). Despite an overabundance and relative uniformity of oligomannose glycans upon the surface gp120 component (49, 50), many neutralizing antibodies nonetheless target protein epitopes that lie beyond this 'glycan shield'. Although glycan-specific broadly neutralizing antibodies have been isolated [such as clone PGT 128 which neutralizes over 70% of HIV-1 subtypes tested (51)], they originate from 'elite neutralizers' (defined by the authors as individuals capable of *in vitro* neutralization of pseudoviruses across several clade groups) (52). Such individuals have been infected for at least three years prior to screening (52). Indeed, oligomannose-dependent broadly neutralizing antibodies potentially require at least 2 years to manifest (53), suggesting a level of immune tolerance towards these host-synthesized self-glycans. Furthermore, it has been demonstrated that broadly neutralizing antibodies can arise from unmutated common ancestors and subsequent descendants that are autoreactive and polyreactive (54). Secondly, other broadly neutralizing antibodies may display features atypical of immunoglobulins such as extended CDR3 loops (54, 55), tyrosine sulfation of CDR3 (56), or binding via framework regions (57) which point to inherent structural constraints that require elongated maturation, and molecular evolution to overcome.

In contrast, there is evidence that VLRs readily and specifically bind glycans. This may be due to similarity in function to IgM which naturally bear anti-glycan specificities (albeit with polyreactivity) (38). In comparison to IgM, VLRBs isolated by Hong

et al. were capable of specifically distinguishing between anomeric forms of the pan-carcinoma Thomsen-Friedenreich antigen while binding with affinities in the nM to pM range (43). Additionally, clones binding to gp120 and polymannose were also isolated from the repertoires of naïve animals. Collins et al. demonstrated the superior specificity of the O13 anti-H-trisaccharide type II VLRB compared to the UEA-1 lectin used in blood typing. In contrast to the VLR, the lectin focuses on fucose and is unable to differentiate between several fucose-containing (37).

Although, most antigen-binding residues are located within β-strands of the VLR's concave surface, the contribution of the LRRCT can be crucial for contact. The LRRCT protrusion is comparable to the loop formed by the CDR3 of particular and peculiar camelid and shark single-chain antibodies (46, 47). In one example, VLRB.2D's LRRCT loop penetrates into the enzyme activity site of HEL and over 75% of the HEL residues bound by VLRB.2D are identical to those bound by the single-chain Igs (36) (**Fig. 1.3b** and **1.3c**). When presented with the same antigen, the relatively planar variable regions of IgH-IgL lead to a preference for likewise flat epitopes such as that bound by HyHEL5 (**Fig. 1.3d**). However, there is no evidence that VLRs are destined to bind clefts. For one, the length of LRRCT inserts in VLRBs are variable to a degree where certain clones will be incapable of forming loops. Secondly, existing structures such as that of VLR RBC36 (45) and GP1bα (35) describe LRRCT loops cooperating with the concave surface to pocket or encircle antigen rather than penetrate it. Antigenicity is a matter of context where antibody structure, tolerance, selection, and immune response are determinants.

## *1.8 Variable lymphocyte receptors as tools for the discovery of human biomarkers*

With the availability of a cast of complementary tools such as anti-VLRB Igs (for example, clone 4C4), VLRs are compatible with or can be easily adapted for almost every application implicating conventional antibodies. VLRBs have been used in affinity purification, Western blotting, immunofluorescence, enzyme-linked immunosorbent assay (ELISA), immunohistochemistry, mass spectrometry, crystallography, etc. (39, 41, 43). They are specific affinity reagents and we aim to demonstrate their

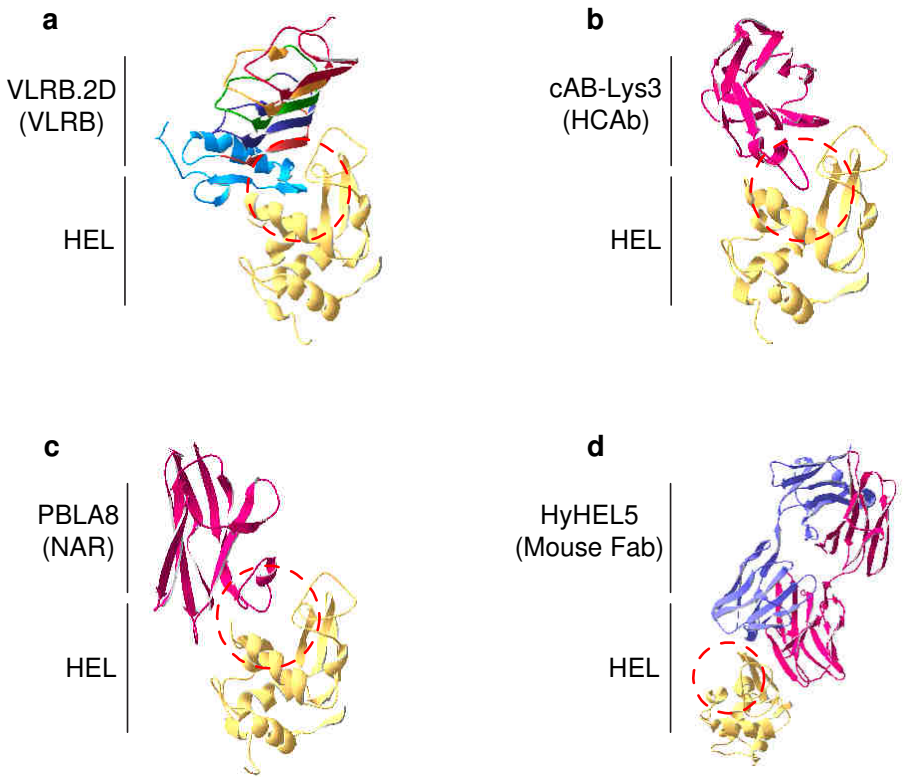


**Figure 1.3 | Antigen recognition by a VLR receptor and several immunoglobulin-based receptors.** When presented with an identical antigen, immunoglobulin (Ig)-based and VLR immune receptors can produce antibodies with differing binding characteristics. This is the basis of our research – namely, that VLR-based immune systems will readily produce antibodies of interest towards epitopes not readily recognized by Igs. The solved crystal structure of Ig- and VLR-based receptors in complex with hen egg lysozyme (HEL) allows us to speculate on similar and dissimilar features. The flexible and length-variable LRRCT loop as presented by **a** | VLRB.2D (PDB ID: 3G3A) is akin to the extended CDR3 loops of single-chain **b** | camelid heavy chain antibodies (HCAbs) (PDB ID: 1mel) and **c** | shark new antigen receptors (NARs) (PDB ID: 1t6v). Dashed red circles highlight the enzymatic cleft of HEL which may be preferred by these atypical-loop forming antibodies, highlighting the VLRB LRRCT as deterministic in antigen binding. In contrast, **d** | IgH-IgL antibodies do not readily form such loops and may prefer planar epitopes as demonstrated by the antigen-binding fragment (Fab) HyHEL5 (PDB ID: 1yqv). HEL is consistently cantaloupe throughout and oriented similarly to highlight the active site. IgH and IgL are colored violet and purple, respectively. Ribbon models created with Swiss-PdbViewer 4.1 (ExPASy).

novelty, and support their position alongside conventional antibodies as research and potentially clinical tools.

In the first example of the isolation of a human cell surface antigen-specific VLRB, our laboratory demonstrated the applicability of an anti-human CD5 VLRB, VLR32, in affinity purification and mass spectrometry identification (41). This antibody was isolated from larvae immunized with peripheral blood mononuclear cells (PBMCs). Among 151 monoclonal VLRs, VLR32 was one of the few clones to both uniquely bind human T cells and segregate them from non-T cells. The pull-down subsequently identified CD5 as the antigen with subsequent experiments revealing binding of VLR32 to $CD5^+$ B cells as well. Additional comparisons with conventional anti-CD5 suggest that VLR32 is a pan-CD5-reactive antibody.

In a subsequent study, from animals immunized with primary multiple myeloma bone marrow aspirates, our laboratory isolated VLRB MM3 which binds uniquely to human plasma cells (58). In a familiar development, VLRB MM3 affinity-purified CD38, a cell surface receptor strongly up-regulated in plasma cells. Unexpectedly however, pan-CD38 reactivity would be a misnomer for VLRB MM3 as it does not bind other CD38-expressing cells such as monocytes, NK cells and T cells. VLRB MM3's binding pattern for all subpopulations of plasma cells at every stage of differentiation classifies it more accurately as pan-plasmablast and plasma cell-reactive. Notably, VLRB MM3 binding kinetics were associated with CD38 enzymatic activity unlike the reactivity of a conventional anti-CD38 antibody tested. VLRB MM3 reactivity being inhibited by a non-hydrolysable analog of the CD38 substrate suggests that its method of binding is reminiscent of VLRB.2D and its affinity for the enzymatic cleft of HEL rather than for a superficial epitope.

With evidence of the feasibility and applicability of VLRs as research tools, VLRs may also translate to clinical diagnostic or prognostic tools as evidenced by VLRB MM3. In preliminary evaluations of reactivity to multiple myeloma patients, 15% of patients' multiple myelomas were non-reactive and lack of VLRB MM3 binding is

correlated with poor prognosis (58). Owing to the unique properties and atypical specificities characterized thus far for VLRs, many discoveries await in human immunophenotyping and biomarker discovery that bear biological and clinical implications.

## *1.9 Thesis statement*

In 1890, immunologists Kitasato and von Behring immunized non-human animals to derive clinically invaluable reagents – in this case, anti-diphtheria antitoxin (59). In the same vein, we are also looking towards non-human animals, albeit a more ancient lineage, as precious sources of antibodies.

Focusing on humoral immunity, amongst jawed vertebrates such as mammals, birds, reptiles, amphibians, bony fishes, and cartilaginous fishes, we observe disparity in genetics (*Ig* locus organization; unique or absent *Ig* isotypes; and even lack of MHC class II), mechanism (presence/absence of class switching and germinal centres), cellular composition (follicular dendritic cells or lack thereof), and tissues (lymph nodes only observed in mammals thus far) (7). Agnathans lack these features altogether, having separated from jawed vertebrates prior to the emergence and divergence of Ig-based immunity. Over 450 million years of separate evolutionary selective pressures has culminated in an alternative VLR-based immune system that is uniquely shaped by this history and adapted to these pressures. Dissimilar immune responses and immune targets have been documented amongst vertebrates (7, 15, 36, 60). Thus, the ontogeny of lamprey lymphocytes and the structure of VLRs will likely result in differences in antigens that can or cannot be readily recognized and in epitopes that can or cannot easily be bound. How will this alternative form of adaptive immunity respond when presented with antigenic determinants of interest?

**We hypothesize that the jawless sea lamprey's adaptive immune system – the sum of the function of this anticipatory system with the form assumed by its antigen receptors – can provide reagents that will not encounter the same structural and tolerogenic constraints as conventional immunoglobulin antibodies.** Thus, VLRs can complement existing Ig antibodies in biotechnology and clinical applications.

Here, we examine the applicability and feasibility of the VLR antibody platform in producing potential research and clinical tools. From our successes and failures, we detail methodologies (**Fig. 1.4**) for the isolation of human serum biomarker-specific VLRs and describe several promising monoclonal antibodies that we identified in this venture (**Chapter 2**). We also studied VLRB N8, an antibody isolated separately (**Fig. 1.4**) which binds specifically to antigen-experienced human memory B and plasma cells (**Chapter 3**). Supporting our hypothesis, this unique binding pattern led us to discover the previously uncharacterized tyrosine sulfation of human leukocyte antigen (HLA) class I, potentially furthering our understanding of B cell biology in health and disease (**Chapter 4**).

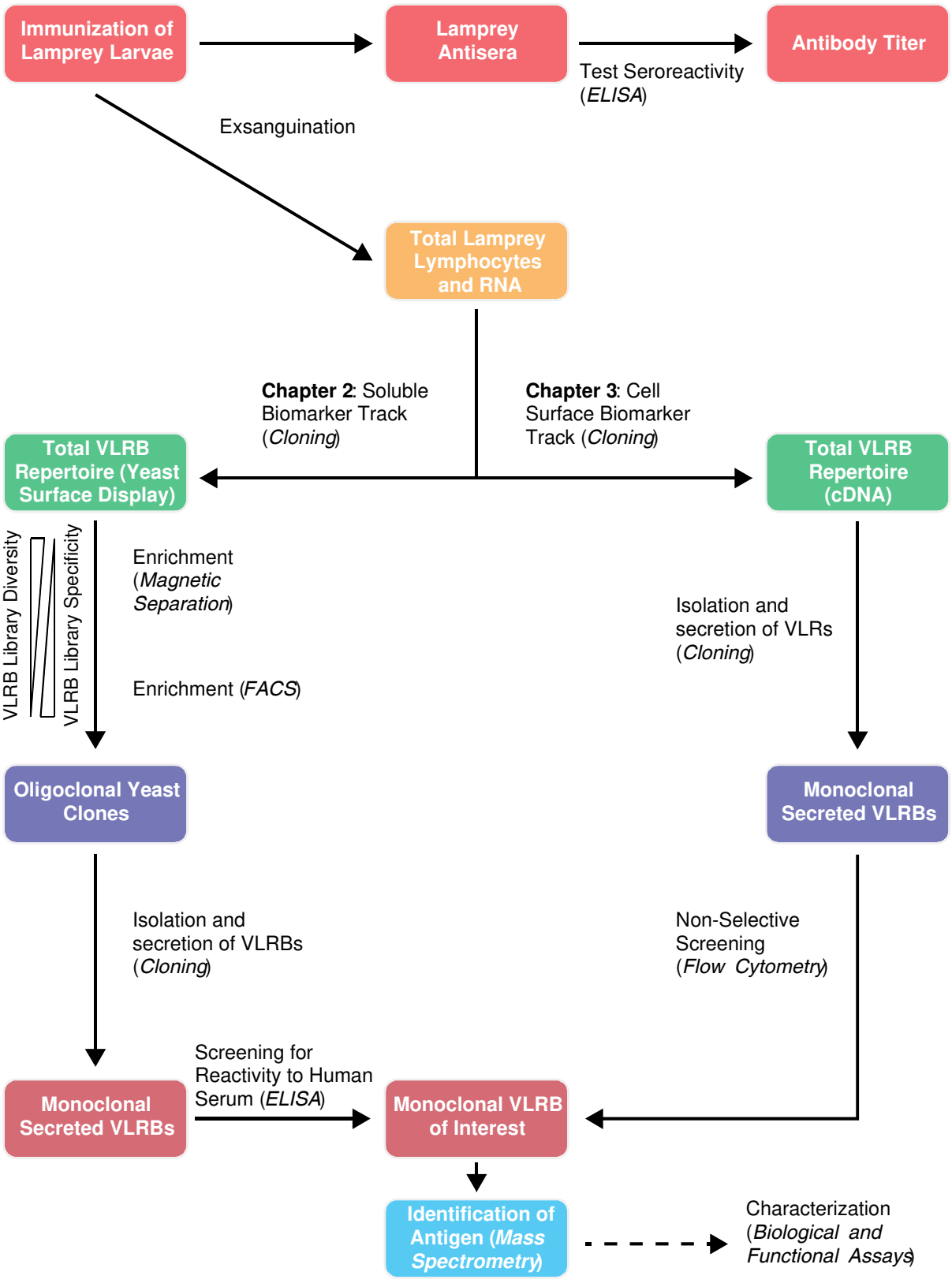
Immunization of Lamprey Larvae
Lamprey Antisera
Antibody Titer
Test Seroreactivity (ELISA)
Exsanguination
Total Lamprey Lymphocytes and RNA
Chapter 2: Soluble Biomarker Track (Cloning)
Chapter 3: Cell Surface Biomarker Track (Cloning)
Total VLRB Repertoire (Yeast Surface Display)
Total VLRB Repertoire (cDNA)
VLRB Library Diversity
VLRB Library Specificity
Enrichment (Magnetic Separation)
Enrichment (FACS)
Isolation and secretion of VLRs (Cloning)
Oligoclonal Yeast Clones
Monoclonal Secreted VLRBs
Isolation and secretion of VLRBs (Cloning)
Non-Selective Screening (Flow Cytometry)
Monoclonal Secreted VLRBs
Screening for Reactivity to Human Serum (ELISA)
Monoclonal VLRB of Interest
Identification of Antigen (Mass Spectrometry)
Characterization (Biological and Functional Assays)

**Figure 1.4 | Isolation of biomarker-specific VLRB antibodies.** This chart is an overview of the procedure followed for isolation of either serum biomarker-specific VLRB antibodies (**Chapter 2**) or cell surface marker-specific VLRB antibodies (**Chapter 3**). Briefly, from the blood of immunized lamprey larvae (top left), immunization efficacy is reflected by seroreactivity of animal sera as tested by enzyme-linked immunosorbent assay (ELISA). Total lymphocytes are separated and their RNA isolated for cloning of the total *VLRB* repertoire either displayed on the cell surface of yeast (**Chapter 2**) or secreted from a mammalian expression system (**Chapter 3**). In the former approach (isolation of serum biomarker-specific VLRB antibodies, **Chapter 2**), the total VLRB library as displayed on a laboratory yeast strain is subjected to cell sorting and separation to derive an incrementally specific but also decrementally diverse collection of VLRB antibodies. This enriched library is extracted from yeast and cloned into a mammalian expression system for secretion of monoclonal VLRB antibodies. At this stage, individual VLRB antibody clones are screened for reactivity to human serum antigen by ELISA. Enrichment procedures are bypassed in the isolation of surface marker-specific VLRB antibodies (**Chapter 3**) but follows the same principle to isolate monoclonal VLRB antibodies of interest. Identification and characterization of the antigen and epitope bound follows (**Chapter 3**) which are necessary to elucidate potential functional and clinical implications (**Chapter 4**).

# Chapter 2 | Discovery of Human Serum Biomarkers of Disease Using Lamprey Variable Lymphocyte Receptors

Justin T.H. Chan[1], Heng Sun[1], Réjean Lapointe[2]
and Götz R.A. Ehrhardt[1]

## Abstract

Cancer and autoimmune diseases are current and projected major public health challenges. Through early detection or diagnosis, they share the common thread of being predictable, or can be diagnosed to a degree. Much progress has been made in the diagnosis of infectious diseases because in many cases, the etiological agent is well known. In contrast, the same cannot be said for non-communicable diseases, which we now appreciate to be complex traits influenced by everchanging environmental contributions. For these diseases, the etiology is multifactorial, any attempt to detect disease must be extensive, and treatment must be multi-pronged.

Two variables of patient outcome are timing/stage of diagnosis and the efficacy of therapy. Patient survival is maximized when diagnoses are at early non-invasive stages. However, whereas a large majority of diseases such as breast cancer are diagnosed at stage I, only a minority of lung cancers are diagnosed in this non-invasive state, leading to a poor outcome for the remainder of patients. Moreover, two diseases diagnosed at the same stage will not necessarily have the same outcome because therapeutic options are limited or not effective. These disparities can be addressed by specific biomarkers of disease that can serve as both an indicator of disease for diagnosis or a target for treatment.

Here, we explored the applicability of sea lamprey variable lymphocyte receptor antibodies for the clinical detection, identification, and characterization of human serum biomarkers of disease. Based on triple-negative breast cancer as our research area, an immunization strategy was devised to elicit responses to soluble antigen. From the total antibody repertoire of immunized sea lamprey larvae, we have established cell separation- and cell sorting-based approaches to isolate variable lymphocyte receptor clones that can correctly stratify patients and healthy individuals. The output is a method applicable to a plethora of complex diseases from which we isolated several candidate tools/monoclonal antibodies for potential detection, diagnosis, and prognosis of breast cancer.

## Author Affiliations

1. The Department of Immunology of the University of Toronto.
2. The Centre de recherche du Centre hospitalier de l'Université de Montréal of the Université de Montréal.

## Acknowledgments

We would like to thank Ms. Dionne White for accommodating and performing yeast sorting in her flow cytometry facility.

Thank you to Renuka Ramlogan for producing monoclonal VLRB antibodies, some of which were screened as part of this chapter.

We would also like to express our gratitude to Kun Shen for preparing some of the material for yeast surface display culture and screening.

## Declaration of Contributions

The experiment depicted in **Fig. 2.2** was conducted with the aid of Mr. Heng Sun.

## 2.1 Introduction

In Canada, the five-year survival rate upon diagnosis of cancer ranges from high (over 86% for prostate, melanoma, and breast cancer) to low (a mere 8% for pancreatic cancer and 17% for lung cancer) (61). Tumors such as breast cancer originate from relatively superficial sites and have far more positive outcomes than cancers of visceral organs, the former being detectable by means of visual, digital (palpation) and imaging techniques leading to 80% of breast cancers being diagnosed at stages I and II. Conversely, diagnosis of lung cancer is less successful with only 30% of patients diagnosed at the same stages. Moreover, breast cancers and lung cancers *in situ* have disparate five-year survival rates upon diagnosis: 99% and 30% for stage I disease, respectively. The variables of method of diagnosis/detection, of timing of diagnosis/detection, and of treatment efficacy can all be improved with suitable and specific biomarkers that indicate disease and/or can be targets for therapy.

### *2.1.1 Biomarkers of disease*

To enable detection of disease or characterization of disease phenotype requires the analysis of indicators known as biomarkers. Biomarkers can be macromolecules such as DNA, RNA, and/or protein that are perturbed qualitatively or quantitatively by altered homeostasis/physiology. Correspondingly, cytogenetic analysis, gene expression profiling, and immunohistochemistry can inform clinicians of underlying disease.

An area of active research is the application of biomarkers towards early detection of asymptomatic disease in which healthy tissue can be indiscernible from eventual disease tissue (62). Therefore, detection at a premature stage requires indirect measurement of markers that are premonitions of abnormality – this is especially true for cancers that are neither easily seen nor felt. Even well after onset or during active disease, biomarkers can inform us of disease severity or prognosis.

The information that can be derived from the measurement of biomarkers depends not only on temporal but also spatial factors. Solid tumors such as carcinomas (for example, breast cancer) can be sampled for tissue to detect intracellular Ki-67

(63) or the targetable Her2/neu receptor (64, 65). Non-tissue sources such as human serum may be the desired option for hematologic malignancies such as leukemias that are not always solid, or myelomas difficult to access in the bone marrow (66). From such sources, the information derived is often indirect because the tumor itself is not analyzed. However, serum markers can be produced or shed by cancerous cells (65), can reflect the microenvironment of a tumor (67), and can sometimes be detected more easily than tumor-derived antigen (68) – all forms can potentially provide diagnostic and/or prognostic value. Additionally, atypical sources of biomarkers can include cerebrospinal fluid (69) or nipple aspirate (70) for diseases such as multiple sclerosis (MS) and breast cancer, respectively. Since blood-derived antigen/biomarkers can be comprehensive indicators of host health and can be collected non-invasively, they are studied and evaluated nonetheless for solid tumors such as breast cancer.

### *2.1.2 Breast cancer as our source of antigen – biomarkers and discovery techniques*

In 2017, 25% of new cancer diagnoses in Canadian women were cases of breast cancer (61). Ductal carcinoma represents about 80% of all mammary carcinomas (71). Survival rates are not as dire as for cancers of internal organs owing to the mammography imaging technique. However, this method remains imperfect with detection of ductal carcinoma being 67.8% sensitive and 75% specific (72). Additionally, successful detection is complicated by density of the tissue, density of tumor, and is observer-dependent. Thus, patients stand to benefit from fewer false positive detections, fewer unnecessary surgical resections, and earlier detection with current five-year survival rates being 99% for stages zero and one but plunging to below 26% for stage four in the United States (73). The current landscape of tried-and-tested biomarker discovery methods involve mostly quantitative expansive profiling of transcriptome or proteome.

Focusing on nucleic acids as indicators of disease, in a retrospective transcription profiling of 117 invasive breast carcinoma biopsies, van't Veer et al. identified 70 significantly differentially regulated genes allowing accurate classification of good and

poor prognosis patients (74). A prognosis profile optimized for 91% sensitivity (with a corresponding 73% specificity) was established allowing segregation of patients who did or did not experience distant metastases in a five-year period. This microarray test has now been commercialized in the form of MammaPrint (Agendia) in the United States. Nucleic acids are therefore reliable biomarkers. However, being a prognosis profile, overt disease/cancer growth is required as evidenced by the inclusion criteria for large and concentrated tumors (up to 5 cm across and containing at least 50% tumor cells) in this study. Being based on quantification, such approaches do not account for the ultimate post-translational modifications nor cell surface phenotype of the tumor. A non-redundant approach will need to offer value for early disease detection as well as allow qualitative analysis.

A method that addresses some of the above limitations is mass spectrometry profiling of breast cancer patient serum. The patient samples are indirect relative to the source of the disease, the tumor. However, it is a necessary caveat for early detection and, being the downstream product of what is sequenced in genomics or measured in transcriptomics, the nature of samples may better reflect physiological outcome. In one such experiment – the profiling of the serum of 48 stage II and III breast cancer patients versus healthy controls – 20 peaks were significantly different between experimental and control conditions (75). However, in this study, van Winden and colleagues were unable to replicate the differences observed in a previous study: either peak intensities were unchanged, or trends were reversed in the latter (67). Being a technique that measures two parameters (mass and charge), there is no technical limitation to detecting protein fragments, isoforms and glycoforms that represent not only quantitative but also qualitative changes. There is evidence of the former in the form of truncated C3a anaphylotoxin (67), and proteolytic products produced by carboxypeptidase N (76). However, mass spectrometry has not yielded any promising biomarker glycoforms yet, possibly due to sensitivity and resolution limits in probing human serum, or the caveat that mass spectrometry cannot differentiate polysaccharides identical in composition but differing in glyosidic linkage.

An avenue for biomarker discovery that is largely unexplored is the application of affinity reagents such as antibodies. In an express application of autoantibodies, Le Naour et al. tested patient and control sera for reactivity to antigen (77) – the reactive Igs themselves and their targets were both considered potential circulating markers of breast cancer. Conventional serodiagnostic tests for infectious diseases quantify seroreactivity to pure recombinant protein. However, because the antigen is unknown, Le Naour et al. used whole cell lysate from the SUM-44 breast carcinoma cell line to which serum samples either reacted or did not react. Isoelectric focusing and electrophoresis separated the lysate with the human sera serving as the 'primary antibody' in an immunoblot. Through this technique, three forms of RS/DJ-1, differing in charge but not in mass were identified. The protein modifications were detectable with autoantibodies from a subset of patients but not with serum from any healthy individuals whereas RS/DJ-1 was detectable in the circulation of patients. Thus, this study detected modified breast cancer circulating proteins that potentially differ in glycan composition and/or linkage, supporting application of these potential glycoforms as biomarkers. However, whether applying monoclonal anti-RS/DJ-1 antibodies or human sera, the detection of the three forms was always as a triad and therefore, no conclusion can be drawn about whether Ig used in this study were glycan-specific or if their epitopes were purely proteinaceous and incapable of separating the forms. Thus, potentially stronger discriminants of disease (glycoforms of other proteins) may have gone undetected due to self-reactive antibodies being limited by tolerance and the lack of suitable reagents.

Taking lessons from all that has gone before, an approach to biomarker discovery that is complementary rather than redundant cannot rely solely on quantitative differences nor on biopsies of disease tissues. We hypothesize that a new class of affinity reagents, namely VLR antibodies, can enable discovery of protein biomarkers that have yet to be detected by conventional mass spectrometry or antibody-based methods.

### *2.1.3 Rationale for applying variable lymphocyte receptors to seromarker discovery*

There is evidence supporting the lamprey immune system as a platform for raising specific antibodies, and slowly mounting evidence of VLRs having unique properties. Most pertinent is evidence that when presented with the same antigen, the resulting antigen receptors will preferentially bind epitopes distinct from those targeted by conventional IgH-IgL antibodies (36, 58). These distinct epitopes can potentially include qualitative differences such as post-translational modifications with capacity to differentiate disease from health.

Aberrant glycosylation is characteristic of cancer [reviewed by Dube and Bertozzi (78)] and represents changes that are non-templated and thus not accounted for by transcriptomics. Many biomarkers are glycoproteins such as CA125 in ovarian cancer and prostate-specific antigen in prostate cancer. The altered glycosylation of the latter distinguishes it from the same antigen in controls, providing value in diagnosis of prostate cancer among cases of benign hyperplasia (79). Elevated glycosylation also occurs in breast carcinoma as evidenced by increased staining of fixed breast cancer tissue by the L-PHA lectin (80). In another study, 34 glycoproteins from patient tissue were preferentially affinity-enriched by L-PHA compared to control tissue (81). Several known breast cancer biomarkers such as HER2/neu and MUC1 are surface glycoproteins but are not confined to tissue in disease conditions. The former is a member of the human epidermal growth factor receptor family whereas the latter is an integral membrane mucin whose O-glycosylation is decreased in breast cancer (68). However, both can be aberrantly shed into blood (65) – the prognostic testing for CA15-3 (secreted MUC1) is currently performed in the clinic.

As introduced in *1.7*, VLRs are excellent glycan-specific reagents with Collins et al. demonstrating enhanced specificity of an anti-H-trisaccharide type II VLR compared to the UEA-1 lectin currently used for O erythrocyte blood typing (37). Knowing that elevated and aberrant glycosylation are associated with breast cancer, and that

several serum biomarkers are glycoproteins, we sought to harness the unique properties of VLRs and the organisms bearing them in the discovery of circulating breast cancer biomarkers.

### *2.1.4 Eliciting VLRB immune responses to soluble antigens*

Although high-titer anti-HEL adult lamprey plasma was elicited by immunization with HEL in complete Freund's adjuvant (42), neither alum-precipitated nor polystyrene bead-coated bovine serum albumin elicit VLRB production or lymphoblasts (32) in lamprey larvae. Immunization of lamprey larvae with complete Freund's adjuvant led to high mortality rates and no detectable circulating agglutinins could be detected against the immunogens bovine gamma globulin or serum albumin (15).

As an alternative, we evaluated existing known immunogens and designed an approach in which soluble antigen is covalently linked to immunogenic human cell lines. In this context, antigen is no longer in solution and we hypothesize that it will render serum antigen immunogenic, allowing us to isolate monoclonal VLRB antibodies that can bind to and correctly classify human serum from healthy individuals and breast cancer patients.

## 2.2 Results

### *2.2.1 Lamprey larvae respond to antigen that is coupled to carrier cell lines*

The larval form of *Petromyzon marinus* responds readily to particulate antigen such as human cell lines (15, 32, 41, 58) but reactivity to soluble antigen is elusive (15, 32). Previously, our laboratory immunized lamprey larvae with cell lines and primary human cells (41, 58). The isolation of specific monoclonal VLRBs suggests that cell surface molecules are antigenic. We thus sought to adapt human cells as a host for the display of exogenous antigen.

To demonstrate feasibility of this approach, we initially covalently linked monoclonal mouse IgG to the surface of paraformaldehyde-fixed Jurkat cells via a two-step EDC and Sulfo-NHS treatment (**Fig. 2.1a**). The crosslinked antigen was readily detectable on coupled cells but not on cells that were mock-treated (**Fig. 2.1b**).

As a prelude to targeting more complex antigen preparations, lamprey larvae were challenged with murine CD130 that was first fused to human crystallisable fragment (Fc) and then coupled to Jurkat cells. Increased seroreactivity of immunized but not naïve animal sera to plate-adsorbed CD130-Fc suggests that a humoral response was elicited by immunization (**Fig. 2.2**). Our results indicate that soluble proteins are rendered antigenic to lamprey larvae via covalent linkage to a cell line.

### *2.2.2 Lamprey larvae immunization*

To target serum-derived antigen, we pooled plasma from three triple-negative breast cancer patients with invasive late-stage disease. The independent specimens were therefore equally represented, increasing the likelihood of identifying genuine disease-specific targets common to the three patients but decreasing the representation of polymorphic protein not shared among the three donors. We reasoned that this approach might decrease the likelihood of isolating anti-alloantigen VLRs which detect disease-unrelated differences.

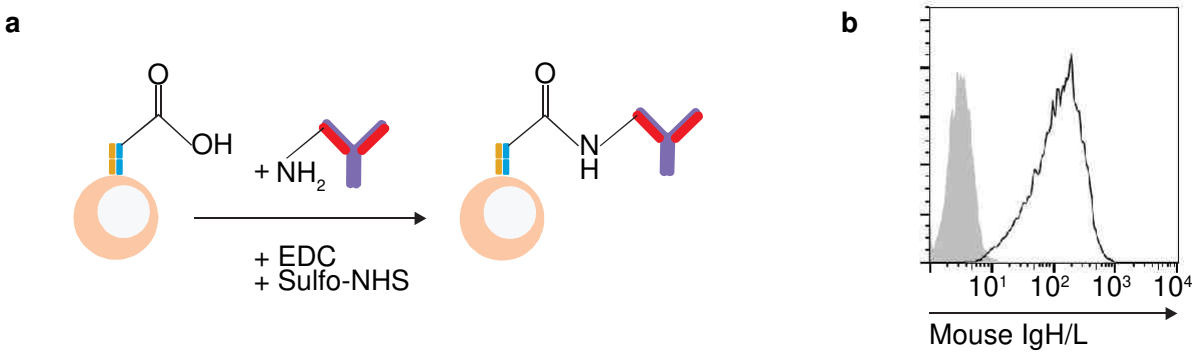


**Figure 2.1** | **Coupling of soluble antigen to the cell surface of carrier cells. a** | A graphical depiction of EDC and Sulfo-NHS crosslinking: on the surface of a paraformaldehyde-fixed cell, a cell surface protein with an exposed carboxyl group is activated by chemical treatment for amide linkage to primary amines on a target polypeptide. **b** | Monoclonal mouse antibody (clone 413D12) was covalently linked to the surface of paraformaldehyde-fixed Daudi cells via EDC and Sulfo-NHS. Crosslinked antigen was subsequently detected by flow cytometry using polyclonal goat anti-mouse Ig reagent (open histograms) whereas cells chemically treated in the absence of a protein coupling partner displayed no detectable mouse Ig (filled histograms). The flow cytometry plot is representative of every such reaction performed in parallel with each immunization and immunogen preparation.

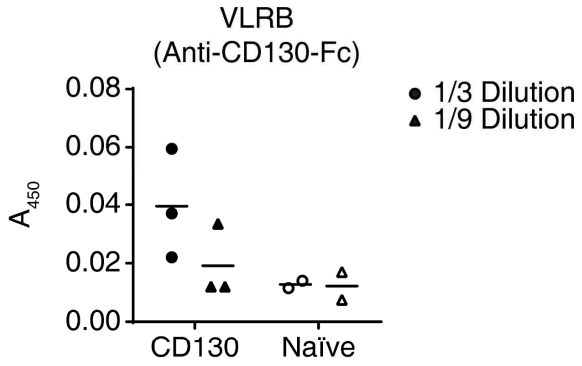


**Figure 2.2 | Lamprey seroreactivity to the CD130 immunogen.** An antibody titer to CD130 was measured by enzyme-linked immunosorbent assay using CD130-Fc adsorbed directly to microwells followed by incubation with animal plasma from one of three immunized animals or one of two naïve animals. Any VLRB bound to the fusion protein was detected using anti-VLRB clone 4C4. Sera was diluted prior to use as indicated by the different symbol shapes. Filled symbols each represent seroreactivity of one immunized animal while hollow symbols each represent seroreactivity of one naïve animal. ELISA absorbance values shown are background-subtracted.

To subvert an immune response to human albumin and IgG, we next depleted patient specimens of these two major constituents of blood with estimated serum depletion efficiency upwards of 80% (**Fig. 2.3**). Pooled patient samples were covalently linked to either the T cell leukemia Jurkat, or the triple-negative breast cancer MDA-MB-231 (82). The latter cell line was included in anticipation that a portion of the immune response will be directed towards cell line-endogenous antigen which may comprise of antigen ultimately shed into circulation during pathogenesis (65).

Previous studies highlighted dosage and immunization regimen as determinants for obtaining a maximal response from lamprey larvae (32). We modeled our immunization protocol on these bases with dosages of approximately 10 million human cells and up to three immunizations (**Fig. 2.4**). Several immunization strategies are outlined in **Fig. 2.4**. Onto animal cohorts B and D, we imposed regimens alternating in cell scaffold to enrich and focus the animal's immune response towards exogenous antigen. In the event of antigen competition (as in, the response towards cell surface endogenous antigen eclipsing that of exogenous coupled antigen), diversifying the cell support but preserving the artificially displayed antigen may help evoke breast cancer patient antigen-specific VLRs.

From the blood of exsanguinated animals, we separated lamprey lymphocytes and collected the animal plasma. For animal cohorts A to D, seroreactivity towards soluble breast cancer patient antigen was tested via ELISA. The ELISA readout for seroreactivity to breast cancer antigen was comparatively weak relative to specific VLRB responses elicited toward particulate antigens (32, 40), especially when taking into account that naïve plasma was the lowest in circulating VLRB (**Fig. 2.5a**). However, reactivity was consistently increased over that of a naïve animal (**Fig. 2.5b**) and comparable to that elicited against the single antigen CD130-Fc tested in preliminary experiments (**Fig. 2.2**). *VLRB* transcription and circulating VLRB are also known to be up-regulated upon immunization (17, 32) and we invariably observed elevated VLRB in all immunized animals (**Fig. 2.5a**). In line with these observations, the most abundant levels of plasma VLRB were not always the strongest in seroreactivity (**Fig. 2.5**),

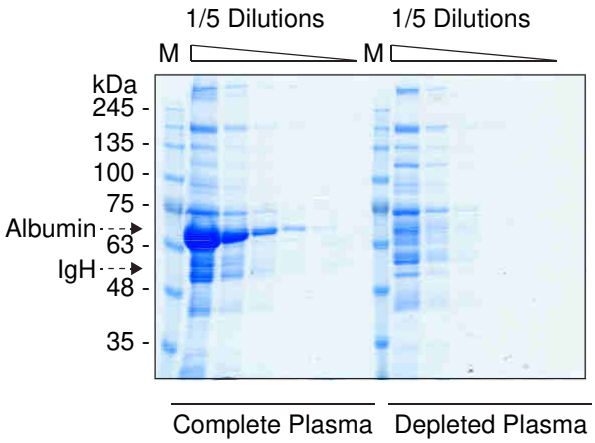


**Figure 2.3 | IgG and albumin depletion from human breast cancer plasma specimens.** Displayed is a GelCode Blue protein stain of serially diluted breast cancer plasma specimens before (left half of gel) and after (right half of gel) depletion of human IgG and albumin. This result is representative of every such procedure performed prior to covalent coupling to carrier cells and immunizations. From left to right, triangles indicate dilutions of specimens between adjacent lanes. Positions of albumin and IgG are indicated by dashed arrows and marker lanes are indicated by the letter 'M' above appropriate lanes.

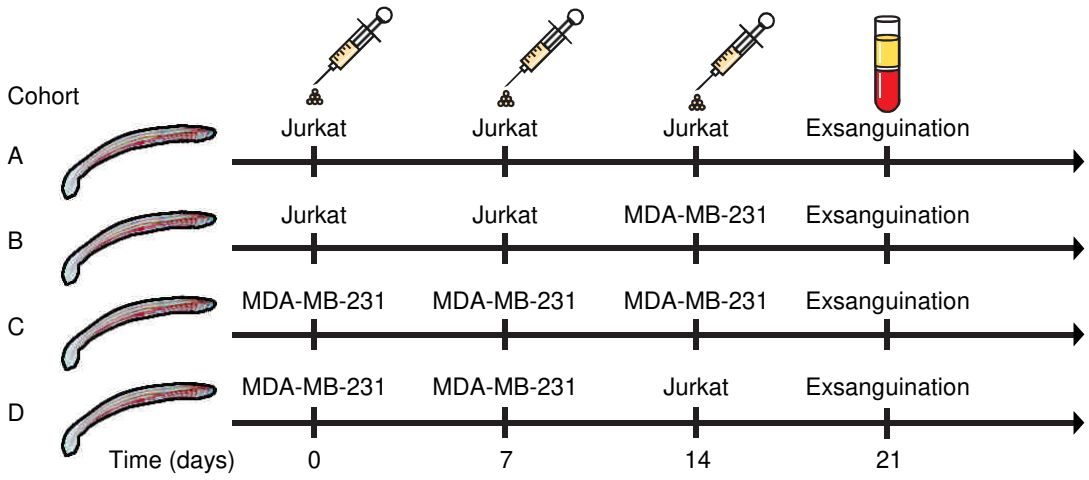


**Figure 2.4 | Strategies for immunization of lamprey larvae with serum antigen-coupled carrier cells.** Immunization strategies for eight experimental animals are shown in which two animals per cohort received various treatments. Breast cancer patient antigen was coupled to the indicated cell lines and comprised the immunogens. We administered the first immunization at day 0 and animals were ultimately exsanguinated 21 days post-primary immunization for isolation of lamprey plasma and lymphocytes, and generation of VLRB antibody libraries. The lamprey larva image is a derivative of 'Lamprey larva unlabelled' by Tracyanne and is used under CC BY-SA 3.0 (https://creativecommons.org/licenses/by-sa/3.0/).

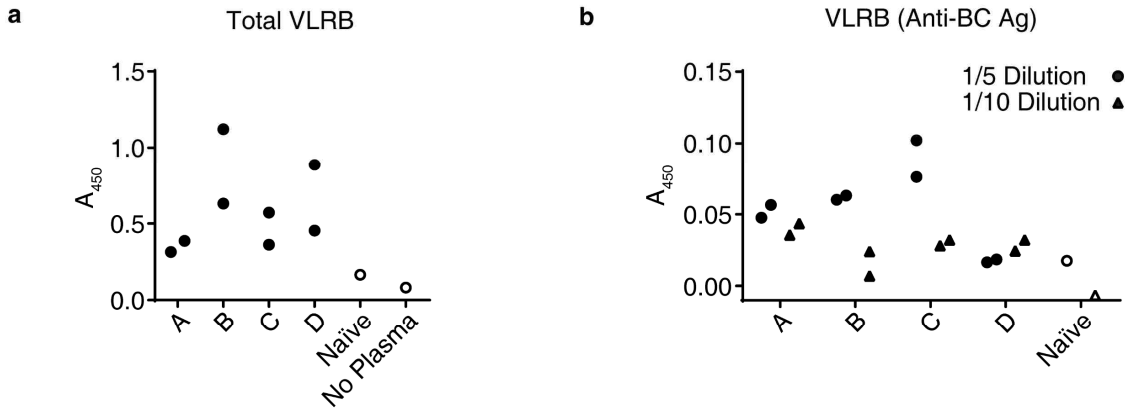


**Figure 2.5 | Lamprey seroreactivity to breast cancer patient plasma antigen.** A VLRB titer specific to the breast cancer patient-derived antigen (BC Ag) was detected by biotinylating the target antigen: namely, pooled IgG- and albumin-depleted patient plasma. **a |** The presence of plasma VLRB was measured by enzyme-linked immunosorbent assay (ELISA) using two anti-VLRB monoclonal antibodies – 4C4 and 5-8A3 sandwiched a 1/20 dilution of lamprey plasma. **b |** In a separate assay, diluted lamprey plasma was captured before testing reactivity to biotinylated antigen via the ELISA approach depicted in **Fig. 2.13**. Numbers represent background-subtracted values. Circles and triangles in **b** represent assays performed with 1/5 or 1/10 dilutions of lamprey larvae plasma, respectively. Each filled symbol represents one of two animals, originating from cohorts A to D as outlined in **Figure 2.4** whereas the open symbols represent a naïve animal or absence of animal plasma.

suggesting that a qualitative, antigen-specific response was elicited rather than a quantitative antigen-indiscriminate response. The highest seroreactivity was from animal cohort C, immunized exclusively with the MDA-MB-231 cell line acting as perhaps more than a scaffold. We performed additional immunizations with breast cancer serum antigens coupled to the Daudi Burkitt's lymphoma cell line. Seroreactivity of these animal cohorts were not assessed by ELISA but *VLRB* cDNA was included for subsequent VLRB library generation.

### *2.2.3 Isolation and screening of human serum antigen-reactive VLRB antibodies*

Our prior work demonstrated the isolation of antigen-specific VLRBs from the screening of hundreds of monoclonal VLRB antibodies from total/non-selected libraries (41, 58). However, we probed fewer than 1% of all clones represented in the VLRB libraries in this approach. To screen virtually all VLRB antibodies within a library, we leveraged the yeast surface display (YSD) system (83).

Pancer et al. pioneered the application of YSD in flow cytometry and/or magnetic separation for the isolation of specific VLR antibodies (42, 43) (**Fig. 2.6**). Through the fusion of VLRB antibodies to the Aga2p molecule, the recombinant protein is expressed on the surface of the *Saccharomyces cerevisiae*-based EBY100 yeast strain via disulfide linkage to the complementary Aga1p constituent (**Fig. 2.6d**). Due to its tryptophan auxotrophy, nutritional selection yields successfully transformed yeast. *VLRB* library expression is inducible with galactose-containing growth medium and surface VLRB expression is verifiable via detection using anti-hemagglutinin (HA) epitope tag antibodies (**Fig. 2.6**).

We generated VLRB libraries with PCR amplification that comprised two steps: the primary amplification was achieved with primers specific to invariant regions of *VLRB* cDNA and secondary amplification was performed with oligonucleotides that incorporated regions homologous to the YSD vector (**Fig. 2.6a**). We electroporated inserts and linearized vector following which the yeast repaired the gap in the latter

**Figure 2.6 | Total lamprey *VLRB* can be introduced into the EBY100 yeast strain for surface display of recombinant antibodies.** Total lamprey *VLRB* was cloned from immunized lamprey larvae for yeast surface display. This figure depicts the process.

**a** | Into mature *VLRB* sequences (green), we introduced sequences homologous [depicted in red and grey (HA tag)] to the yeast surface display vector pCTCON2-N1.

**b** | Linearized vector [black, also encodes Aga2p agglutinin component (lime)] and amplified *VLRB* inserts derived from animals were electroporated into the EBY100 yeast strain.

**c** | The EBY100 auxotrophic strain of yeast is amenable to selection and endogenously expresses Aga1p (pink). EBY100 has the intrinsic ability to efficiently repair gaps such as those we introduced into the pCTCON2-N1 vector. The linearized vector is mended through recombination (depicted as dashed crosses) with inserts.

**d** | Aga2p-linked proteins are thus introduced into the yeast and compatible for surface display through disulfide linkage to Aga1p.

**e** | Through the display of VLRB upon the yeast surface, the affinity of the receptor for any tagged antigen can be tested because of compatibility with flow cytometry-based assays and techniques. Screening procedures such as cell-based selection, separation, and enrichment procedures are also enabled by the yeast scaffold.

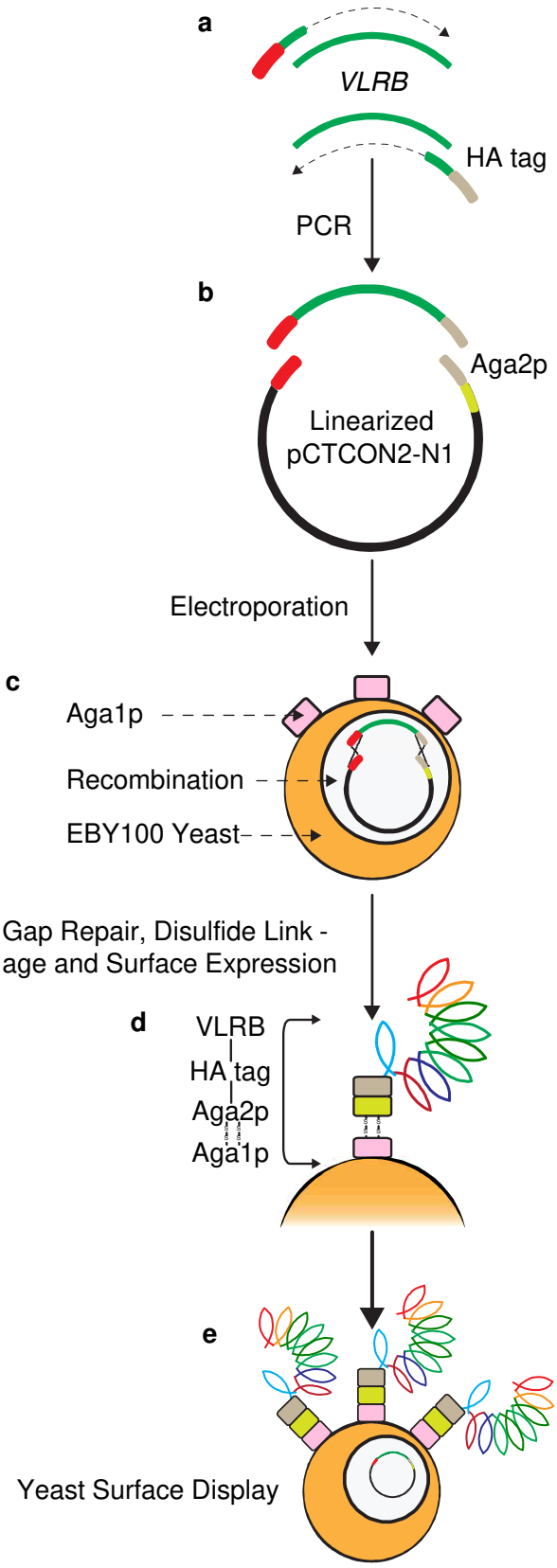

via recombination with the former, *VLRB* secondary amplicons (**Fig. 2.6c**). Thus, VLRB libraries were generated independently using cDNA derived from individual immunized animals. Together, we were able to construct a library with an estimated combined size of 2.5 million independent yeast clones. The same procedure was undertaken to transform EBY100 yeast with negative control VLR4, a monoclonal VLRB antibody reactive to the BclA antigen of *Bacillus anthracis* exosporium coat protein. Following galactose induction, it is noted that, as observed by ourselves and others (42, 43), whether in polyclonal or monoclonal yeast, a subpopulation of yeast cells are consistently non-inducible for cell surface expression of the transgene. We nonetheless determined that transformed yeast libraries and monoclonal *VLR4*-transfected yeast both successfully expressed surface VLRB antibody (**Fig. 2.7**).

Screening of YSD libraries generally requires either a known antigen, an antigen which can be fluorescently labeled, or one which can be immobilized for selection of reactive antibody clones. To isolate VLRB antibody clones reactive to unknown antigen, we biotinylated total serum antigen and, via Western blot analysis, we subsequently demonstrated that biotin labeling was comparable between independent human specimens (**Fig. 2.8**).

VLRB library-transformed cells were incubated with biotinylated breast cancer patient serum antigen in three sequential rounds of magnetic separation, and one round of FACS. Thus, we achieved an approximately 50-fold increase in serum antigen-reactive yeast cells relative to initial libraries (**Fig. 2.9**, top). However, enrichment of breast cancer serum antigen-reactive clones was likewise accompanied by enrichment of clones reactive to antigen derived from healthy donors (**Fig. 2.9**, middle). We did not observe reactivity when libraries were incubated with streptavidin reagent but without antigen exposure, suggesting that positive selection was specific (**Fig. 2.9**, bottom). At both the nascent and ultimate stage (represented by the leftmost and rightmost columns respectively of **Fig. 2.9**), the YSD library was parsed into individual colonies/clones of which over 340 were randomly tested for reactivity to biotinylated human serum antigen. We reasoned that independent VLRB-expressing clones would produce distinguishable binding profiles determined by affinity of antigen receptors

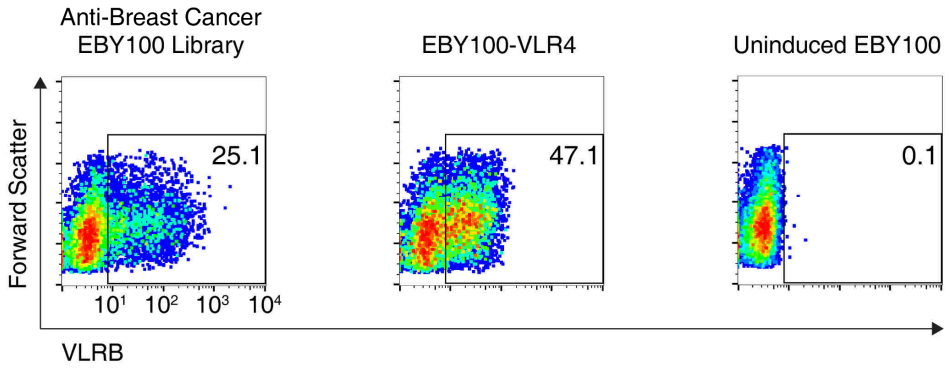


**Figure 2.7 | Induction of VLRB fusion proteins on the surface of *Saccharomyces cerevisiae* EBY100 cells.** Surface-expressed VLRB fusion proteins were detected by flow cytometry using anti-hemagglutinin epitope tag (clone 12Ca5) antibody following a 24-hour culture of yeast in galactose-containing medium. Numbers indicate the percentage of VLRB-expressing yeast cells. Note that even monoclonal yeast such as cultures uniformly encoding control *VLR4* are not 100% inducible at the population level for surface expression.

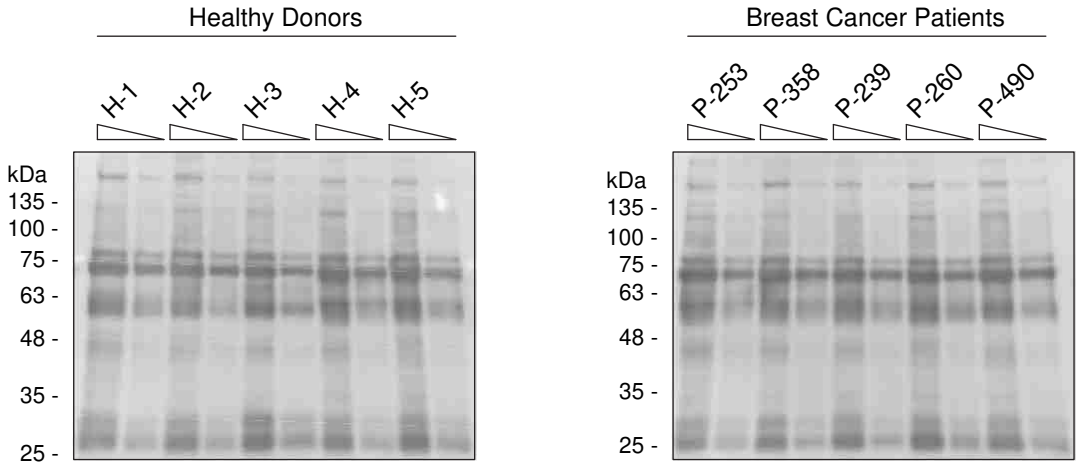


**Figure 2.8 | Biotinylation of individual breast cancer patient- and healthy donor-derived serum antigens.** Shown is a streptavidin-horseradish peroxidase Western blot of independent control and patient plasma/serum specimens that were biotinylated to enable detection and enrichment procedures. The first three samples within each group (H-1, H-2 and H-3 from healthy donors; P-253, P-358, and P-239 from patients) were combined for positive selection and yeast surface display screening purposes. Samples shown here were three-fold diluted.

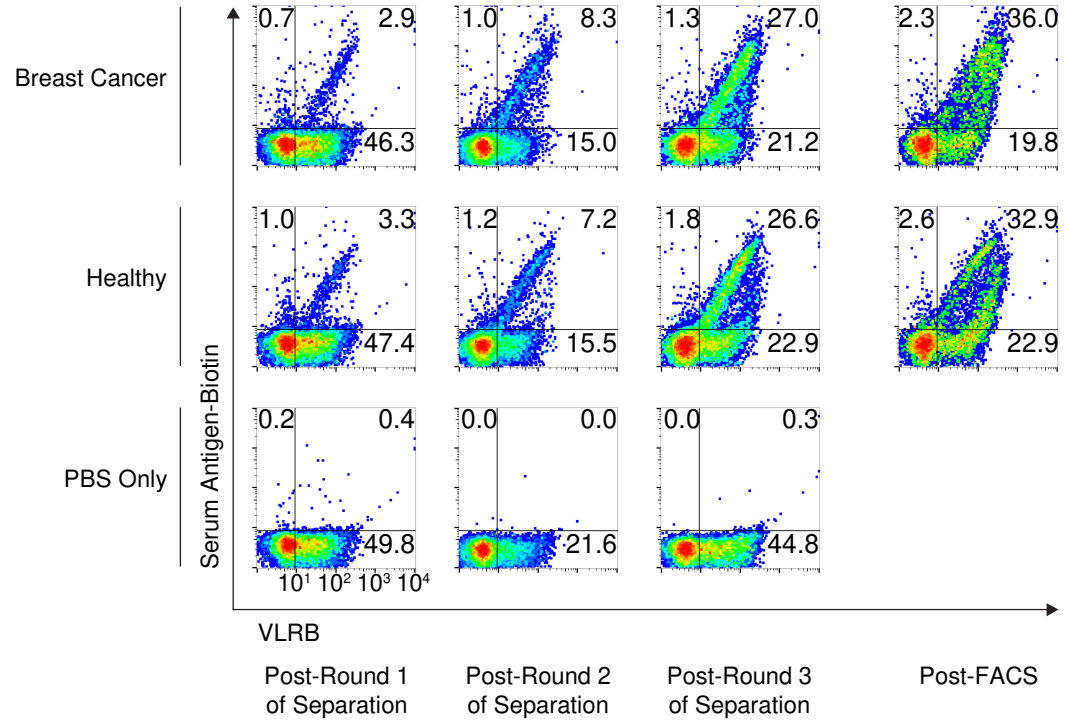


**Figure 2.9 | Positive selection of a breast cancer serum antigen-reactive yeast surface display library.** A compiled yeast surface display library was incubated with biotinylated breast cancer serum antigen. Reactive cells were enriched via anti-biotin magnetic beads in three sequential rounds of magnetic separation, and sorted for VLRB-expressing and antigen-binding yeast clones in an ultimate fluorescence-activated cell sorting (FACS) procedure. The degree of reactivity to breast cancer serum antigen (top row), to serum antigen derived from healthy donors (middle row), or in the absence of antigen (bottom row) was measured by flow cytometry after each round of magnetic separation or FACS. Numbers in the top right quadrant represent the proportion of $VLRB^{+}$ serum antigen-reactive cells. Note that enrichment equally selected for yeast clones reactive to serum antigen derived from healthy individuals.

and concentration of antigen in serum. Disparate binding profiles were observed for several monoclonal VLRBs (**Fig. 2.10a**). Screening and intraclonal juxtaposition of reactivity to breast cancer serum antigen versus healthy donor serum antigen allowed us to remove 51/341 clones which were non-VLRB-expressing despite induction, 99/341 whose antigen receptors were non-reactive, and 149/341 which were serum antigen-reactive but did not discernibly discriminate between human antigen. This last category is represented by monoclonal VLRB JC-AD and VLRB JC-AF in **Fig. 2.10b**. We selected 26 of the 42 remaining clones for sequencing of the VLRB insert. Alignment revealed that 22/26 clones were identical (**Fig. 2.10c**) and the reactivity of this clonotype is represented by VLRB JC-J (**Fig. 2.10b**). VLRBs JC-C, JC-F and JC-J were preferentially reactive to breast cancer patient serum-derived antigen whereas VLRBs JC-B and JC-D preferentially reacted to serum antigen donated by healthy individuals. Among antibodies tested, VLRBs JC-B and JC-D displayed the most disparate binding profiles when comparing binding to the two types of human specimens.

In the wake of the excessive selection/sorting that allowed a single yeast clonotype to pervade in the library, and our inability to distinguish unique VLRBs by subtly different binding profiles, we opted for a different screening approach. In an alternative procedure, library enrichment was limited to two rounds of magnetic separation, culminating in a library consisting of 10 to 15% of cells reacting to breast cancer patient and healthy donor serum antigen (**Fig. 2.11**). Subsequently, *VLRB* inserts were extracted from polyclonal yeast cultures by PCR and cloned into the mammalian expression vector 367HH-SP-ASA. This vector integrates 6-histidine and HA epitope tags for purification and detection (**Fig. 2.12a**). We randomly sampled clones from this resulting library followed by PCR analysis. The variability in number of LRRV inserts suggests that polyclonality was maintained (**Fig. 2.12b**).

Plasmids encoding individual *VLRB* sequences were transfected into HEK293T cells from which VLRB-containing supernatant can be readily used in applications such as ELISA or can be purified by nickel affinity chromatography for applications necessitating higher purity such as immunoprecipitation (IP). Through this approach, multimeric VLRB molecules were successfully detected by Western blot under non-

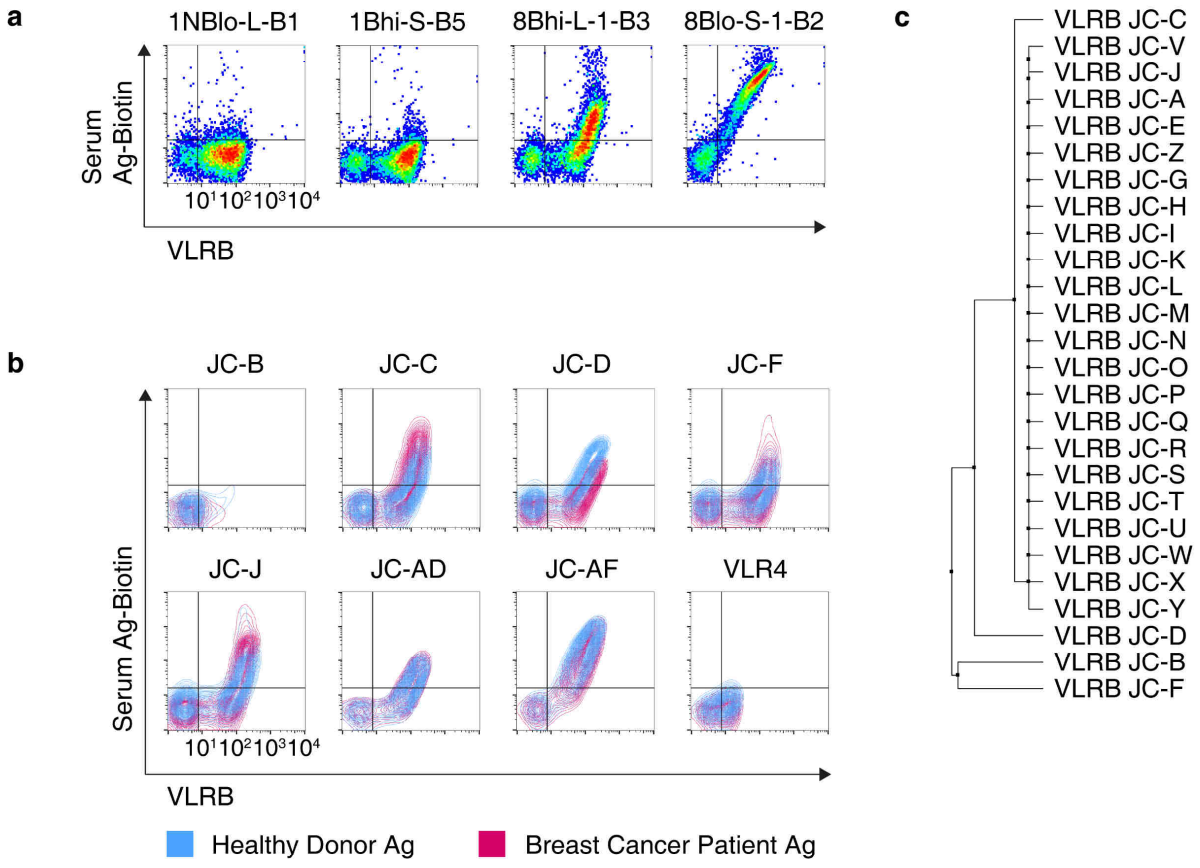


**Figure 2.10 | Monoclonal yeast surface display clones vary in reactivity to serum antigen and display distinct flow cytometry staining profiles. a |** Through the screening of monoclonal yeast surface display (YSD) VLRB-expressing clones, independent yeast/VLRB clonotypes reacted variably despite being incubated with the same human antigen (Ag) specimen. Four VLRB-expressing representative clones illustrate (from left to right) no detectable antigen binding; minimal binding or Ag scarcity; antigen binding achieved only with sufficient VLRB expression; and VLRB expression not being a limiting factor in binding an antigen. **b |** Select monoclonal YSD VLRB clonotypes vary in reactivity and binding profile to breast cancer patient serum antigen versus healthy donor-derived antigen. Correlation between VLRB expression and antigen binding was disparate in clones VLRB JC-B, VLRB JC-C, VLRB JC-D, VLRB JC-F and VLRB JC-J when comparing reactivity to Ag of two different sources whereas VLRB JC-AD and JC-AF bound antigen indistinguishably. Reactivity of negative control monoclonal VLR4 is included. VLRB expression was detected by anti-hemagglutinin tag (clone 12Ca5) staining and binding to biotinylated Ag was detected by a streptavidin reagent. **c |** Sequencing of *VLRB* inserts revealed that 22 candidate clones were identical with their reactivity represented by VLRB clone JC-J in **b**. Average distance phylogenetic tree was constructed using the BLOSUM62 matrix.

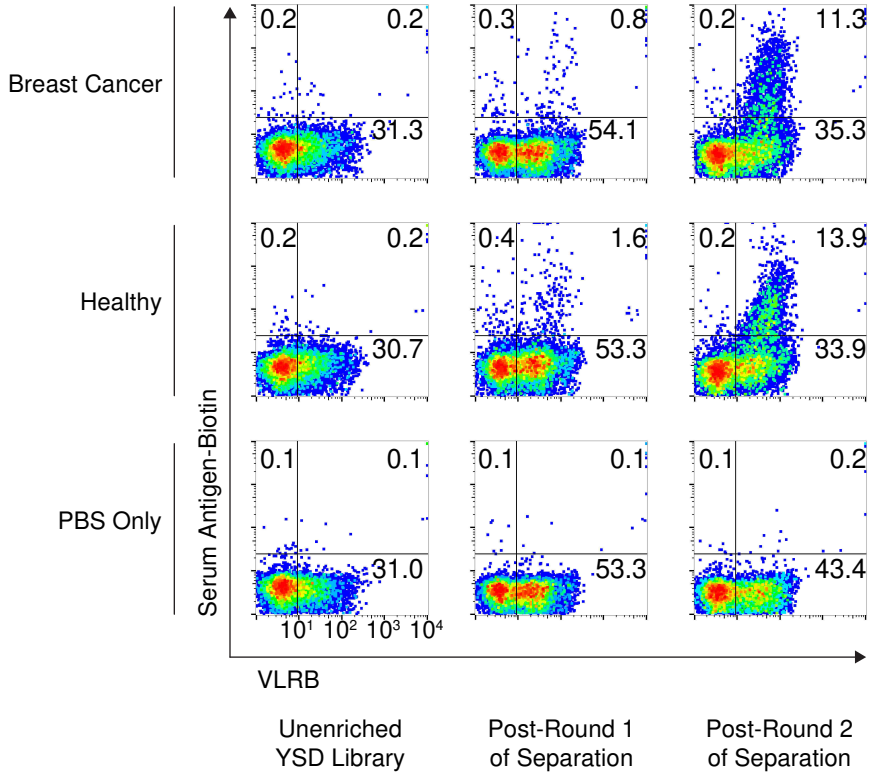


**Figure 2.11 | Limited positive selection of a yeast surface display library for reactivity to breast cancer patient serum antigen.** Yeast surface display library enrichment was performed as described in **Fig. 2.9** but with the overarching protocol limited to two cycles of magnetic separation without a final FACS procedure. Reactivity was measured before enrichment or after each round of magnetic separation. The percentage of VLRB-expressing yeast surface display cells reacting to breast cancer patient serum antigen (top row), healthy donor-derived serum antigen (middle row), or no antigen (PBS only, bottom row) are shown in the top right quadrant of each plot.

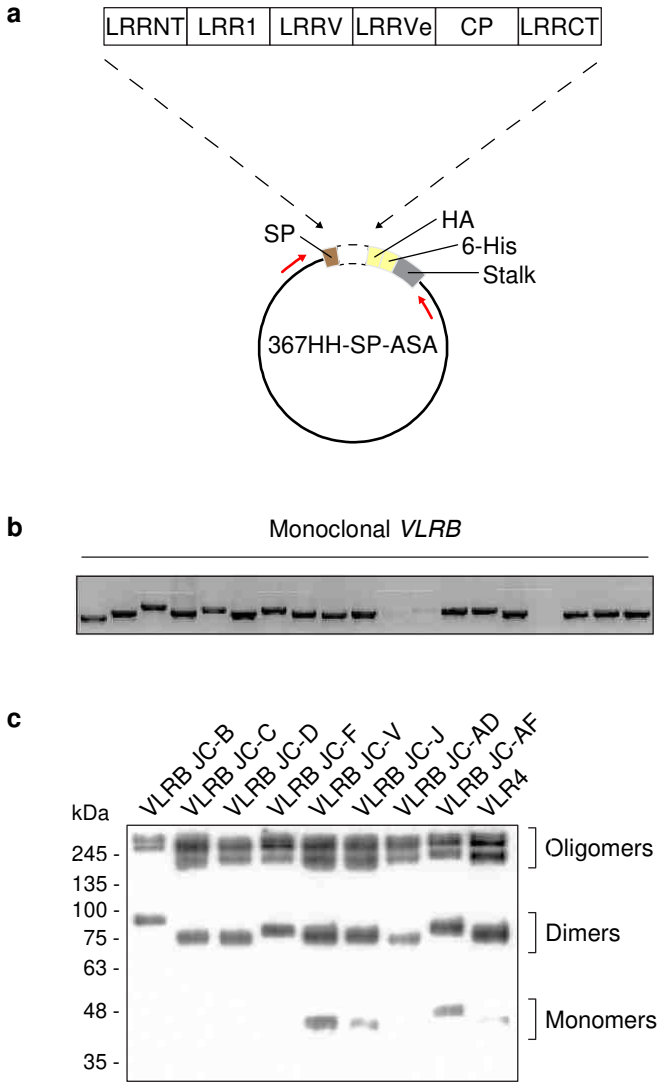


**Figure 2.12 | Purification of several serum antigen-reactive monoclonal VLRB antibodies originating from enriched yeast surface display libraries. a** | For secretion of VLRB antibodies, *VLRB* inserts were molecularly cloned from positively selected yeast surface display libraries into the multiple cloning site (dashed enclosure in the circular vector) of mammalian expression vector 367HH-SP-ASA. The lamprey signal peptide (SP) along with hemagglutinin (HA) epitope and 6-histidine (6-His) tags are labeled on 367HH-SP-ASA and incorporated into *VLRB* inserts. **b** | Colony PCR was performed on 19 randomly selected clones using oligonucleotides flanking the invariant regions of *VLRB* inserts (depicted as red arrows in **a**). Note the length differences which reflect variation in the number of LRRV inserts incorporated into mature *VLRB* and the overall library complexity. **c** | Select serum antigen-specific or control VLR4 recombinant antibodies were purified by nickel affinity chromatography. Shown is a 4C4 (anti-VLRB) immunoblot of non-reduced protein. Note the size disparity reflecting the number of LRRV inserts, and that the majority of disulfide-linked high molecular weight multimers are maintained.

reducing conditions (**Fig. 2.12c**). To evaluate candidate monoclonal VLRB antibodies that have demonstrated serum antigen reactivity, including the five select VLRB clones isolated from our initial approach (**Fig. 2.10b**), we designed a modified sandwich ELISA in which VLRB antibodies are used to capture biotinylated human serum antigen that is then detected by streptavidin-coupled reagents (**Fig. 2.13**).

The two-dimensional array in **Fig. 2.14** depicts reactivity of independent monoclonal VLRB antibodies to each of 10 biotinylated human serum antigen specimens equally divided into two age- and sex-matched groups: specimens of breast cancer patient or healthy donor origin. Each column represents one human serum antigen specimen and each row represents one monoclonal VLRB antibody. Hierarchical clustering reveals pairs and clusters of monoclonal VLRBs that formulate similar binding profiles (**Fig. 2.14b**).

By measuring reactivity of monoclonal VLRB antibodies to a set of human specimens as well as performing statistical analyses, we determined that the majority of monoclonal VLRB antibodies did not discriminate between antigen of breast cancer patient origin and healthy donor origin. However, the reactivity of four monoclonal VLRB antibodies to antigen from the two sources was significantly different whereas a proceeding group of seven antibodies approached significance (**Fig. 2.15**). Notably, VLRB JC-C and VLRB AL-63 display biphasic staining patterns within the breast cancer category. Importantly, the binding profile of VLRB AL-85 suggests that this antibody reacts with an antigen found in all breast cancer patient serum specimens but absent in all reciprocal specimens originating from healthy donors.

### *2.2.4 Immunoprecipitation of serum antigen using monoclonal VLRB antibodies as affinity reagents*

To associate a VLRB-reactive serum antigen with breast cancer pathology requires identification of the target antigen. Prior studies demonstrated the feasibility of applying VLRBs as affinity reagents for purification and mass spectrometric identification of cell surface protein antigens (41, 58). To explore whether this approach can be adapted toward serum antigens, we used VLRB JC-B for immunoprecipitation of its

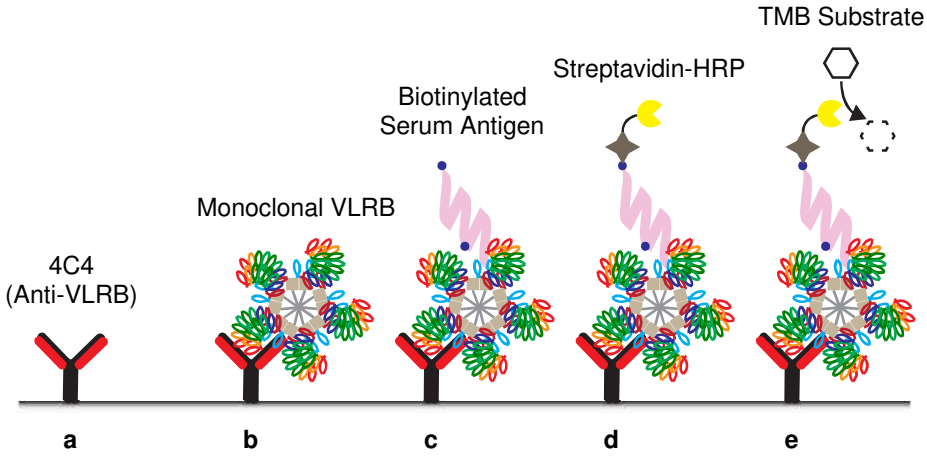


**Figure 2.13 | Design of a sandwich enzyme-linked immunosorbent assay to measure VLRB reactivity to human serum antigen. a** | Anti-VLRB clone 4C4 was first adsorbed to microwells. **b** | The coating of 4C4 is a constant and delimits the subsequent binding of monoclonal VLRB in all wells. **c** | VLRB serves as the capture antibody for biotinylated serum antigen with biotin depicted as blue circles. **d** | Detection of any bound serum antigen was achieved using streptavidin-horseradish peroxidase (HRP). **e** | Addition and oxidation of the TMB substrate allows a quantitative comparison of VLRB reactivity to independent human serum antigen specimens between monoclonal VLRBs.

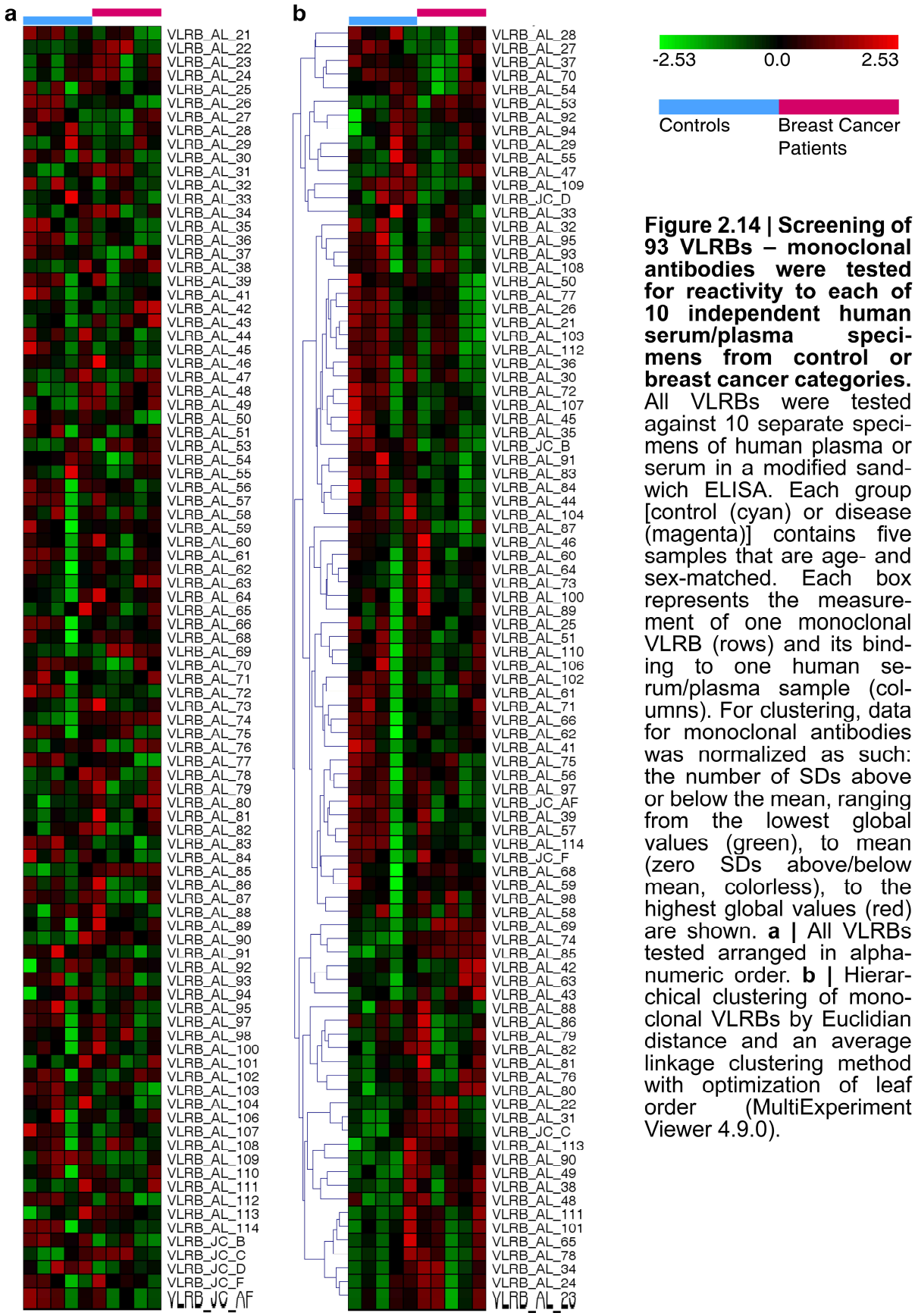


**Figure 2.14 | Screening of 93 VLRBs – monoclonal antibodies were tested for reactivity to each of 10 independent human serum/plasma specimens from control or breast cancer categories.** All VLRBs were tested against 10 separate specimens of human plasma or serum in a modified sandwich ELISA. Each group [control (cyan) or disease (magenta)] contains five samples that are age- and sex-matched. Each box represents the measurement of one monoclonal VLRB (rows) and its binding to one human serum/plasma sample (columns). For clustering, data for monoclonal antibodies was normalized as such: the number of SDs above or below the mean, ranging from the lowest global values (green), to mean (zero SDs above/below mean, colorless), to the highest global values (red) are shown. **a |** All VLRBs tested arranged in alpha-numeric order. **b |** Hierarchical clustering of monoclonal VLRBs by Euclidian distance and an average linkage clustering method with optimization of leaf order (MultiExperiment Viewer 4.9.0).

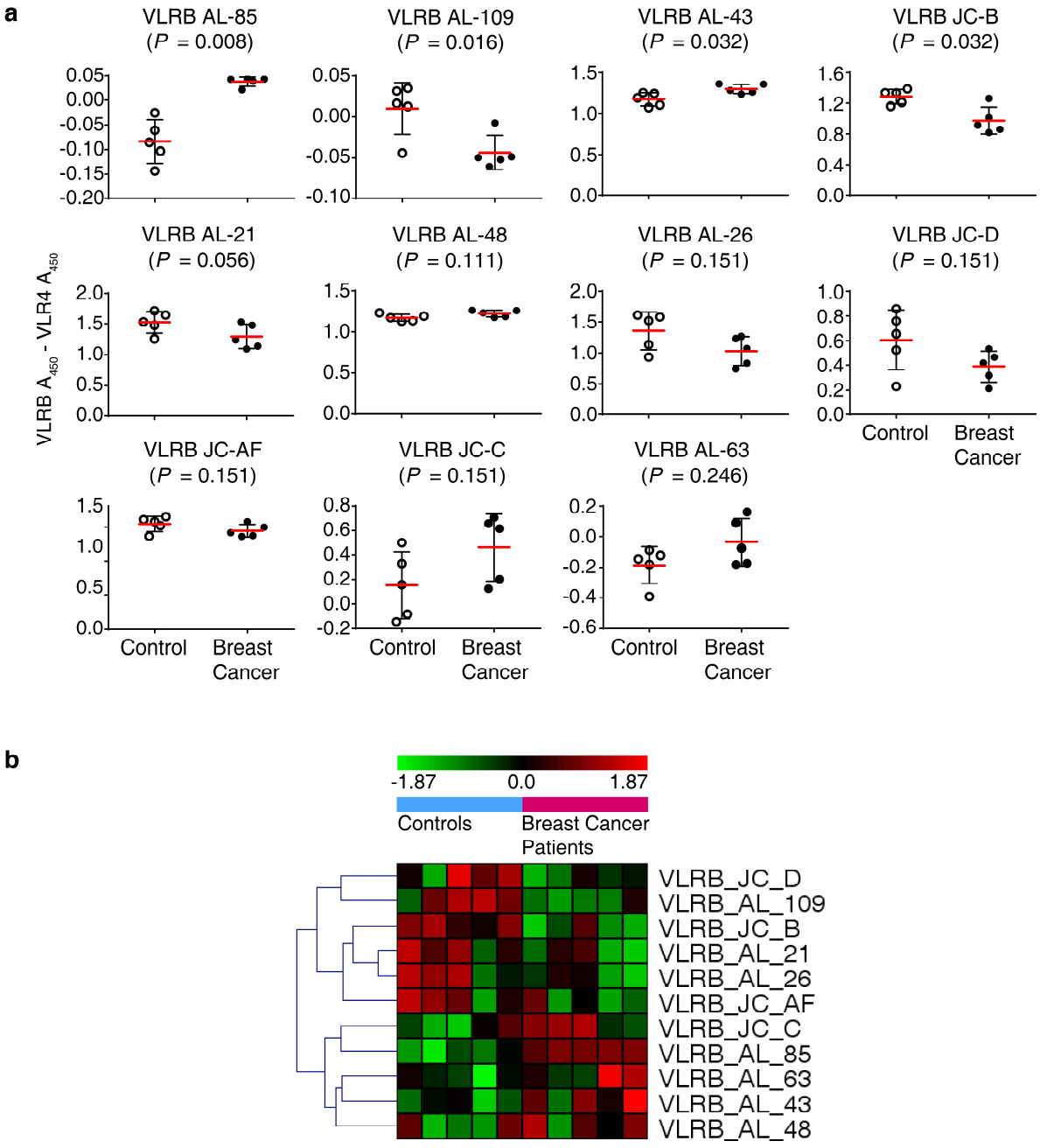


**Figure 2.15 | Monoclonal VLRB antibodies can differentiate human samples of breast cancer origin from those of healthy individuals.** Using a modified sandwich enzyme-linked immunosorbent assay (ELISA), we measured VLRB antibody reactivity to human serum antigen. Shown are background-corrected (subtraction of VLR4 negative control signal) ELISA readings. Using each human sample as a measurement, we determined whether the means were significantly different between VLRB antibody binding to control and disease specimens. **a |** Select VLRBs displaying significantly ($P < 0.05$) or near significantly different means ($0.05 < P < 0.25$) between groups are shown. Red lines depict means +/- standard deviation (black error bars). Statistical significance was determined with the Mann-Whitney U test. Note the different y-axis scales reflecting the disparate binding magnitudes of VLRB antibodies. **b |** Hierarchical clustering (as described in **Fig. 2.14**) of the 11 candidate monoclonal VLRB antibodies.

cognate antigen from healthy donor serum. Only in a condition containing serum-reactive VLRB JC-B, but not those containing negative control VLR4 nor conditions in which VLR antibody was omitted, was a 75 kDa protein detectable by immunoblotting (**Fig. 2.16a**). Similarly, the 75 kDa candidate antigen was detected when visualizing sodium dodecyl sulfate polyacrylamide gel electrophoresis (SDS-PAGE)-separated immunoprecipitate by a total protein stain (**Fig. 2.16b**). These experiments demonstrate the specificity of VLRB-antigen interactions and suggest that monoclonal VLRB antibodies are applicable toward serum biomarker purification and identification.

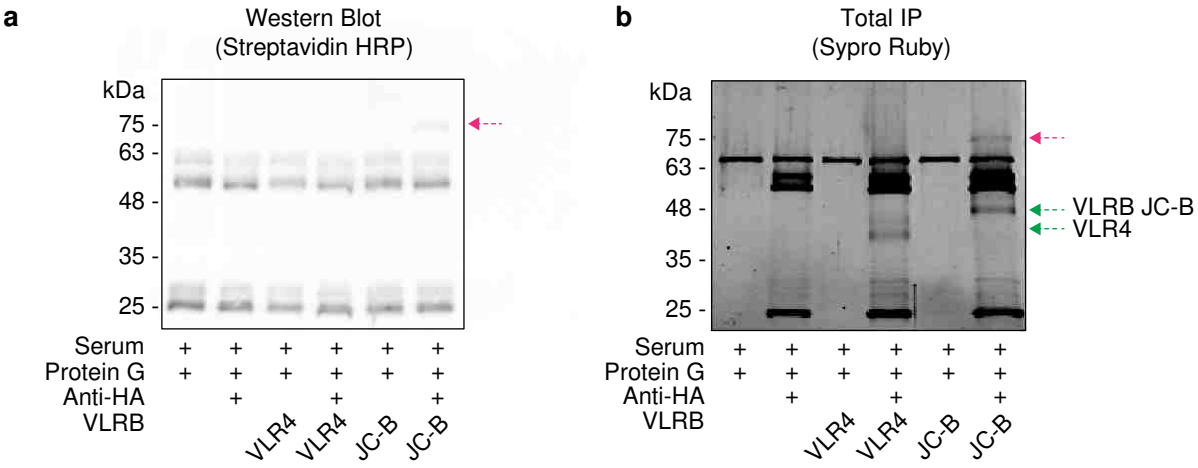


**Figure 2.16 | Serum-reactive monoclonal VLRB JC-B specifically immunoprecipitates a 75 kDa antigen.** VLRB JC-B or negative control VLR4 were incubated with human albumin- and IgG-depleted serum antigen derived from a healthy donor. VLRB was captured by mouse anti-hemagglutinin (HA) epitope tag antibody (clone 12Ca5) and protein G. Immunoprecipitate (IP) was reduced, denatured, and resolved by SDS-PAGE before detection by **a** | streptavidin reagents in Western blot for detection of co-immunoprecipitated biotinylated serum antigen or **b** | Sypro Ruby stain for detection of co-immunoprecipitated non-biotinylated serum antigen (Total IP). The purified 75 kDa antigen is indicated by red arrows whereas pulled down immunoprecipitating VLRBs are indicated by green arrows and detectable only when visualizing total protein.

## 2.3 Discussion

Here, we evaluated the prospect of applying VLRB antibodies of the evolutionarily distant sea lamprey as a novel class of reagents towards the discovery of human serum biomarkers. In addition to being collected non-invasively, serum and circulating markers can support detection, diagnosis, prognosis, post-treatment monitoring, and therapeutic intervention of disease. Through this endeavor, we discovered several promising monoclonal VLRB antibodies. The identity and nature of the antigens/epitopes recognized and their capacity to accurately stratify disease and health must be determined.

Previous studies have noted the proclivity of the lamprey larval immune response to particulate antigen (15, 32, 41, 58) whereas responses directed toward soluble antigen were weak (15, 32). In this study we overcame this constraint by the chemical crosslinking of soluble antigens to the surfaces of carrier cells lines and leveraging the antigenicity of these human cells. Whether targeting a single-antigen preparation of the model antigen CD130 or a complex mixture of human serum antigen, we elicited an adaptive immune response to both antigen preparations after coupling them to carrier cells (**Figs. 2.2** and **2.5**). However, VLRB antibody titers were weak when compared to those elicited by particulate antigens such as mammalian erythrocytes or viral particles (32, 40) suggesting that the majority of animal responses were directed toward carrier cell endogenous surface antigen. The artificial and dispersed coupling of the over 10,000 human serum proteins (84) likely did not recapitulate the valency nor the density of known immunogenic endogenous antigens: the surface antigens HLA class I and CD38, respectively bound by monoclonal VLRB antibodies N8 (**Chapter 3**) and MM3 (58), are known to be highly expressed on their VLRB-reactive B cell subsets (85). Furthermore, detection of serum antigen binding was likely also hampered by incomplete or limited biotinylation. Thus, the measurement of seroreactivity from the polyclonal repertoire of immunized animals was likely an underestimate reflecting only the detectable portion of bound antigen rather than total bound antigen.

In contrast to mammalian antigen receptors of heavy and light chain composition, VLR antibodies are generated by iteration of a single gene and are uniquely suited for screening *en masse* using display technologies such as YSD. Magnetic separation and FACS approaches are dependent on antigens targetable for positive selection/enrichment which are correspondingly determined by the degree of biotinylation. A disadvantage of this approach is that 20-50% of transformed yeast, whether monoclonal or polyclonal, could not be induced for VLRB surface expression (**Fig. 2.7**). Therefore, depletion strategies targeting clones with reactivity to healthy donor-derived serum antigen would preserve this population of *VLRB*-encoding but surface VLRB-non-expressing cells. We attempted to compensate for this caveat by preincubation of YSD libraries with non-biotinylated serum antigen prior to addition of labeled breast cancer patient antigen. This proved ineffective, as evidenced by the large number of monoclonal VLRB antibodies reacting to both antigens derived from breast cancer patient serum and healthy donor serum. This can likely be explained by the level of recombinant VLRB expression upon the yeast surface, numbering approximately 10,000 per cell (86), which could not be saturated especially when this valency is extrapolated to an entire culture/library. The inevitability of yeast binding to both healthy control and experimental antigen led us to hypothesize that if we let it be without attempting to preoccupy surface receptors, we could apply a novel FACS approach for biotin-based enrichment. By measuring two dimensions of reactivity, namely reactivity to control and breast cancer patient antigen that are each labeled differentially with distinct fluorochromes, can we specifically sort out yeast that are disproportionately positive to healthy or breast cancer patient antigen? Ideally, double-positive yeast would be disregarded, and only mono-reactive clones labeled with a single fluorochrome would be sorted, and their VLRB antibodies retrieved for analysis.

The majority of the 93 monoclonal VLRB antibodies screened did not differentiate healthy control and breast cancer patient specimens. However, select VLRB antibodies accurately stratified patient specimens from healthy donor specimens while achieving statistical significance or approaching it (**Fig. 2.15a**). Despite these promising results, only limited conclusions can be drawn from 10 human specimens of only

two categories. Whether for single- or multi-variable statistical analyses, measurements/number of specimens should outnumber predictors (VLRB antibodies) at least 15:1 to avoid overfitting and chance observations (87). For multinomial analyses, human sera from additional categories must be acquired. Much like how rheumatoid arthritis specimens are a control for those originating from systemic lupus erythematosus (SLE) patients, more accurate controls for breast cancer patient sera would be sera donated by patients with benign breast lesions or from those with mastitis/breast infection. Moreover, circulating antigen can originate from more nuanced categories (instead of crude 'breast cancer' or 'control' as dependent variables). VLRB candidates can be tested on patient samples and correlated with patient and tumor characteristics such as menopause status, stage/invasiveness/lymph node status, p53 expression, and tumor growth receptor expression.

Several candidate VLRB antibodies displayed differential and readily detectable signals in reactivity to serum antigen (**Fig. 2.15**). Protein antigens recognized by VLRB AL-43 and VLRB JC-B may therefore be increased or decreased in abundance, respectively, in breast cancer patients compared to healthy individuals. Alternatively, signals may be altered by differential post-translational modification such as glycosylation as occurs in malignancy (78, 80, 81) for which detection can benefit from VLRB antibodies and their unique properties (37). Differentially binding monoclonal VLRB antibodies such as VLRB AL-85 on the contrary display faint but reproducible binding to antigen from breast cancer patient serum but not from healthy donors. These comparatively weak signals may reflect circulating markers induced by pathology, as opposed to serum antigen such as VEGF that is present under homeostasis (88). It is tempting to speculate that known antigen such as HER2 or CA15-3 shed from tumor cells (65) or as-yet-unidentified antigen may be selectively displaced from malignant cells and therefore also serve as a potential therapeutic target for an anti-serum antigen monoclonal VLRB antibody. Breast cancer differs by stage, histological type, subtype/hormone receptor expression, as well as polymorphism in patient immunity and antigen presentation. Therefore, the biphasic binding to breast cancer patient antigen by VLRB JC-C and VLRB AL-63 may indicate the stratification of patient subsets.

Previous studies have highlighted the unique antigen recognition characteristics of VLRB antibodies (36, 37, 58). While the identification of a single pan-breast cancer-specific biomarker shared by all patients is unlikely, our study demonstrates the applicability of VLRB antibodies for the detection and identification of serum biomarkers with potential for diagnosis, prognosis, or monitoring of not only breast cancer patients, but also patients suffering from other malignancies or autoimmune diseases.

.

## 2.4 Materials and Methods

### *2.4.1 Human serum/plasma antigen specimens*

Human plasma from five triple-negative breast cancer patients (P-253, P-358, P-239, P-260, and P-490) were generously donated by Dr. Réjean Lapointe [Centre de recherche du Centre hospitalier de l'Université de Montréal (Montréal, Québec, Canada)]. These samples were respectively age-matched to healthy donor plasma. All specimens were collected after having obtained written informed consent from the donor.

### *2.4.2 Preparation of immunogen*

For compatibility with downstream applications, whole patient plasma was first dialyzed against a 500 to 1,000-fold excess (volume) of phosphate-buffered saline (PBS) overnight, at 4°C. This was done with the D-Tube Dialyzer Maxi from MilliporeSigma (3.5 kDa MWCO, St. Louis, MO, USA).

For IgG and albumin depletion, we used the Qproteome Albumin/IgG Depletion Kit (Qiagen, Hilden, Germany) while applying three times more plasma than recommended (we included plasma in equal parts from patients P-253, P-358, and P-239) to each depletion column. Otherwise, we performed the protocol as recommended. Depletion was verified by GelCode Blue Stain Reagent (Thermo Fisher Scientific, Waltham, MA, USA). For equal comparison of the GelCode Blue stain, an aliquot of whole pooled plasma (representing 'no depletion') was diluted such that its volume matched that of the sample after depletion (the depletion protocol dilutes plasma about ten-fold). Whenever necessary, antigen was quantified via the BCA Assay Kit (Thermo Fisher Scientific, Waltham, MA, USA).

These depleted patient antigen samples were then linked to carrier cells via a two-step protein coupling reaction. Firstly, EDC and Sulfo-NHS (Thermo Fisher Scientific) were used to activate cell surface carboxyl groups to form an amine-reactive intermediate. For every 20 million cells, we used 0.4 mg/mL of EDC and 1.1 mg/mL of Sulfo-NHS in 100 mM MES, 150 mM NaCl, pH 6.0 buffer. After a 15-min ambient

temperature incubation, 1.4 µL of 2-mercaptoethanol per mL of cell suspension was used to quench the reaction and prevent activation of the carboxyl groups in target antigen proteins. After PBS washes, we resuspended the activated cells in recombinant protein solution (up to 2 mg/mL diluted in PBS) and incubated for two hours at ambient temperature. Finally, the reaction was quenched with 20 mM Tris, pH 7.0 for 15 min, cells were washed with PBS. The procedure was conducted according to the manufacturer's instructions except for the first protein source being carrier cell surface integral and peripheral proteins rather than a pure protein binding partner. A parallel reaction with monoclonal antibody 413D12 was performed with each coupling of human antigen to cell lines (**Fig. 2.1b**).

### *2.4.3 Lamprey larvae immunization*

We experimented exclusively on non-metamorphosed lamprey larvae, specifically the species *Petromyzon marinus*. Wild animals were captured from the tributaries of Lake Michigan (Lamprey Services, Ludington, MI. USA). Animals ranging from 60 to 120 mm in length were kept in captivity as approved by the animal care committee of the University of Toronto. Animals were housed in aquariums containing air stone-aerated water (kept at a constant ~18°C). The bedding consisted of very fine sand to mimic natural habitats and to allow the species-specific behavior of burrowing. Animals were fed brewer's yeast on a weekly basis.

Animals were first anesthetized with a solution of 0.1 g/L of tricaine mesylate, 0.14 g/L of $NaHCO_3$ in non-distilled water for 5 min. For each lamprey larva, we intracoelomically injected ten million patient antigen-linked antigen-displaying cells suspended in 66.6% PBS (isotonic to animal bodily fluid). Various immunization schedules were attempted and are outlined in **Fig. 2.4**. The T cell leukemia Jurkat, Burkitt's lymphoma Daudi, and breast adenocarcinoma MDA-MB-231 (a generous gift from the laboratory of Dr. Maria Rozakis Adcock) were included in immunizations. All cell lines used in this study were cultured at 37°C and incubated in 5% $CO_2$. We killed animals using a ten-fold concentration of the anesthetic before severing and exsanguinating animals. Animal blood was collected in 66.6% PBS with 1.5 to 3 USP units of heparin rather than EDTA.

### *2.4.4 Isolation of animal plasma and cloning of total lymphocyte VLRB*

From each animal, we harvested around 0.2 mL of whole blood. Lymphocytes were isolated by density centrifugation in 55% Percoll in 66.6% PBS and the buffy coat collected. The animal plasma was diluted for VLRB capture in ELISA as described (**Fig. 2.3**) before detection with the 1-Step Ultra TMB-ELISA Substrate Solution (Thermo Fisher Scientific, Waltham, MA, USA).

Lamprey lymphocytes were spun down at 3,000 *g* and we followed the manufacturer's protocol for homogenization using the QIAshredder and RNeasy Mini Kit (both sourced from Qiagen, Hilden, Germany). All steps up to this point should be sufficient to exclude anticoagulant from downstream reactions. SuperScript II or SuperScript III Reverse Transcriptase (Invitrogen, Carlsbad, CA, USA) were the systems of choice for purification of total lymphocyte cDNA. Random hexamer primers were used for the reverse transcription of 500 ng of starting RNA material. Primers 645 and 646 (*2.4.13*) were used to amplify total *VLRB* through 20 cycles of PCR.

### *2.4.5 Biotinylation of human serum/plasma antigen*

To enable detection of human circulating antigen using streptavidin reagents, we covalently linked plasma and serum (whole or depleted) to biotin using EZ-Link Sulfo-NHS-LC-Biotin (Thermo Fisher Scientific, Waltham, MA, USA). This procedure was conducted according to the manufacturer's instructions using two-hour labeling in ice. Reagents were proportioned for a 1 to 5 mg/mL solution of a 75 kDa protein (an approximation for the heterogeneous protein mixture in serum), and we used a 20-fold molar excess of biotin. After this step, we performed dialysis anew as described in *2.4.2*, to remove excess biotin that was not covalently linked. Samples were denatured in 1% sodium dodecyl sulfate (SDS) 10% glycerol, 20 mM Tris pH 6.8 sample buffer. Successful biotinylation was assessed by immunoblotting with streptavidin-horse radish peroxidase (HRP) (**Fig. 2.5**) and imaged with the DNR Bio Imaging Systems (Neve Yamin, Israel) MicroChemi 4.2. Samples were diluted in PBS 1% bovine serum albumin (BSA) for use or storage (at -20°C).

### *2.4.6 Generating yeast surface display libraries*

For YSD, we worked exclusively with EBY100 (89), an auxotrophic strain of *Saccharomyces cerevisiae*. Relevant features include the inability to biosynthesize tryptophan due to a prematurely terminated *trp1*, and a galactose-inducible *Aga1p* gene, a subunit of the yeast cell mating molecule α-agglutinin. We modified the pCTCON2 vector for the surface display of N-terminus-exposed polypeptide chains – the pCTCON2-N1 vector was designed to fuse C-termini of inserted *VLRB*s to yeast galactose-inducible *Aga2p*. The Aga2p-fused chain is linked to the membrane-bound Aga1p subunit via disulfide bonding and will display VLRBs in their natural orientation. We selected for autotrophic transformed yeast expressing pCTCON2-encoded *trp1* by incubation in tryptophan-deficient medium.

| YPD | Mass per 100 mL of Sterile ddH2O |
|---|---|
| Peptone | 2 g |
| Yeast Extract | 1 g |
| Dextrose* | 2 g |

Prior 645/646-amplified *VLRB* libraries were subjected to another 20 cycles of PCR amplification with oligonucleotides 661 and 662 (*2.4.13*). These prospective inserts were then co-electroporated into EBY100 along with NheI- and AgeI-linearized pCTCON2-N1 according to the protocol pioneered by Chao et al. (83) but with 2 µg total of DNA consisting of a vector:insert ratio of 1:36 (assuming that inserts are 700 bp on average). Animal total lymphocyte cDNA were kept separate throughout the process but combined after YSD library generation for subsequent magnetic separation or FACS. Electroporated yeast were either kept in solution in bulk or serially plated to isolate monoclonal yeast. Yeast solutions and plates were stored at 4°C short-term (1-3 months) for experimentation.

YPD was used as a non-selective yeast growth medium consisting of amino acids essential to yeast. Synthetic dextrose plus casein amino acids (SDCAA) was used as a tryptophan-deficient medium containing dextrose for optimal yeast growth

whereas SGCAA was used for inducing recombinant protein expression with 95% of the dextrose in SDCAA replaced with galactose to induce the GAL promoter.

| SDCAA | Mass per 100 mL of Sterile ddH2O |
|---|---|
| $Na_2HPO_4$ | 0.54 g |
| $NaH_2PO_4$ | 0.86 g |
| Dextrose* | 2 g |
| Yeast Nitrogen Base* | 0.67 g |
| Casamino Acids* | 0.5 g |

| SGCAA | Mass per 100 mL of Sterile ddH2O |
|---|---|
| $Na_2HPO_4$ | 0.54 g |
| $NaH_2PO_4$ | 0.86 g |
| Galactose* | 1.9 g |
| Dextrose* | 0.1 g |
| Yeast Nitrogen Base* | 0.67 g |
| Casamino Acids* | 0.5 g |

We cultured yeast at 30°C in aerobic conditions whereas induction was at ambient temperature. For induction, monoclonal yeast colonies were picked and incubated in 0.5 mL of SGCAA overnight. For induction of yeast libraries, cultures in SDCAA starting at an $OD_{600}$ of 0.1 at most were grown until cultures reached an $OD_{600}$ of 1 to 3. Next, induction in SGCAA was as above but at a starting $OD_{600}$ of 0.5.

### *2.4.7 Magnetic separation and FACS of YSD libraries*

YSD libraries were enriched using the EasySep Biotin Positive Selection Kit from Stemcell Technologies (Vancouver, BC, Canada) according to the manufacturer's instructions. However, we used biotinylated depleted patient plasma (50 µg/mL) instead of biotinylated antibody as a target. To ensure equal representation of

* added last as a sterile-filtered portion after the rest of the solution is autoclaved.

diverse clones that make up the library, we always initiated separation with a ten-fold excess of yeast cells relative to calculated starting library size.

### *2.4.8 Purification of monoclonal VLRBs*

Oligonucleotide pairs 645 and 658 (*2.4.13*) were used to extract monoclonal *VLRB*s from yeast. *VLRB*s were separately cloned into the 367HH-SP-ASA vector – based on the pIRESpuro2 vector but reintegrating the lamprey signal peptide for secretion and the invariant VLRB stalk for detection and multimerization; incorporating a 6-histidine and an HA tag for purification and detection, respectively; mutated and therefore immunized against NheI star activity.

Constructs were transfected into HEK293T cells which served as a mammalian expression system. We used the polyethylenimine (PEI) method for transfection using a 3:1 (mass:mass) ratio of PEI:DNA. Cells were selected with 1 µg/mL of puromycin. We harvested total supernatant which was separated from cell debris and stray 293T cells by centrifugation at 250 *g* with prolonged deceleration. Dulbecco's modified Eagle's medium-based HEK293T supernatant was buffer-exchanged with PBS using the Pellicon XL Cassette (30 kDa MWCO) from MilliporeSigma (St. Louis, MO, USA). Filtrate below the MWCO was near-completely eliminated at least twice, each instance bringing about addition of 1 volume (relative to the starting supernatant) of PBS into the system. Finally, retentate was concentrated to 10 to 20% of the original volume. Supernatant was then vacuum-filtered in Corning (Corning, NY, USA) 500 mL Filtration Systems (0.22 µm, sterilizing and low protein-binding).

For each litre of supernatant, we supplemented with 5 mM imidazole and we captured 6-histidine tag-VLRBs using 1.5 to 2 mL (packed volume) of Ni-NTA Agarose beads (Qiagen, Hilden, Germany) at 4°C. Beads were then washed once with 10 mM imidazole in PBS, once with 420 mM NaCl, 20 mM imidazole in PBS, and bound protein was eluted with 250 mM imidazole in PBS. Samples were then dialyzed overnight against PBS at 4°C using 10,000 MWCO SnakeSkin Dialysis Tubing (Thermo Fisher Scientific, Waltham, MA, USA).

We concentrated samples using the 30 kDa MWCO Vivaspin 6 tubes (GE Healthcare, Chicago, IL, USA) or Corning (Corning, NY, USA) Spin-X UF 6 10 kDa MWCO tubes according to the manufacturer's instructions. Purified material was denatured as described in *2.4.5* and evaluated with GelCode Blue Stain Reagent or 4C4 immunoblotting. Purified VLRB was stored in 0.5% $NaN_3$ at -80°C long-term.

### *2.4.9 Flow cytometry or ELISA screening of monoclonal VLRBs*

Yeast induced overnight were then incubated with 100 µg/mL of complete biotinylated pooled human serum/plasma. Excess human serum/plasma antigen was washed away before yeast were co-stained with streptavidin-phycoerythrin (PE) and anti-HA tag 12Ca5- fluorescein isothiocyanate. Data was acquired on the Guava easyCyte 6HT (MilliporeSigma, St. Louis, MO, USA).

ELISA microplates were coated overnight at 4°C with anti-VLRB 4C4. Excess coating antibody was washed away with PBS 1% BSA. Subsequent steps were all conducted at ambient temperature. Wells were blocked with PBS 7% milk for two hours. The blocking solution was washed and replaced with monoclonal VLRB antibody (at 5 µg/mL in PBS 1% BSA) that was allowed to bind to 4C4 for an hour. Excess VLRB antibody was also washed and, subsequently, biotinylated non-depleted serum/plasma (at 10 µg/mL) was exposed to coated wells for an hour. The wells were ultimately rinsed and the penultimate reagent, streptavidin-HRP, was added and maintained for an hour. After the final wash, we detected bound streptavidin-HRP with the TMB Substrate Kit (Thermo Fisher Scientific, Waltham, MA, USA) according to the manufacturer's instructions. The reaction was brought to a halt with 2M $H_2SO_4$ after 5 to 10 min, and the absorbance at 450 nm measured using the Multiskan Go (Thermo Fisher Scientific, Waltham, MA, USA).

### *2.4.10 Immunoprecipitation of human serum antigen bound by a monoclonal VLRB antibody*

IP of serum antigen was performed on the biotinylated and albumin- IgG-depleted serum from individual H-3. We firstly cleared serum of components binding non-specifically to protein G sepharose beads via a one-hour incubation with the beads at

4°C. Beads were spun down and the cleared supernatant was collected for a subsequent overnight 4°C IP using 2 µg of VLR antibody, 5 µg of anti-HA (clone 12Ca5) and fresh beads. 25 µL of a 50% protein G sepharose bead slurry was used in both the clearing procedure and IP.

After the overnight IP, beads were washed thrice with PBS and twice with PBS 0.1% Triton X-100 prior to denaturation in reducing SDS sample buffer described in *2.4.5* but further supplemented with 10% 2-mercaptoetthanol and 50 mM dithiothreitol (DTT). Samples were resolved by SDS-PAGE after which immunoprecipitate was detected by streptavidin-HRP immunoblotting or via Sypro Ruby Protein Gel Stain (Molecular Probes, Eugene, OR, United States) according to the manufacturer's 'Basic Protocol'. When following this protocol, we used non-biotinylated starting material for IP. Sypro Ruby stain was visualized with the Bio-Rad (Hercules, CA, United States) ChemiDoc.

### *2.4.11 Data and statistical analyses*

Flow cytometry analyses were performed using FlowJo V10 (FlowJo). We performed ELISA analyses using GraphPad Prism Version 6.01.

Average distance phylogenetic tree was constructed with the BLOSUM62 matrix on Jalview 2.10.4. Input sequences were derived from sequencing oligonucleotides 723 and 724 (*2.4.13*) specific to vector regions of mammalian expression vector 367HH-SP-ASA.

We performed hierarchical clustering using MultiExperiment Viewer 4.9.0 (90).

Serum/plasma specimens were not considered paired for the purpose of statistical analysis. The means of the reactivity of individual VLRBs to breast cancer patient serum antigen versus healthy donor antigen were compared using the Mann-Whitney U test.

### *2.4.12 Antibodies and affinity reagents*

| Clone, Affinity Portion, and Fluorochrome | Specificity | Species of Origin | Application(s) | Provider |
|---|---|---|---|---|
| 12Ca5-(Alexa Fluor 488) | HA-tag | Mouse | Flow Cytometry (10 μg/mL)<br>IP (5 μg) | Produced by an in-house hybridoma. It was labeled using the Alexa Fluor 488 Labeling Kit (Thermo Fisher Scientific, San Jose, CA, USA) |
| 4C4 | Invariant stalk of VLRB | Mouse | Flow Cytometry (10 μg/mL)<br>Western Blot (0.25 μg/mL)<br>ELISA Plate Coating (4 μg/mL) | Produced by an in-house hybridoma. |
| 5-8A3 | Invariant stalk of VLRB | Mouse | ELISA (4 μg/mL) | Produced by an in-house hybridoma. |
| Anti-Mouse IgH/L | Mouse IgH and IgL chains of $IgG_{1, 2a, 2b, 2c, 3}$ IgM and $IgA_{1, 2}$ | Goat (Polyclonal) | Flow Cytometry (1:300) | Southern Biotech (Birmingham, AL, USA) |
| Anti-Mouse-HRP | Mouse IgH and IgL chains of IgG | Horse | ELISA (1:3,000) | Cell Signaling Technologies (Danvers, MA, USA) |
| Streptavidin-HRP | Biotin | n/a | ELISA (1:3,000)<br>Immunoblot (1:10,000) | Cell Signaling Technologies (Danvers, MA, USA) |
| Streptavidin-PE | Biotin | n/a | Flow Cytometry (1.67 μg/mL) | Southern Biotech (Birmingham, AL, USA) |

### 2.4.13 Oligonucleotides

| Internal Designation | Specificity | Primer Sequence (5' to 3') | Orientation Relative to Target | Application/Description |
|---|---|---|---|---|
| 645 | *VLRB* LRRNT | TGC GGC TAG CTG TCC CTC GCA GTG TTC KTG | Sense | 645 includes an NheI site. It clones *VLRB* out of total lymphocyte cDNA and into pCTCON2-N1. 645 amplifies only a portion of LRRNT but includes the entirety of the variable region.<br><br>This same primer is also used for cloning of *VLRB* from pCTCON2-N1 into 367HH-SP-ASA. |
| 646 | *VLRB* Stalk | ATT ACC GGT AGG CTT GGG TTT CTG GGT TG | Anti-Sense | 646 includes an AgeI site. It clones *VLRB* out of total lymphocyte cDNA and into pCTCON2-N1. With 645, 646 flanks *VLRB* to encompass the entirety of the variable region. |
| 658 | *VLRB* | TAT AAC CGG TGG GCT GCG GCG AGG TGG TG | Anti-Sense | Along with 645, 658 clones *VLRB* from pCTCON2-N1 into 367HH-SP-ASA |
| 661 | 645-amplified *VLRB* | TTC AAT ATT TTC TGT TAT TGC TTC AGT TTT AGC AGC TAG CTG TCC CTC GCA GTG | Sense | 661 is meant to be used for second-step PCR of 645 amplicons. This is enabled by 20 bases of homology with 645.<br><br>661 introduces an additional 34 bases of homology between *VLRB* inserts and pCTCON2-N1, facilitating yeast gap repair. |
| 662 | 646-amplified *VLRB* | GGT ATC TAC CTT CAA TCG TCG AGC TAT TGT CCT TAC CGG TAG GCT TGG GTT TC | Anti-Sense | 662 is meant to be used for second-step PCR of 646 amplicons. This is enabled by 21 bases of homology with 646.<br><br>662 introduces an additional 34 bases of homology between *VLRB* inserts and pCTCON2-N1, facilitating yeast gap repair. |
| 723 | *VLRB* | TAT ATC GAT CCA CCA TGT GGA TCA AGT GGA | Sense | 723 is used for amplification of 367HH-SP-ASA-inserted *VLRB* from bacterial colonies but it can |

| | | | | |
|---|---|---|---|---|
| | | | | also be used for sequencing of inserts in that vector. |
| 724 | *VLRB* | TAT GCG GCC GCT CAA CGT TTC | Anti-Sense | 724 is used for amplification of 367HH-SP-ASA-inserted *VLRB* from bacterial colonies but it can also be used for sequencing of inserts in that vector. |

# Chapter 3 | A Tyrosine Sulfation-Dependent HLA Class I Modification Identifies Memory B Cells and Plasma Cells

Justin T.H. Chan[1], Yanling Liu[1], Srijit Khan[1], Jonathan R. St.-Germain[2], Chunxia Zou[3], Leslie Y.T. Leung[1], Judi Yang[1], Mengyao Shi[1], Eyal Grunebaum[4], Paolo Campisi[5], Evan J. Propst[5], Theresa Holler[5], Amit Bar-Or[6], Joan E. Wither[1], Christopher W. Cairo[3], Michael F. Moran[2], Alexander F. Palazzo[7], Max D. Cooper[8] and Götz R.A. Ehrhardt[1]

## Abstract

Memory B cells and plasma cells are antigen-experienced cells tasked with the maintenance of humoral protection. Despite these prominent functions, definitive cell surface markers have not been identified for these cells. We report here the isolation and characterization of the monoclonal VLRB N8 antibody from the evolutionarily distant sea lamprey that specifically recognizes memory B cells and plasma cells in humans. Unexpectedly, we determined that VLRB N8 recognizes the HLA class I antigen in a tyrosine sulfation-dependent manner. Furthermore, we observed increased binding of VLRB N8 to memory B cells in individuals with autoimmune disorders multiple sclerosis and systemic lupus erythematosus. Our study indicates that lamprey VLR antibodies uniquely recognize a memory B cell- and plasma cell-specific post-translational modification of HLA class I, the expression of which is up-regulated during B cell activation.

## Author Affiliations


1. Department of Immunology, University of Toronto, Toronto, ON, Canada
2. Department of Molecular Genetics, Hospital for Sick Children, Toronto, ON, Canada
3. Alberta Glycomics Centre and Department of Chemistry, University of Alberta, Edmonton, AB, Canada
4. Division of Immunology and Allergy, Hospital for Sick Children and University of Toronto, Toronto, ON, Canada
5. Department of Otolaryngology – Head and Neck Surgery, Hospital for Sick Children and University of Toronto, Toronto, ON, Canada
6. Department of Neurology, University of Pennsylvania School of Medicine, Philadelphia, PA, USA
7. Department of Biochemistry, University of Toronto, Toronto, ON, Canada
8. Department of Pathology and Laboratory Medicine and Emory Vaccine Center, Emory University School of Medicine, Atlanta, GA, USA


## Acknowledgments


We thank Ms. Dionne White and Ms. Joanna Warzyszynska for educating and assisting us on multi-color flow cytometry analysis of primary human lymphocytes.

We thank Ms. Hui Zhang, Ms. Eliza Lee, and Mr. Mathew Truong for technical support for radiolabeling and phosphorimaging work.

We are grateful to Ms. Diane Nhieu for help with making some of the DNA constructs used in this chapter.


## Declaration of Contributions

The data presented in **Figs. 3.1**, **3.2, 3.6, 3.7** and **3.10** were collected and analyzed with the help of Dr. Yanling Liu, and Judi Yang whereas the experiment depicted in **Fig. 3.8** was designed with the help of Dr. Srijit Khan. The data presented in **Fig. 3.3** was generated by Shabab Ali. Drs. Jonathan R. St-Germain and Michael F. Moran conducted the experiment and analysis for **Table 3.1**.

## 3.1 Introduction

Memory B cells and plasma cells serve a key function in providing long-lasting humoral protection to pathogenic challenge, both in the context of natural infections and following vaccinations (91, 92). Despite these central roles, many questions remain unanswered about these cells, including the functions of subpopulations of human memory B and plasma cells, regulatory mechanisms governing their activation, and the basis of their longevity. One impediment to answering these questions is the paucity of suitable markers for specific memory B cell identification. Blood memory B cells in humans are identified by the expression of CD27 (93, 94), whereas tissue-based memory B cells are recognized as $CD19^{+}/IgD^{-}/CD38^{-}$ (95, 96). Although widely used as a marker for memory B cells, CD27 is also expressed on germinal center (GC) B cells, plasma cells, and many non-B lineage cells (97, 98), and several studies identified memory B cell populations lacking CD27 expression (99-101). Consequently, memory B cells are currently best defined as antigen-experienced B cells, which are not engaged in an ongoing immune reaction, rather than described by the expression of well-defined cell surface markers. To address this issue, we developed a structure-based approach for the identification of cell surface antigens on memory B cells using the VLR antibodies of the jawless vertebrate sea lamprey (*Petromyzon marinus*).

Despite observations of adaptive immune responses by jawless vertebrates – that is, lampreys and hagfishes – over 50 years ago (15, 102), no orthologues of conserved prototypical adaptive immune genes, such as HLA or recombining B cell and T cell antigen receptors, could be identified in evolutionarily distant jawless vertebrates. Only recently, the molecular basis of adaptive immune responses in jawless vertebrates was defined with the discovery of clonally diverse VLR anticipatory receptors (17). This receptor system provides a potential repertoire exceeding $10^{14}$ clonotypes (17, 18, 103). Unlike antibodies of jawed vertebrates, which use the Ig fold as the basic structural unit, the VLRB antibodies consist of β-sheet-forming LRR units. Structural analyses of monoclonal VLRB antibodies in complex with protein and carbohydrate antigens indicate that residues of VLRB antibodies located on the inner

concave surface and a variable loop structure emanating from the C-terminal capping LRR unit interact with the antigen (36, 45, 104). We reasoned that the radically different protein architecture of VLR antibodies and the large evolutionary distance of jawless vertebrates from jawed vertebrates would allow the generation of monoclonal VLR antibodies to antigens, which conventional mammalian antibodies do not readily recognize because of structural or tolerogenic constraints.

In previous studies, we established monoclonal VLR antibodies as a new class of research reagents for discovery of biomarkers on human lymphocytes and plasma cells (41, 58). Here, we report the isolation of the monoclonal antibody VLRB N8, reactive with an epitope that is expressed specifically on HLA class I on memory B and plasma cells, is up-regulated on memory B cells in autoimmune disorders and is dependent on tyrosine sulfation of HLA class I, indicating that HLA class I-dependent immune responses are subject to an as-yet unexplored level of immune regulation.

## 3.2 Results

### *3.2.1 VLRB N8 specifically recognizes human memory B and plasma cells*

In an effort to generate novel reagents targeting late stages in B lineage differentiation, we screened 628 monoclonal VLRB antibodies from a library generated from lymphocytes of sea lamprey larvae immunized with a cocktail of the plasmacytoma cell lines NCI-H929, U266, and RPMI 8226. Monoclonal VLRB antibodies that displayed reactivity to these cell lines were further evaluated for recognition of primary lymphocytes. One of these VLRB antibodies, VLRB N8, recognized human $CD27^{+}/IgD^{-}$ memory B cells, and $CD27^{+}/IgD^{+}$ marginal zone-equivalent cells (**Fig. 3.1a**, top), blood B lineage cells whose somatically mutated antigen receptor sequences are indicative of post-GC status (93, 105, 106). The VLRB N8 antibody did not react with T cells, non-B/T lineage cells, or monocytes (**Fig. 3.1a**, top). When tonsil samples were used to evaluate VLRB N8 reactivity with tissue-based lymphocytes, we found that VLRB N8 again strongly recognized memory B in addition to recognizing plasma cells (**Fig. 3.1a**, bottom). VLRB N8 only very weakly detected a small number of naïve B cells and detected no GC B cells or non-B lineage cells. Sequence analysis revealed that VLRB N8 contains four variable LRRV units and is thus larger than average VLRB molecules (**Fig. 3.1b**) (23, 107).

Analysis of VLRB N8-reactive cell frequencies showed that nearly all circulating memory B cells were reactive with the lamprey antibody (**Fig. 3.1c**). In contrast, VLRB N8 reacted strongly with 70 to 80% of tonsillar memory B and plasma cells (**Fig. 3.1c**). In tonsil, the immunoregulatory Fc receptor-like 4 (FCRL4) molecule characterizes a morphologically and functionally distinct subpopulation of $CD20^{hi}/CD21^{lo}$ memory B cells (108). Using FCRL4 as a marker to discriminate defined memory B cells subpopulations, we determined on 14 additional tonsil specimens that $FCRL4^{+}$ memory B cells were found more frequently among VLRB $N8^{lo/-}$ memory B cells than $FCRL4^{-}$ memory B cells (**Fig. 3.1d**). This predominant memory B cell/plasma cell

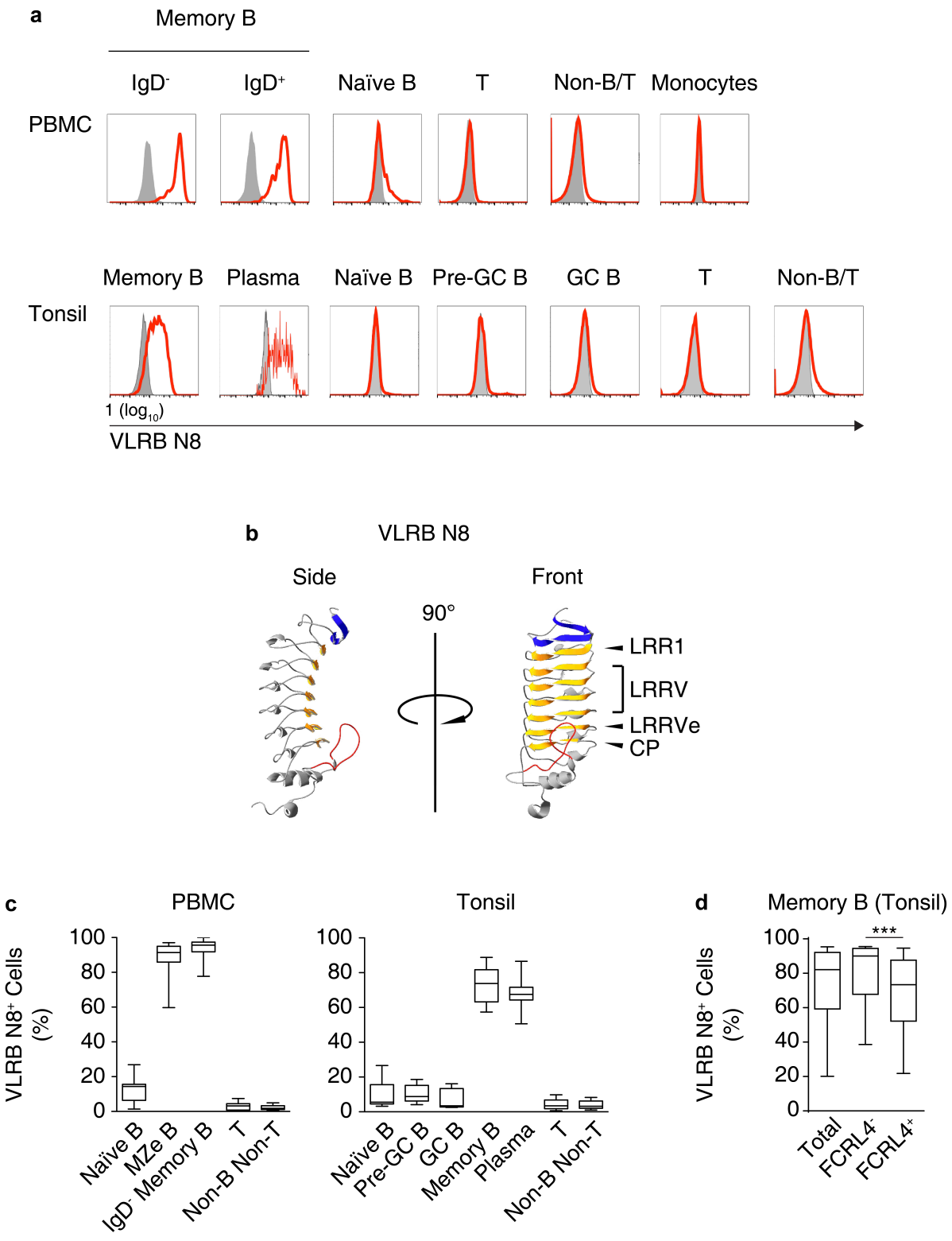
a
Memory B
IgD-
IgD+
Naïve B
T
Non-B/T
Monocytes
PBMC
Memory B
Plasma
Naïve B
Pre-GC B
GC B
T
Non-B/T
Tonsil
1 (log10)
VLRB N8
b
VLRB N8
Side
Front
90°
LRR1
LRRV
LRRVe
CP
c
PBMC
Tonsil
VLRB N8+ Cells (%)
100
80
60
40
20
0
Naïve B
MZe B
IgD- Memory B
T
Non-B Non-T
Naïve B
Pre-GC B
GC B
Memory B
Plasma
T
Non-B Non-T
d
Memory B (Tonsil)
***
Total
FCRL4-
FCRL4+

**Figure 3.1 | VLRB N8 recognizes human memory B and plasma cells in blood and tonsils. a** | Peripheral blood mononuclear cells (PBMCs) were separated into memory B cells ($CD19^+/IgD^-/CD27^+$), marginal zone-equivalent (MZe) B cells ($CD19^+/IgD^+/CD27^+$), naïve B cells ($CD19^+/IgD^+/CD27^-$), non-B non-T cells ($CD19^-/CD3^-$), and T cells ($CD19^-/CD3^+$). A representative of 12 examined PBMC specimens is shown. Human tonsillar lymphocytes were separated into the following subpopulations: memory B cells ($CD19^+/IgD^-/CD38^-$), plasma cells ($CD19^+/IgD^-/CD38^{hi}$), naïve B cells ($CD19^+/IgD^+/CD38^-$), pre-germinal center (Pre-GC) B cells ($CD19^+/IgD^+/CD38^+$), GC B cells ($CD19^+/IgD^-/CD38^+$), non-B non-T cells ($CD19^-/CD3^-$), and T cells ($CD19^-/CD3^+$). A representative example of 14 analyzed tonsil specimens is shown. VLRB N8 reactivity by flow cytometric analysis is indicated by solid red lines and VLR4 reactivity (specific for the BclA antigen of the exosporium of *Bacillus anthracis*) as a negative control is shown as a solid grey histogram. **b** | Ribbon model of a monomeric antigen-binding unit of VLRB N8. Parallel β-sheets lining the inner concave surface encoded by the N-terminal capping LRR are shown in blue and sequences encoded by the LRR1, variable LRRV1-4, LRRVe and connecting peptide (CP) units are depicted in orange. A variable loop protruding from the capping C-terminal LRR is shown in red. The model was generated using the IntFOLD modeling platform (107). **c** | Frequencies of VLRB N8-reactive cells for each analyzed cell population in healthy blood (n = 12) and tonsil samples (n = 14). **d** | Frequencies of VLRB N8-reactive cells between $FCRL4^+$ and $FCRL4^-$ memory B cells from 14 tonsil specimens. Statistical significance was assessed using a Wilcoxon signed-rank test, *** $P < 0.001$; (n = 14).

specificity observed for VLRB N8 has not been demonstrated for any previously reported conventional antibody.

### *3.2.2 VLRB N8 reacts with the HLA class I antigen*

To use VLRB N8 as an affinity reagent for antigen purification and identification, we initially screened panels of human cell lines for recognition by VLRB N8 (**Fig. 3.2**). Analysis of VLRB N8 immunoprecipitates of cell surface-biotinylated VLRB N8-reactive KMS-11 plasmacytoma cells revealed a prominent band of approximately 40 kDa (**Fig. 3.3**). We used tandem mass spectrometry to determine binding partners in VLRB N8 immunoprecipitates and tentatively identified peptides corresponding to sequences of several HLA class I alleles and the HLA class I-associated beta-2 microglobulin (β2m) as the most prevalent protein signals (**Table 3.1**). In the immunoprecipitates, we also detected other molecules for which *cis* interactions with HLA class I have been reported, such as the transferrin receptor (CD71) (109) and HLA class II (110).

To confirm the isolation of HLA class I from VLRB N8 immunoprecipitates, we used KMS-11 cells expressing exogenous HLA A*24:02 green fluorescent protein (GFP) fusion proteins for VLRB N8 IP experiments, followed by detection of endogenous or exogenous HLA class I by Western blotting using anti-HLA class I or anti-GFP antibodies, respectively. These experiments confirmed the initial observation of HLA class I isolation using VLRB N8 as an affinity purification reagent (**Fig. 3.4**). To further confirm the interaction of VLRB N8 with HLA class I, we transfected VLRB N8-reactive KMS-11 cells with small interfering RNA (siRNA) targeting β2m, ablation of which interferes with HLA class I folding, stability, and cell surface expression (111). This inhibition resulted in substantial reduction of HLA class I detection using conventional pan-HLA class I antibodies and even stronger reduction of VLRB N8 binding compared with transfections with scrambled control siRNA (**Fig. 3.5a**). In contrast, binding of VLRB EHT46, recognizing an unknown but ubiquitously expressed antigen, was unaffected, as was the detection of syndecan-1 using a conventional anti-CD138 antibody. Interference of VLRB N8 binding by siRNA-mediated down-regulation of HLA class I was also observed for primary memory B cells (**Fig. 3.5b**). In an independent

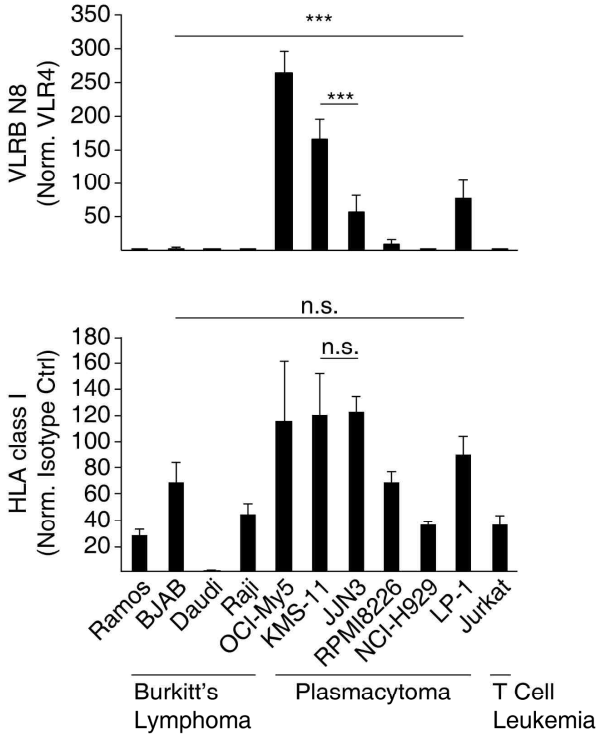


**Figure 3.2 | VLRB N8 binding to cell lines does not correlate with HLA class I cell surface expression levels.** The indicated cell lines were stained with VLRB N8 (top) or conventional anti-pan HLA class I antibodies and analyzed by flow cytometry. Shown are mean +/- SD (n = 4). Values are normalized to negative control VLR4 or isotype-matched control antibodies, respectively. Statistical analysis was performed using a one-way analysis of variance test with Tukey's *post hoc* test. Selected pairings (BJAB and LP-1, or KMS-11 and JJN3) demonstrating significant differences for VLRB N8 binding but lack of significant differences in HLA class I expression are indicated. *** $P < 0.001$, n.s. indicates $P > 0.05$.

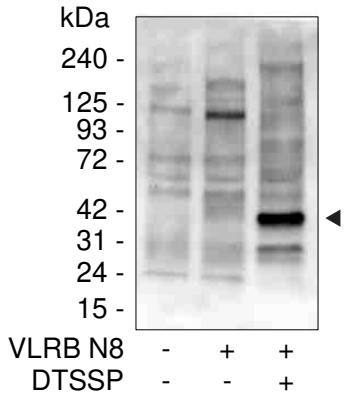


**Figure 3.3 | VLRB N8 immunoprecipitates a prominent 42 kDa protein antigen.** VLRB N8 immunoprecipitates of cell surface-biotinylated KMS-11 cells were resolved on 6 to 14% SDS-PAGE gradient gels, transferred onto nitrocellulose membranes and detected using horseradish peroxidase-labeled streptavidin. DTSSP indicates the addition of a membrane non-permeable, amine-reactive reducible crosslinker prior to cell lysis and immunoprecipitation with monoclonal anti-VLRB antibody 4C4. Depicted is one of three independently performed experiments.

| Rank | Identified Proteins | Accession Number | Molecular Weight |
|---|---|---|---|
| 1 | HLA class I A-24 alpha chain | 1A24_HUMAN | 41 kDa |
| 2 | HLA class I B-55 alpha chain | 1B55_HUMAN | 40 kDa |
| 3 | HLA class I B-51 alpha chain | 1B51_HUMAN | 41 kDa |
| 4 | HLA class I Cw-14 alpha chain | 1C14_HUMAN | 41 kDa |
| 5 | Transferrin receptor protein 1 | TFR1_HUMAN | 85 kDa |
| 6 | HLA class II DRB1-16 beta chain | 2B1G_HUMAN | 30 kDa |
| 7 | Galectin-1 | LEG1_HUMAN | 15 kDa |
| 8 | Beta-2-microglobulin | B2MG_HUMAN | 14 kDa |
| 9 | 4F2 cell-surface antigen heavy chain | B4E2Z3_HUMAN | 56 kDa |
| 10 | Ubiquitin | B4DV12_HUMAN | 17 kDa |
| 11 | HLA class II DR alpha chain | DRA_HUMAN | 29 kDa |
| 12 | Ig gamma-2 chain C region | IGHG2_HUMAN | 36 kDa |
| 13 | Isoform 4 of Low-density lipoprotein receptor | LDLR_HUMAN | 91 kDa |

**Table 3.1** | **Mass spectrometric analysis of VLRB N8 immunoprecipitates.** Displayed are identified proteins that remain following elimination of sequences associated with intracellular molecules and with VLR4 negative control co-immunoprecipitates.

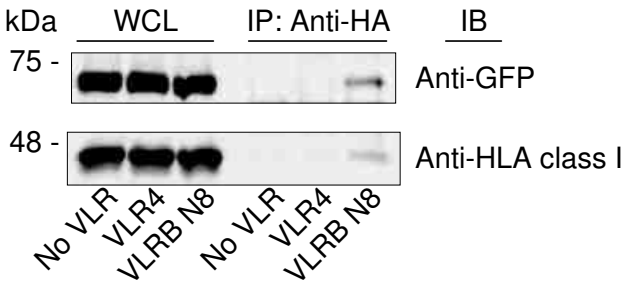


**Figure 3.4** | **Immunoprecipitation of HLA class I with VLRB N8.** KMS-11 cells expressing exogenous HLA A*24:02-GFP fusion proteins were preincubated with VLR4, VLRB N8 or without VLR antibodies followed by crosslinkage with DTSSP. The cells were lysed in 1% Nonidet P-40 lysis buffer and the cell lysate subjected to immunoprecipitation (IP) using anti-hemagglutinin (HA) tag antibodies. The whole cell lysates (WCL) and immunoprecipitates were subjected to SDS-PAGE and transferred onto nitrocellulose membranes. The membranes were cut into two sections with the top section immunoblotted (IB) with anti-green fluorescent protein (GFP) antibodies for the detection of exogenous HLA A*24:02-GFP and the bottom section incubated with anti-HLA class I clone HC-10 for the detection of endogenous HLA class I.

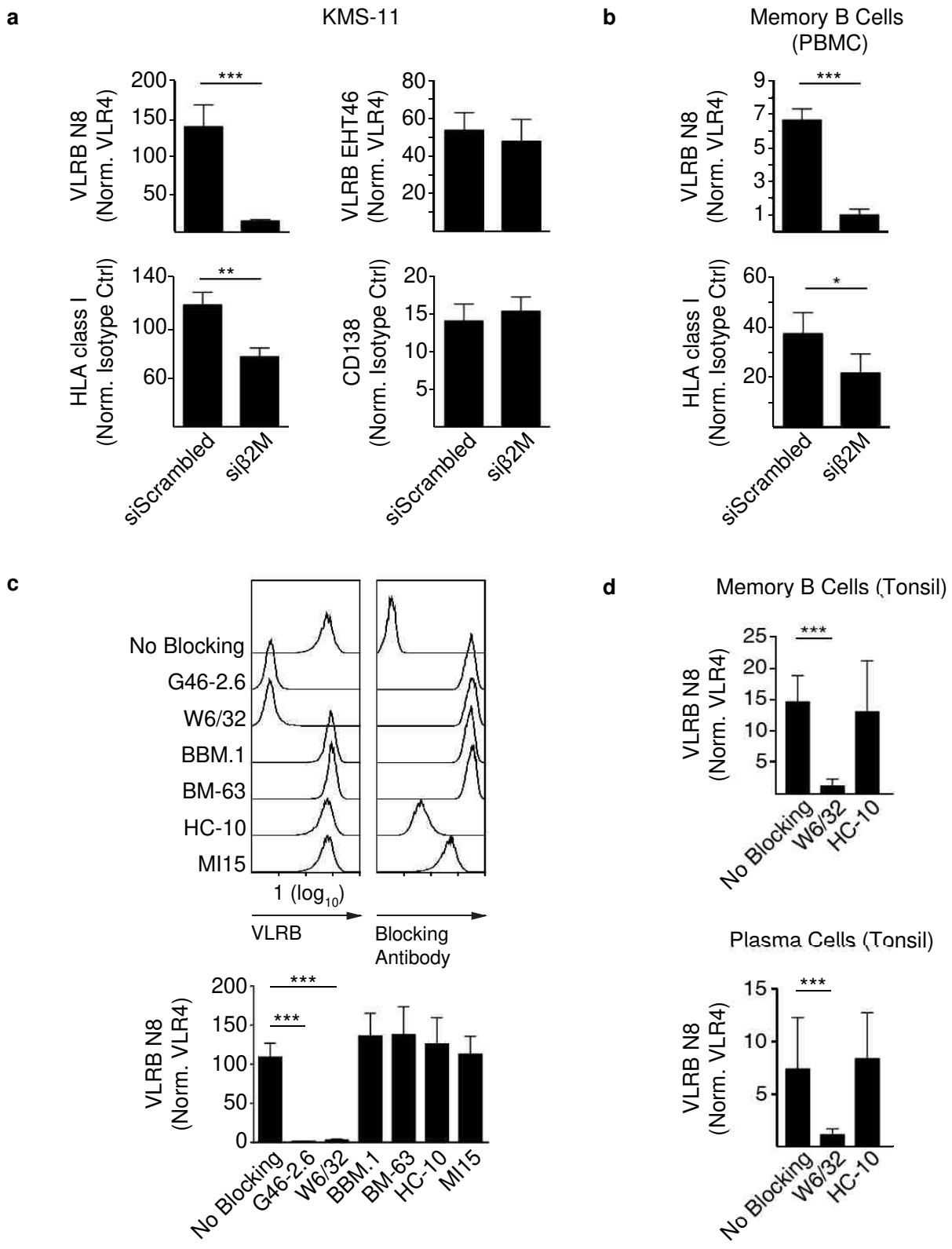
a
KMS-11
VLRB N8 (Norm. VLR4)
VLRB EHT46 (Norm. VLR4)
HLA class I (Norm. Isotype Ctrl)
CD138 (Norm. Isotype Ctrl)
siScrambled
siβ2M
b
Memory B Cells (PBMC)
c
No Blocking
G46-2.6
W6/32
BBM.1
BM-63
HC-10
MI15
1 (log10)
VLRB
Blocking Antibody
d
Memory B Cells (Tonsil)
Plasma Cells (Tonsil)

**Figure 3.5 | VLRB N8 recognizes a memory B/plasma cell-specific epitope of HLA class I. a** | KMS-11 cells and **b** | primary human memory B cells from peripheral blood mononuclear cells (PBMC) were transfected with siRNA targeting β2m (siβ2m) or scrambled control siRNA (siScrambled) before analysis for VLRB N8 reactivity (top row). Modulation of HLA class I cell surface expression was assessed using conventional anti-HLA class I antibodies (bottom row). Off-target effects of transfected siRNA were assessed by staining with VLRB EHT46 and conventional anti-CD138, respectively. **c** | Pan-HLA class I antibodies block the recognition of HLA class I by VLRB N8**.** KMS-11 cells were preincubated with anti-HLA class I antibodies G46-2.6 or W6/32, anti-β2m antibodies BBM.1 or BM-63, free HLA class I heavy chain-detecting HC-10 antibodies, or anti-CD138 antibodies before the addition of VLRB N8. The binding of VLRB N8 (left) or the blocking antibodies (right) was assessed by flow cytometric analysis. Median fluorescence intensities normalized to negative control VLR4 or isotype-matched control antibodies +/- SD (n = 5) are shown. **d** | Pan HLA class I antibody W6/32 blocks the recognition of HLA class I by VLRB N8. Tonsillar lymphocytes were preincubated with anti-HLA class I antibodies W6/32 or HC-10, followed by evaluation of VLRB N8 binding. Median fluorescence intensities normalized to negative control VLR4 or isotype-matched control antibodies +/- SD (n = 12) are shown. Statistically significant differences of $P < 0.05$ were determined with Student's *t* test (**a** and **c**), and Wilcoxon signed-rank test (**b** and **d**), and were indicated by * $P < 0.05$, ** $P < 0.01$, and *** $P < 0.001$.

experimental approach, we observed that VLRB N8 binding to KMS-11 cells was completely blocked by pretreatment with the W6/32 and G46-2.6 pan-HLA class I antibodies, but not the HC-10 anti-HLA class I antibody, reported to detect β2m-free HLA class I α-chains (**Fig. 3.5c**) (112). On the other hand, anti-β2m antibodies BBM.1 and BM-63 did not interfere with VLRB N8 binding to KMS-11 cells. As expected, pretreatment with anti-CD138 antibody had no effect on the binding of VLRB N8 to KMS-11 cells. Blocking of VLRB N8 recognition of HLA class I using anti-HLA class I antibody W6/32 was also observed for primary memory B and plasma cells (**Fig. 3.5d**). These experiments indicate that VLRB N8 recognizes a unique HLA class I epitope on memory B/plasma cells that is absent on other hematopoietic cells.

### *3.2.3 VLRB N8 reactivity does not correlate with HLA class I cell surface expression levels*

The specific interaction of VLRB N8 with memory B/plasma cells contrasts with the ubiquitous expression pattern of HLA class I. Binding of VLRB N8 to panels of cell lines revealed that HLA class I recognition by VLRB N8 does not correlate with HLA class I cell surface expression levels (**Fig. 3.2**). We then extended our investigation into the reactivity of VLRB N8 with primary circulating and tissue-based cells relative to HLA class I expression. Median fluorescence intensities of VLRB N8 observed for memory B or plasma cells were consistently increased over values observed with other cell populations (**Fig. 3.6**, top row). We found strongly increased VLRB N8 binding to memory B cells for a subset of individuals diagnosed with the SLE and MS autoimmune disorders. Increased VLRB N8 binding was also seen for class-switched $CD27^-$ atypical memory B cells that have been observed in the circulation of patients with SLE and MS (101, 113). HLA class I expression was increased on some of the analyzed cell populations, although only to a modest degree (**Fig. 3.6**, bottom row), an observation resulting in characteristic increased ratios of VLRB N8 signals normalized to HLA class I, indicating independence of VLRB N8 recognition of HLA class I from HLA class I cell surface expression levels. This was most evident in comparisons of tonsillar memory B and plasma cells with GC B cells, B lineage cell populations with comparable HLA class I expression levels that are either strongly VLRB N8-reactive

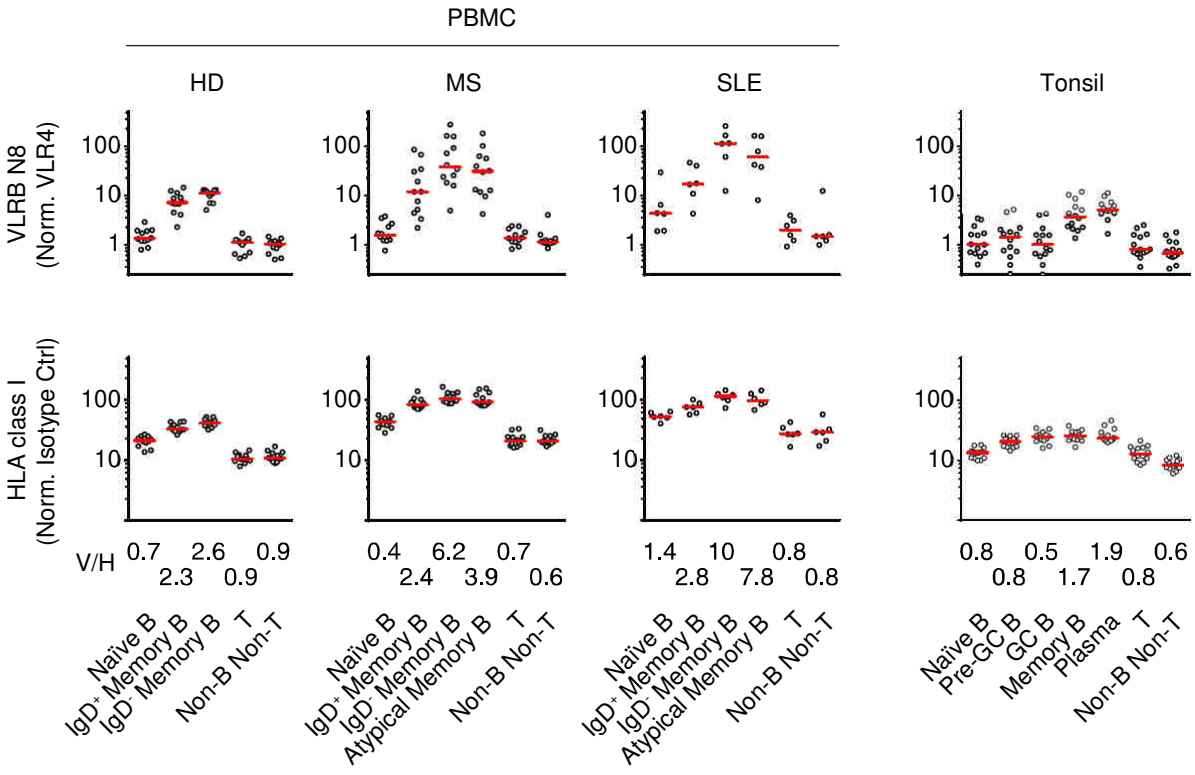


**Figure 3.6 | VLRB N8 reactivity does not correlate with HLA class I cell surface expression levels.** Blood from healthy donors (HD) and individuals diagnosed with multiple sclerosis (MS) or systemic lupus erythematosus (SLE), or tonsillar lymphocytes were analyzed for VLRB N8 binding (top row) and HLA class I binding (bottom row). Peripheral blood mononuclear cells (PBMC). Cell populations were gated as described in **Fig. 3.1**. Atypical memory B cells are defined as $CD19^{+}/CD3^{-}/IgD^{-}/CD27^{-}$. Median values for each population are indicated by red horizontal bars. V/H indicates the numerical values of the median of VLRB N8 signals normalized to the corresponding value of HLA class I.

(memory B and plasma cells) or non-reactive (GC B cells), respectively (**Fig. 3.6** and **Fig. 3.7**), and in comparative analyses of cell lines for HLA class I expression and VLRB N8 reactivity (**Fig. 3.2**).

### *3.2.4 VLRB N8 recognition of HLA class I is induced following B cell activation*

Since memory B and plasma cells are antigen-experienced B cells, we investigated whether antigen encounter could promote VLRB N8 recognition of B lineage cells. We stimulated cells of the VLRB N8 non-reactive BJAB Burkitt's lymphoma cell line with phorbol 12-myristate 13-acetate (PMA) and ionomycin (PMA-I) to simulate the response to antigen receptor signaling. Under these conditions, BJAB cells became VLRB N8-reactive without significant changes in HLA class I expression levels (**Fig. 3.8a**). VLRB N8 reactivity was acquired with relatively slow kinetics and maintained for the duration of the experiment (120 hours; **Fig. 3.8b**, top), although VLRB N8 binding decreased toward the end of the time course. HLA class I expression levels remained unchanged for each of the examined time points (**Fig. 3.8b**, middle), thereby resulting in strong increases of VLRB N8/HLA class I ratios (**Fig. 3.8b**, bottom). Similar to PMA-I stimulation, ligation of the antigen receptor with anti-Ig antibodies induced VLRB N8 reactivity of BJAB cells (**Fig. 3.8c**, top). Interferon (IFN) gene signatures are frequently observed in individuals with autoimmune disorders such as MS and SLE (114-117). In light of our observation of the strongly increased VLRB N8 binding to memory B cells from MS and SLE samples, we were interested in the potential of IFN to induce VLRB N8 reactivity. Stimulation of BJAB cells with type I or with type II IFN resulted in the induction of VLRB N8 binding to these cells (**Fig. 3.8c**, middle panels). Moreover, combinations of suboptimal concentrations of anti-Ig antibodies with type I or type II IFN resulted in further enhancement of VLRB N8 binding (**Fig. 3.8d**). In contrast, treatment of BJAB cells with a Toll-like receptor ligand (CpG) failed to induce VLRB N8 reactivity (**Fig. 3.8c**, bottom). These results demonstrate that B cell activation by antigen encounter or cytokine stimulation induces a unique epitope on HLA class I to allow binding of the VLRB N8 antibody to B lineage cells.

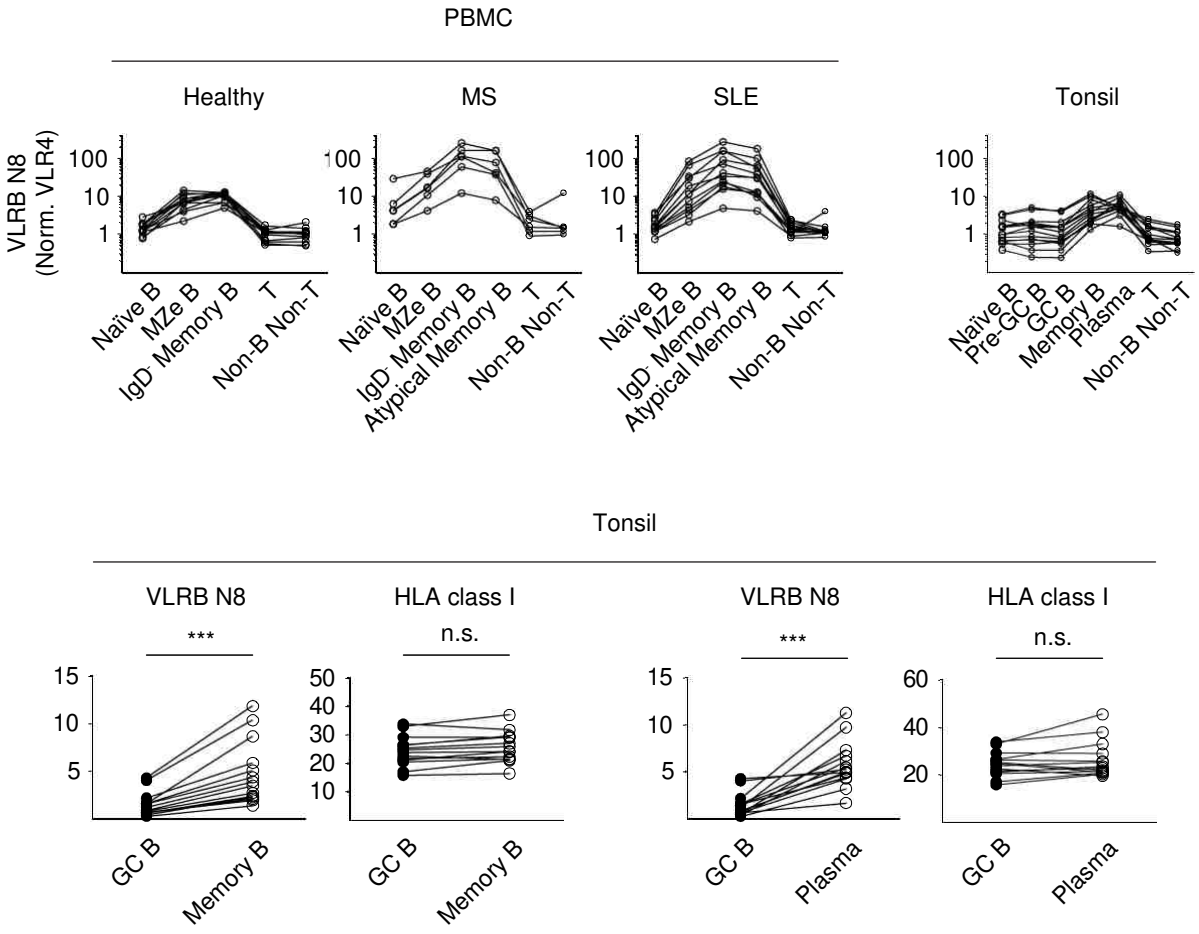


**Figure 3.7 | Recognition of HLA class I by VLRB N8 on memory B cells and plasma cells is independent of HLA class I expression levels.** (Top row) Depicted are median fluorescence values of VLRB N8 normalized to negative control VLR4 for the indicated cell populations from circulating and tissue-based lymphocytes. Note that in multiple sclerosis (MS) and systemic lupus erythematosus (SLE) samples, VLRB N8-reactive cells are consistently strongly or moderately reactive within each individual sample. Marginal zone-equivalent (MZe) B cells. Germinal center (GC) B cells. (Bottom row) Depicted are median fluorescence values of VLRB N8 normalized to negative control VLR4 and HLA class I normalized to isotype-matched control antibodies of tonsillar germinal center B cells in comparison to memory B cells or plasma cells. Note that VLRB N8 consistently recognized memory B and plasma cells but not GC B cells while the HLA class I levels of these cell populations remained unchanged. Statistical significance was determined using a Friedman test followed by Dunn's multiple comparison test, *** $P < 0.001$, not significant (n.s.); n = 14.

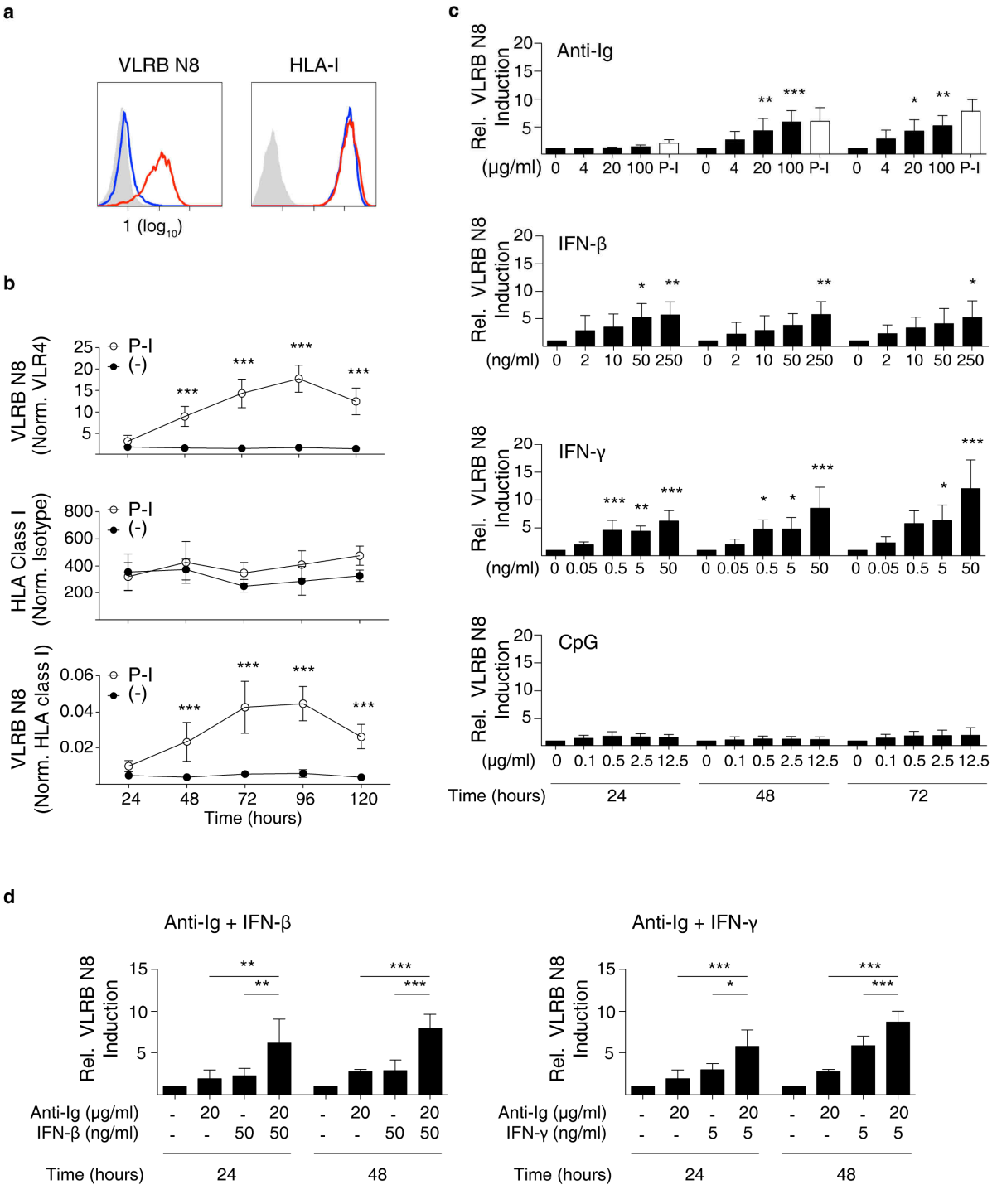
a
VLRB N8
HLA-I
1 (log10)
b
VLRB N8 (Norm. VLR4)
HLA Class I (Norm. Isotype)
VLRB N8 (Norm. HLA class I)
P-I
(-)
Time (hours)
c
Anti-Ig
IFN-β
IFN-γ
CpG
Rel. VLRB N8 Induction
(μg/ml)
(ng/ml)
Time (hours)
d
Anti-Ig + IFN-β
Anti-Ig + IFN-γ
Anti-Ig (μg/ml)
IFN-β (ng/ml)
IFN-γ (ng/ml)
Time (hours)

**Figure 3.8** | **Induction of VLRB N8 binding following B cell activation. a** | BJAB cells were stimulated with PMA and ionomycin (P-I) for one hour and analyzed for VLRB N8 reactivity and HLA class I expression levels after 72 hours (red open histograms). Antibody binding obtained without stimulation is depicted in blue open histograms, and filled grey histograms represent the VLR4 and isotype control specimens. **b** | Time course of BJAB response after stimulation with PMA and ionomycin. VLRB N8 binding normalized to negative control VLR4 (top), HLA class I expression normalized to isotype-matched control antibodies (middle) or the ratio of VLRB N8 relative to HLA class I (bottom) are shown. Statistical significance was determined using a multiple *t* test corrected with the Holm-Šídák method. **c** | BJAB cells were treated with the indicated stimuli and VLRB N8 binding and HLA class I expression levels were measured as in **a**. Induction of VLRB N8 was determined by normalizing VLRB N8/HLA class I ratios to the corresponding unstimulated controls. Bars indicate mean +/- SD (n = 4). Statistical significance was determined using one-way analysis of variance with Dunnett's test. For comparison, the VLRB N8 signals following PMA and ionomycin treatment are included in the graphic for anti-Ig responses (open bars). **d** | Induction of VLRB N8 binding to BJAB cells following costimulation with anti-Ig and interferon (IFN). Induction of VLRB N8 reactivity was assessed as in **c**. Statistical significance was determined using one-way analysis of variance with Tukey's post test. Statistically significant differences are indicated by * $P < 0.05$, ** $P < 0.01$ and *** $P < 0.001$.

### *3.2.5 VLRB N8 recognizes a tyrosine sulfation-dependent epitope on HLA class I*

Recognition of HLA class I by VLRB N8 independently of HLA class I cell surface expression levels suggested that the epitope recognized by VLRB N8 could be formed by a post-translational modification of HLA class I. No alternative glycosylation of HLA class I on VLRB N8-reactive cells could be determined. In addition to glycosylation, cell surface receptors are frequently sulfated on tyrosine residues, a post-translational modification mediated by the tyrosylprotein sulfotransferase 1 (TPST1) and TPST2 enzymes using 3′-phosphoadenosine-5′-phosphosulfate (PAPS) as a sulfate donor (118). Treatment of VLRB N8-reactive KMS-11 cells with $NaClO_3$, an inhibitor of PAPS biosynthesis (119), resulted in a strong reduction of VLRB N8 reactivity without modulation of HLA class I cell surface expression levels (**Fig. 3.9a**). Similarly, incubation of BJAB cells with $NaClO_3$ following PMA-ionomycin treatment also reduced the induction of VLRB N8 reactivity (**Fig. 3.9b**). The PAPS biosynthesis inhibition affects both sulfation of carbohydrate moieties and tyrosine residues. To discriminate between these sulfation reactions, we used short hairpin RNA (shRNA) to target the TPST1 and TPST2 tyrosine sulfotransferases in BJAB cells (**Fig. 3.9c**). HLA class I recognition of VLRB N8 following antigen receptor ligation of BJAB cells was strongly reduced in BJAB cells expressing *TPST2*-targeting shRNA, but not in cells expressing *TPST1*-targeting shRNA or negative control *GFP* shRNA (**Fig. 3.9d**).

In subsequent experiments, we used a metabolic labeling approach to directly demonstrate tyrosine sulfation of HLA class I in response to antigen receptor engagement (**Fig. 3.9e**). These experiments showed low levels of sulfate incorporation in HLA class I in our BJAB model system in the absence of B cell stimulation. Antigen receptor engagement resulted in significant increases in HLA class I tyrosine sulfation, which was inhibited by shRNA targeting *TPST2* but not *TPST1* nor negative control shRNA targeting *GFP*. Lastly, to validate that our *TPST2*-dependent *in vitro* stimulation system could reflect tyrosine sulfation in primary B lineage cells, we determined the presence of *TPST* transcript levels in tonsillar B cell populations. Quantitative reverse transcription polymerase chain reaction demonstrated that *TPST1* and *TPST2* transcripts

were detected in all tonsillar B cell populations with strong increases of *TPST2* mRNA in the plasma cell compartment (**Fig. 3.9f**). Combined, these experiments indicate that the unique recognition of memory B and plasma cells by VLRB N8 is dependent on cell type-specific tyrosine sulfation modifications of HLA class I.

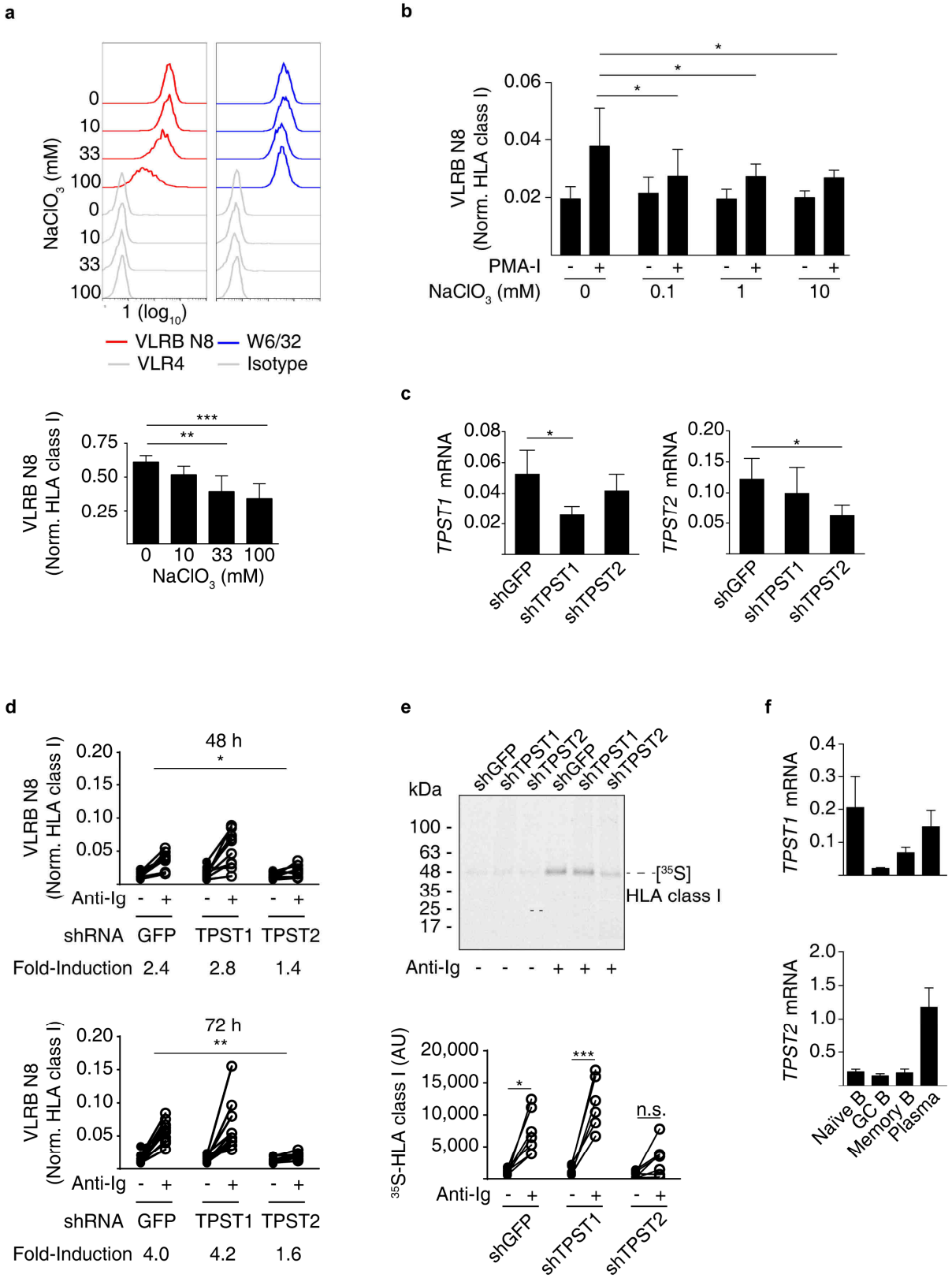
a
NaClO3 (mM)
0
10
33
100
1 (log10)
VLRB N8
W6/32
VLR4
Isotype
VLRB N8 (Norm. HLA class I)
NaClO3 (mM)
b
VLRB N8 (Norm. HLA class I)
PMA-I
NaClO3 (mM)
c
TPST1 mRNA
TPST2 mRNA
shGFP
shTPST1
shTPST2
d
48 h
72 h
Anti-Ig
shRNA
GFP
TPST1
TPST2
Fold-Induction
2.4
2.8
1.4
4.0
4.2
1.6
e
kDa
[35S] HLA class I
35S-HLA class I (AU)
n.s.
f
TPST1 mRNA
TPST2 mRNA
Naive B
GC B
Memory B
Plasma

**Figure 3.9 | VLRB N8 recognizes a tyrosine sulfation-dependent antigen on HLA class I. a** | KMS-11 cells were cultured in the presence of the indicated concentrations of $NaClO_3$ for 48 hours followed by flow cytometric measurement of VLRB N8 (red histograms) and HLA class I reactivity (blue histograms). A representative experiment is depicted in the top panel and VLRB N8/HLA class I ratios from five independent experiments are shown in the bottom bar diagram, depicted as means +/- standard deviation (SD). Statistical significance was determined using one-way analysis of variance with Dunnett's test (n = 5). **b** | Inhibition of VLRB N8 recognition of HLA class I on BJAB cells following PMA and ionomycin (PMA-I) stimulation. Cells were stimulated for one hour with PMA and ionomycin, and VLRB N8 and HLA class I binding were assessed following a 36-hour culture with the indicated concentrations of $NaClO_3$. Mean +/- SD of VLRB N8 signals normalized to HLA class I is shown. Statistical significance was determined using two-way analysis of variance with Dunnett's test (n = 4). **c** | shRNA-mediated down-regulation of *TPST1* and *TPST2* in transduced BJAB cells was verified by quantitative RT-PCR. Transcript levels of *TPST1* (left) and *TPST2* (right) of the indicated cell populations are depicted as means +/- SD (n = 3). Statistical significance was determined using a Student's *t* test. **d** | shRNA-transduced BJAB cells were stimulated with anti-Ig (20 µg/ml) followed by the assessment of VLRB N8 and anti-HLA class I recognition. Numbers indicate the mean fold-induction of HLA class I normalized VLRB N8. Statistical significance for induced VLRB N8 binding was determined using a one-way analysis of variance test with Tukey's *post hoc* test (n = 9). **e** | Tyrosine sulfation of HLA class I following antigen receptor engagement. A representative autoradiogram (left) of anti-HLA class I immunoprecipitates of unstimulated and stimulated BJAB cells and the quantitation (right) of six independent experiments are shown. $[^{35}S]SO_3$ incorporation is shown with arbitrary units (AU). Statistical significance was determined using paired Student's t test (n = 6). **f** | Cell populations were gated as described in **Fig. 3.1** prior to sorting. Means +/- SD of quantitative RT-PCR of *TPST1* or *TPST2* normalized to *HPRT* from five independent tonsil specimens are shown. Statistically significant differences are indicated by * $P < 0.05$, ** $P < 0.01$, and *** $P < 0.001$; n.s., $P > 0.05$.

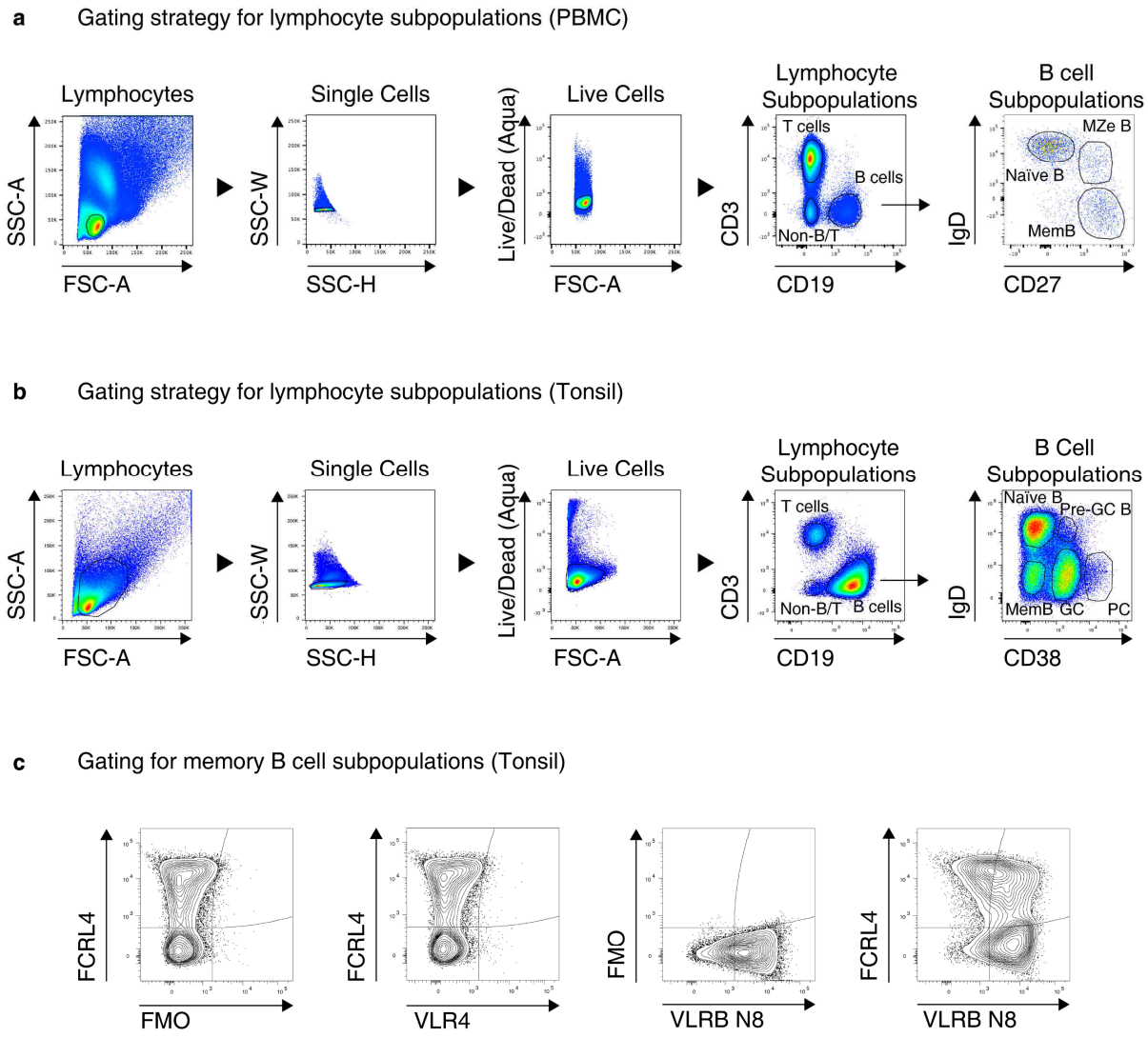


**Figure 3.10 | Gating strategies for evaluation of lymphocyte populations from human blood and tonsillar tissue. a |** Peripheral blood mononuclear cells (PBMCs) were purified using ficoll density gradient centrifugation and incubated with anti-CD3, anti-CD19, anti-IgD, anti-CD27 and VLRB antibodies. Shown is the gating strategy for the indicated subpopulations of a representative blood sample. Memory B cells (MemB). Plasma cells (PC). **b |** Tonsillar lymphocytes were purified using ficoll density gradient centrifugation and incubated with anti-CD3, anti-CD19, anti-IgD, anti-CD38 and VLRB antibodies. Shown is the gating strategy for the indicated subpopulations of a representative tonsil sample. Germinal center B cells (GC B). Plasma cells (PC). **c |** We determined reactivity of VLRB N8 to memory B cell subpopulations by staining with anti-FCRL4 antibodies. Cells determined as memory B cells are depicted using the antibody panel described and shown in **b**.

## 3.3 Discussion

In the present study, we used the nonconventional VLR antibody platform of the evolutionarily distant sea lamprey for the discovery of a biomarker on memory B and plasma cells. The unexpected discovery of HLA class I as the antigen recognized by VLRB N8 on memory B and plasma cells independently of HLA class I expression levels suggested that the recognized epitope is likely formed by a post-translational modification of HLA class I. While the only described post-translational modification of HLA class I occurs at a conserved N-linked glycosylation site at position Asn86 of the α1 domain (120), our results are in accordance with tyrosine sulfation of HLA class I following B cell activation. The extracellular domain of HLA class I contains several conserved tyrosine residues, including Tyr59, located within a tyrosine sulfation consensus sequence of the α1 domain. While we demonstrated that the low-level baseline tyrosine sulfation of HLA class I in VLRB N8-non-reactive cells is greatly increased following B cell activation in a TPST2-dependent manner and that it is accompanied by acquisition of VLRB N8 reactivity, the identity of the sulfo-tyrosine residue(s) under steady-state conditions and following B cell activation remains to be determined. Similarly, analysis of the structure of VLRB N8 in complex with HLA class I will determine whether VLRB N8 directly recognizes a sulfo-tyrosine residue or whether VLRB N8 recognizes HLA class I in a tyrosine sulfation-dependent manner without directly engaging the sulfo-tyrosine.

The strong inhibitory effect on VLRB N8 recognition of HLA class I that we observed following the transduction of *TPST2* shRNA is in agreement with microarray studies and our demonstration showing the expression of *TPST2* transcripts in all peripheral B cell compartments and strongly increased *TPST2* levels in the plasma cell compartment (121). Although VLRB N8 does not recognize the vast majority of naïve B lineage cells, these cells display levels of *TPST2* transcripts that are comparable to those observed for VLRB N8-reactive memory B cells. This indicates that tyrosine sulfation events required for VLRB N8 recognition of HLA class I are likely to be regulated on the level of enzymatic activity and are not necessarily dependent on enzyme expression levels.

Sulfation of tyrosine residues has been demonstrated for several cell surface and secreted proteins (122, 123) and can alter the affinities of receptor/ligand interactions (124). Among the various HLA class I functions, the antigen presentation of peptide antigens to the antigen receptor of $CD8^+$ T cells represents arguably one of the most significant protein-protein interactions in adaptive immunity. It will be important to compare antigen presentation by VLRB N8-reactive HLA class I peptide complexes versus complexes not recognized by the VLR antibody. A potential memory B/plasma cell-specific post-translational modification raises the possibility that T cell recognition of a peptide presented on HLA class I by these cells may be subject to an as-yet unexplored level of immune regulation.

Our observation of strongly increased VLRB N8 recognition of HLA class I in SLE and MS indicates the potentially dysregulated tyrosine sulfation of memory B cells in these autoimmune disorders. B cells are increasingly recognized as contributors to the pathophysiology of these disorders (125, 126), including in antibody-independent B cell effector functions such as generation of proinflammatory cytokines by memory B cells in MS (127). It will be important to expand on our initial observation of increased VLRB N8 reactivity in memory B cells found in PBMCs of patients with MS and SLE and to correlate the level of memory B cell recognition by VLRB N8 with clinicopathological parameters. Similarly, it will be of interest to investigate potentially altered tyrosine sulfation of proteins beyond HLA class I.

Cell surface receptors provide the interface where cues of the extracellular microenvironment are detected and integrated into appropriate cellular responses. Post-translational modifications of intracellular proteins are extensively studied and represent a central mechanism controlling protein expression levels and function in response to a diverse set of stimuli. In contrast, protein modifications such as glycosylation of the extracellular domains of cell surface receptors, the highly complex covalent attachment of carbohydrates to asparagine, serine, or threonine residues (128), or sulfation of tyrosine residues, are less well understood. Investigations into the complexities and functional consequences of post-translational modifications of the extracellular domains of cell surface receptors are limited by a paucity of suitable

detection reagents. Our study highlights the unique characteristics of VLR antibodies as a novel class of highly specific, broadly applicable research reagents to detect previously unrecognized epitopes on cell surfaces of otherwise only functionally defined cells. This is of particular interest for epitopes generated by enzymatic activities that may not be revealed in transcriptomic approaches. While the precise nature and the functional properties of the epitope recognized by VLRB N8 remains to be elucidated, our data demonstrate that HLA class I on memory B/plasma cells is structurally distinct from other lymphocytes and may reveal induced tyrosine sulfation as a novel mechanism in the regulation of HLA class I-dependent immune responses.

## 3.4 Materials and Methods

### *3.4.1 Study design*

The goals of this study were to harness the adaptive VLR-based immune system of the sea lamprey to interrogate the cell surface of memory B cells, to isolate monoclonal VLR antibodies with binding patterns distinct from those of conventional antibodies, and to use these VLR antibodies as novel affinity reagents for antigen identification. We used cell line systems for biochemical experiments aimed at identification and characterization of the recognized epitope. We used primary human samples from healthy donors and autoimmune patients to validate specificity of the reagent. All experiments were performed at least three times.

### *3.4.2 Cells and reagents*

Hematopoietic cell lines were grown in RPMI 1640 supplemented with 10% fetal bovine serum (FBS), glutamine, 50 μM 2-mercaptoethanol, and penicillin-streptomycin (100 U/mL). HEK293T cells were grown in Dulbecco's modified Eagle's medium supplemented with 5% FBS, glutamine, and penicillin-streptomycin (100 U/mL). Cells were maintained in a humidified atmosphere at 37°C and 5% $CO_2$. Antibodies to the human cell surface antigens CD19 (clone HIB-19), CD20 [clone H1(FB1)], CD27 (clone M-T271), IgD (clone IA6-2), HLA class I (clone G46-2.6), CD38 (clone HIT-2), and CD138 (clone MI15) were obtained from BD Biosciences (San Jose, CA, USA). Antibodies to CD3 (clone HIT-3a) were obtained from BioLegend (San Diego, CA, USA), and anti-β2m antibody BM-63 was obtained from MilliporeSigma (St. Louis, MO, USA). Anti-HLA class I antibodies HC-10 and W6/32 and anti-β2m antibody BBM.1 were gifts from Dr. David Williams (University of Toronto, Canada). Phycoerythrin (PE)-labeled anti-HLA class I (clone W6/32) was purchased from Thermo Fisher Scientific (Waltham, MA, USA). Anti-6-histidine-PE antibodies (clone AD1.1.10) were obtained from Novus Biologicals (Littleton, CO, USA), and anti-human Ig was obtained from Jackson ImmunoResearch (West Grove, PA, USA). Recombinant IFN-β and IFN-γ were purchased from PeproTech (Rocky Hill, NJ, USA), and CpG was purchased from InvivoGen (San Diego, CA, USA).

Tonsil samples were obtained from the Hospital for Sick Children (Toronto, Ontario, Canada). Peripheral blood was obtained from healthy donors and heparinized. Primary cell sample collections were approved by the ethical review boards of the Hospital for Sick Children, Toronto, and the University of Toronto in accordance with the Declaration of Helsinki. All participants gave written informed consent.

### *3.4.3 Immunization of sea lamprey larvae and generation of monoclonal VLR antibodies*

Sea lamprey (*Petromyzon marinus*) larvae were immunized with a cocktail of human plasmacytoma cell lines (NCI-H929, U266, and RPMI 8226) in 66.6% PBS and boosted twice in two-week intervals before harvesting of lamprey lymphocytes from the blood. VLRB expression libraries were generated as described previously (41). Briefly, total RNA was prepared from the lamprey lymphocytes using RNeasy columns (Qiagen, Hilden, Germany), followed by complementary DNA (cDNA) generation using the SuperScript II system (Invitrogen, Carlsbad, CA, USA). A VLRB expression library was generated by PCR amplification of cDNA using oligonucleotides specific to the signal peptide (5′-ATATGCTAGCCACCATGTGGATCAAGTGGATCGCCACGC-3′) and C-terminal stalk region (5′-ATATACCGGTTCAACGTTTCCTGCAGAGGGCG-3′) of *VLRB* transcripts and cloning of the PCR products into the eukaryotic expression vector pIRESpuro2 (Invitrogen, Carlsbad, CA, USA). To generate monoclonal VLRB antibodies, plasmids encoding *VLRB* sequences were transfected into HEK293T cells using the PEI method as described previously (41, 129). Lamprey immunizations were approved by the animal care committees of the University of Toronto and Emory University.

### *3.4.4 Generation of recombinant monoclonal VLRB antibodies*

VLRB sequences were subcloned into the vector pIRESpuro2-367HH, which contains sequences encoding the invariant VLRB stalk region as well as the 6-histidine and HA epitope tags. The plasmids were transfected into HEK293T cells using the PEI method (41, 129). Culture supernatants were analyzed 3 days after transfection for the presence of VLRB antibodies by Western blotting and used for staining of

primary cells and cell lines. Transfectants were selected on puromycin (1 µg/mL), and purified VLRB antibodies were obtained using Ni-nitrilotriacetic acid affinity chromatography (41).

### *3.4.5 Flow cytometric analysis of VLRB N8 binding to cell lines and primary lymphocytes*

Cell lines were stained with purified monoclonal VLRB antibodies (500 ng/mL in PBS 1% BSA) for 25 min on ice as described (58). Bound VLRB antibodies were detected by subsequent incubation with anti-VLRB antibody 4C4 followed by fluorescently labeled goat anti-mouse antibodies. Alternatively, bound VLRB was detected by incubation with fluorescently labeled anti-VLRB antibody 5-8A3 or with anti-HA epitope tag antibodies. PBMCs and tonsillar lymphocytes were isolated by density gradient centrifugation over lymphocyte separation medium for 20 min at 750 *g*. VLRB-stained primary cells were blocked extensively with 5% normal mouse serum for 15 min on ice before addition of a cocktail of lineage-specific, fluorescently labeled mouse monoclonal antibodies. Dead cells were excluded by propidium iodide (1 µg/mL) or an Aqua dead cell staining reagent (Life Technologies, Burlington, Ontario, Canada). Flow data were acquired using BD FACSCanto II or Millipore Guava easyCyte HT instruments and analyzed using the FlowJo software package (Ashland, OR, USA). Gating strategies for blood and tonsillar lymphocyte cell populations are shown in **Fig. 3.10**.

### *3.4.6 Affinity purification and identification of antigens detected by VLRB N8*

KMS-11 plasmacytoma cells ($1 \times 10^8$) were surface-biotinylated and incubated with VLRB N8 followed by cross-linkage using the amine-reactive, membrane nonpermeable thiol-sensitive DTSSP cross-linker for 30 min at room temperature. The reaction was quenched by addition of 100 mM Tris (pH 7.5) before lysis of the cells in 1 mL of Nonidet P-40 lysis buffer [1% Nonidet P-40, 150 mM NaCl, 5 mM EDTA, and 50 mM Tris (pH 7.5)] in the presence of protease inhibitors [leupeptin (5 µg/mL), pep-

statin (1 µg/mL), aprotinin (5 µg/mL), soybean trypsin inhibitor (10 µg/mL), and phenylmethylsulfonyl fluoride (40 µg/mL)] for 10 min on ice. Cell lysates were centrifuged at 20,000 *g* for 10 min at 4°C, and the supernatants were subjected to immunoprecipitation using 5 µg of anti-HA antibodies and 30 µL of a 50% slurry of protein G Sepharose (GE Healthcare, Pittsburgh, PA, USA). Five percent of the resulting immunoprecipitates was subjected to SDS-polyacrylamide gel electrophoresis (SDS-PAGE), under reducing conditions and analyzed by Western blotting using horseradish peroxidase-labeled streptavidin and enhanced chemiluminesence reagent. The remaining 95% of the immunoprecipitates were eluted in 8 M urea, 100 mM ammonium bicarbonate at 95°C. Eluates were reduced with 10 mM dithiothreitol for 20 min at 60°C, allowed to cool at room temperature, and alkylated with 10 mM iodoacetamide for 15 min at room temperature in the dark. Samples were diluted fourfold in 100 mM ammonium bicarbonate to reach a concentration of ≤2 mM urea before overnight proteolytic digest with trypsin (10 µg/mL) at room temperature. The resulting tryptic peptide samples were acidified with trifluoroacetic acid at a final concentration of 1% before desalting and purification using offline C18 reverse-phase chromatography. Samples were then dried in a vacuum centrifuge and redissolved in 0.1% formic acid for liquid chromatography (LC)-tandem mass spectrometry analysis. Inline C18 reverse-phase chromatography was performed over a 120-min gradient using an integrated nano-LC system (Easy-nLC, Thermo Fisher Scientific, San Jose, CA, USA), coupled to a linear ion trap Orbitrap hybrid mass spectrometer instrument (Orbitrap Elite, Thermo Fisher Scientific, San Jose, CA, USA). Profile mode mass spectrometry spectra were acquired at a 60,000 full width at half maximum resolution in the Orbitrap, whereas tandem mass spectrometry spectra were acquired in the linear ion trap.

### *3.4.7 Peptide and protein identification*

Samples were analyzed with the Sequest (version 1.4.0.288, Thermo Fisher Scientific, San Jose, CA, USA) and X! Tandem [The GPM, version CYCLONE (2010.12.01.1); https://thegpm.org/)] search engines. For both search engines, the human Uniprot database was mined for tryptic peptides. Parent ion tolerance was set to 10 parts per million, and fragment ion mass tolerance was set at 0.60 Da. Variable

modifications included in the search were asparagine and glutamine deamidation, methionine oxidation, cysteine carbamidomethylation, and N-terminal Glu->pyro-Glu, Gln>pyro-Glu and loss of ammonia. Scaffold (version Scaffold_4.3.4, Proteome Software Inc., Portland, OR, USA) was used to visualize and validate peptide and protein identifications. Peptide identifications required a >95% probability based on the PeptideProphet algorithm (130). Protein identifications required a 95.0% probability based on the Protein Prophet algorithm with at least two identified peptides matching the peptide identification criteria. Proteins that could not be differentiated on the basis of tandem mass spectrometry analysis alone were grouped to satisfy the principles of parsimony.

### *3.4.8 HLA class I ablation by siRNA targeting of* β2m *and shRNA-targeting of* TPST1/2

Ablation of *β2m* expression was performed by transiently transfecting KMS-11 cells or primary PBMCs with 10 pmol of *β2m*-specific siRNA or scrambled control siRNA (Silencer Select, Ambion, Grand Island, NY, USA) using the Amaxa Nucleofection T system (Lonza, Allendale, NJ, USA) and O-20 setting. Cells were analyzed for VLR antibody binding and HLA class I expression levels 48 hours after transfection using a BD FACSCanto II instrument and Aqua LIVE/DEAD for dead cell exclusion. *TPST* expression was down-regulated using RNA interference consortium shRNA sequences, TRCN0000330250 targeting *TPST1*, and TRCN0000035732 targeting *TPST2*, cloned into the pLKO vector. HEK293T cells were cotransfected with *TPST* shRNA vector, packaging plasmid psPAX2, and the envelope vector pMD2.G. BJAB cells were incubated with viral supernatants 2 days after transfection and selected with puromycin (0.5 μg/mL) for 5 days followed by antigen receptor ligation and flow cytometric assessment of HLA class I recognition by VLRB N8 and anti-HLA class I antibody W6/32. The reduction of *TPST1/2* transcripts was determined by qRT-PCR using oligonucleotides 5′-CTGGAACGGTGAAGGTGACA-3′ and 5′-GCTCCCCATGCTTAACGATAAT-3′ targeting *TPST1*, and 5′-CAGCTCGGCTATGACCCTTA-3′ and 5′-GCTGGTGTTTTATAGTCCCCTTTC-3′ targeting *TPST2*, respectively. qRT-PCR experiments were performed using the KAPA SYBR FAST

qPCR system (Kapa Biosystems, Wilmington, MA, USA) on a CFX96 Touch Real-Time PCR Detection instrument (Bio-Rad, Hercules, CA, USA), and values were normalized to hypoxanthine-guanine phosphoribosyltransferase expression levels.

### *3.4.9 Blocking of VLRB N8 binding to HLA class I with conventional antibodies*

KMS-11 cells were preincubated with anti-HLA class I antibodies W6/32, G46-2.6, or HC-10, anti-β2m antibodies BBM.1 or BM-63, or anti-CD138 antibodies (2 µg/mL) in PBS supplemented with 0.5% BSA for 10 min on ice. Subsequently, VLRB N8 or VLR4 antibodies were added for an additional 20 min. The cells were washed, bound VLRB antibodies were detected with anti-His-PE-labeled secondary antibodies, and bound blocking antibodies were detected with PE-labeled anti-mouse secondary reagents followed by detection with a Millipore Guava HT instrument. Primary tonsillar lymphocytes were incubated with the previously indicated antibody panels following preincubation with the blocking antibodies. VLRB N8 binding was detected with anti-His-PE antibodies.

### *3.4.10 Modulation of VLRB N8 binding to cell lines*

BJAB cells were stimulated with the indicated concentrations of anti-Ig, CpG, IFN-β, or IFN-γ followed by flow cytometric assessment of VLRB N8 and anti-HLA class I binding. For PMA (50 ng/mL) and ionomycin (2 µg/mL) stimulations, cells were washed once after a one-hour incubation before continued culture in RPMI 1640 medium supplemented with 10% FBS. Anti-Ig stimulations on shRNA-transduced BJAB cells were performed as three independent stimulations each on three independently performed shRNA transductions. Modulation of VLRB N8 recognition of KMS-11 cells following inhibition of sulfation was assessed by culture of the KMS-11 cells in the indicated concentrations of $NaClO_3$. Culture medium was replaced every 12 hours, and VLRB N8 and anti-HLA class I binding were assessed by flow cytometry.

### 3.4.11 Metabolic labeling of BJAB cells

Radiolabeling of BJAB cells was conducted on the basis of a modified protocol for P-selectin glycoprotein ligand-1 (PSGL-1) tyrosine sulfation detection (131). BJAB cells ($1 \times 10^6$) were stimulated for 24 hours with anti-Ig (20 µg/mL) antibodies in RPMI supplemented with 10% FBS, glutamine, 50 µM 2-mercaptoethanol, and penicillin-streptomycin (100 U/mL). Subsequently, the cells were incubated for an additional 24 hours in Eagle's minimum essential medium (Joklik modification for suspension cultures) supplemented with 23.8 mM $NaHCO_3$, 0.4 mM $CaCl_2$, nonessential amino acids, 20 mM HEPES, and 100 µCi/mL $[^{35}S]Na_2SO_4$. Cells were lysed as described, followed by immunoprecipitation with anti-HLA class I clone W6/32 antibodies and the immunoprecipitates resolved by SDS-PAGE on 4 to 15% gradient gels. The gels were dried for 2 hours at 80°C, and $[^{35}S]$ signals were detected using a Typhoon FLA 9500 instrument (GE Healthcare, Chicago, IL, USA).

### 3.4.12 Statistical analysis

Statistical analysis was performed using the GraphPad Prism 6 software package. Statistical significance was determined using Student's *t* test, repeated-measures analysis of variance (ANOVA) with Holm-Šídák *post hoc* test, one-way ANOVA with Dunnett's post test, two-way ANOVA with Dunnett's post test, Wilcoxon signed-rank test, and Friedman test with Dunn's multiple comparison test as indicated.

# Chapter 4 | Discussion

Whether in nature or in research, receptors that vary in form can be adopted for the same purpose. Immune systems that differ in operation and organization at the marrow can employ structurally divergent immune receptors for the same function. This is exemplified by primates opting for Ig superfamily NK cell receptors versus C-type lectin-like NK cell receptors in rodents (22). Likewise, researchers have adapted structurally dissimilar non-human IgH-IgL antibodies, atypical single heavy chain antibodies, and artificial scaffolds such as ankyrin repeat proteins (132) as affinity reagents. In turn, we have applied VLR antibodies as an Ig alternative because they are both structurally distinct and adaptable.

Our application of VLR antibodies stems as much from their intrinsic qualities as it does from the organisms bearing them - jawless vertebrates separated 500 million years ago from gnathostomes and this divergence transcends mere adoption of the VLR antibodies. We hypothesized that the sum of the mechanisms governing this anticipatory system with the form assumed by its antigen receptors can provide reagents that will not encounter the same tolerogenic and structural constraints as conventional immunoglobulin antibodies.

Via immunization of lamprey larvae and eliciting antigen-specific antibodies to circulating antigen (**Chapter 2**) or B cell surface markers (**Chapter 3**), we built an infrastructure supporting the generation of antigen-specific VLRB antibodies. Currently, a pressing need in breast cancer is prognosis of disease to stratify patients who can ultimately benefit from therapy versus those unnecessarily receiving treatments detrimental to quality of life. To this end, we must also evaluate select monoclonal VLRB antibodies isolated in **Chapter 2** and their reactivity to retrospective longitudinal specimens, with the ultimate goal to identify and characterize the antigen to establish a diagnostic/prognostic test. Some of these steps which proceed initial discovery have been undertaken in **Chapter 3**. The ability of VLRB N8 to resolve tyrosine-sulfated HLA class I from its unmodified counterpart is the strongest evidence generated thus far supporting our above hypothesis that the VLR platform can give us insight into

molecular markers omitted or unseen thus far. This new-found modification of a molecule at a most crucial synapse in immunology leads us to speculate that many other cell-cell and receptor-ligand interfaces are subject to modification and regulation beyond those we were privy to observe here. Compared to the CD27 marker for instance, VLRB N8 and its target more specifically characterize human memory B cells while possibly providing clues to the long-term maintenance of the B cell compartment. We envision that application of VLRB antibodies will continue to uncover tools and markers that enable such discoveries in many biomedical and research contexts.

As exemplified by VLRB N8, the isolation of human biomarker-reactive VLRB antibodies raises many more questions than it answers. We must identify what antigen is bound and where the antigen is bound, while posing the question of why reactivity accompanies a particular phenotype or cell population. The latter point of inquiry warrants discussion as exemplified by the isolation of VLRB N8 and discovery that a distinct form of HLA class I exists on antigen-experienced B cells. If this modification is not vestigial upon reaching the cell surface, what is the functional outcome of tyrosine-sulfated molecules? What can modified HLA class I teach us about the molecule's activity, novel interactions, and the expressing B cell population? Exploration of several aspects of HLA class I on memory B and plasma cells beckons.

## *4.1 Tyrosine sulfation of human proteins*

Having validated tyrosine sulfation of HLA class I, it is imperative to review this post-translational modification itself: its specificity/targets, its place among other post-translational modifications, and its functional outcomes. These are knowledge bases upon which we can perhaps deduce the function and role of tyrosine sulfation in the context of HLA class I molecules.

Through the activity of human PAPS synthase[1], dietary inorganic sulfate is converted into PAPS, the universal sulfonate/sulfuryl ($-SO_3$) group donor for all sulfotransferase reactions including those of TPSTs (133). The TPSTs are active in the lumen

[1]*PAPS synthase* A bifunctional enzyme possessing a sulfurylase and kinase domain that takes inorganic sulfate, and two ATP molecules as input to produce PAPS, with ADP and pyrophosphate as byproducts.

of the Golgi apparatus and thus, only secreted or membrane integral proteins can be subject to modification. The current consensus sequence dictates that prospective tyrosines are proximal or adjacent to acidic and small residues (118). In contrast, a consensus site is suggested to be distant from an N-glycan as it can sterically prevent TPST access – one study demonstrated that tyrosine sulfation of mouse IgG2a was only enabled following tunicamycin inhibition of N-glycosylation (134). Based on other observations, it is established that modifiable tyrosines are at least seven aa away from disulfide bond-forming cysteines, from N-glycans, and from hydrophobic residues (118). However, these restrictions are not absolute nor are the rules comprehensive with estimates suggesting that tyrosine sulfation is more common than tyrosine phosphorylation (135).

*TPST1* and *TPST2* are ubiquitously expressed in human tissues including the immune compartments blood, bone marrow, spleen, and thymus (136). The TPSTs are conserved throughout the animal kingdom with human *TPST1* and *TPST2* being 55% and 41% identical, respectively, to *C. elegans TPST1* and *TPST2*; 82% and 62% identical, respectively, to *Danio renio TPST1* and *TPST2*. Due to moderate homology of 77%, the human TPST1 and TPST2 isoenzymes can share substrate specificity – for instance, to P-selectin glycoprotein ligand-1 (PSGL-1) and CCR5 – but differ in affinity (136).

Sulfation is most akin to yet distinct from phosphorylation. Both involve the addition of an 80 Da negatively charged acidic group to a suitable acceptor residue. However, tyrosine O-sulfation occurs strictly on secreted and membrane integral proteins whereas phosphorylation is generally for cytosolic and nuclear processes such as signal transduction [reviewed by Stone et al. (118)]. In stark contrast to phosphorylation, there is no evidence of tyrosine sulfation being physiologically reversible - though it can be removed by a bacterial arylsulfatase (131). This is exceptional compared to phosphorylation and other ‘tunable’ modifications - are the effects of tyrosine sulfation only regulated with the rise (by activity of TPSTs and surface expression) and set (by endocytosis and/or degradation of the host protein)? Furthermore, alt-

hough tyrosine sulfation also occurs within a distinct consensus motif, no corresponding recognition domain equivalent to phospho-tyrosine-binding SH2 domains has been identified for sulfo-tyrosine. Therefore, any sulfo-tyrosine-mediated protein-protein interactions are potentially solely through electrostatic forces and any consensus motif is purely for TPST enzyme specificity. These characteristics need to be considered to infer potential binding partners and functional outcomes of sulfation.

To illustrate how pivotal tyrosine sulfation is for cell-cell communication and in the integration of extracellular cues, we can examine two examples in P-selectin glycoprotein ligand-1 (PSGL-1) and CCR5 in which the modification determines binding. Wilkins et al. observed $^{35}S$ incorporation into PSGL-1 from carrier-free inorganic [$^{35}S$]sulfate and that treatment with bacterial arylsulfatase could prevent interaction with P-selectin (131). Furthermore, $NaClO_3$ as well as mutagenesis targeting the three N-terminal tyrosines of PSGL-1 can prevent binding to P-selectin. Similar studies were conducted to confirm the modification of CCR5 (137). The lack of PSGL-1 sulfation decreases affinity for P-selectin by 30-fold (138) whereas sulfation provides an eight-fold increase in affinity for RANTES in the case of CCR5 (137). PSGL-1 binding is through electrostatic interactions between its negatively charged sulfate and the lectin domain of P-selectin. However, the modification does not act in solitude and determines more than affinity. Differential tyrosine sulfation (along with O-glycosylation of PSGL-1) enable specificity to ligands such as P-selectin and CCL19/21 whereas binding to E-selectin is independent of the modification (139).

As evidence of cell-mediated regulation of tyrosine sulfation: two independent studies observed differences between *in vitro* cell-free sulfation (140) and cell-catalyzed sulfation (122) of the same polypeptide - not only was the choice of tyrosine residues impacted but also the temporal order of reactions. In another example, KPL1, a tyrosine sulfation-dependent antibody for PSGL-1, has reduced reactivity to B cells compared to other PBMCs (141) which suggests lineage-specific regulation of TPST expression or activity.

The tyrosine sulfated residues on CCR5 can also directly interact with a pathogen. In the absence of tyrosine sulfation of CCR5, binding to gp120 and entry of the

JR-CSF strain of HIV was abrogated, as determined by CRISPR-guided deletion of TPST2 or the PAPS transporter SLC35B2 (142). Interestingly, a tyrosine-sulfated monoclonal antibody was capable of neutralizing HIV-1 by mimicking the CCR5 binding site of gp120 (143). CCR5 expression and cell viability were unaffected whether with *TPST2* knockout or *SLC35B2* knockout. Therefore, tyrosine sulfation is potentially targetable for therapy. Overall, the unique properties of tyrosine sulfation can be essential for physiology and pathogenesis alike.

## *4.2 How is tyrosine sulfation regulated in memory B and plasma cells?*

Using a cell line system mimicking BCR crosslinking, we have demonstrated that the inducible VLRB N8 reactivity can be eliminated by silencing *TPST2*. However, like the expression of HLA class I, *TPST* expression is detectable in cell lines, ubiquitous in primary cells (136), and therefore mRNA levels cannot demarcate VLRB N8 reactivity from non-reactivity. Whereas *TPST2* expression is elevated in VLRB N8$^+$ primary plasma cells compared to all other tonsillar B cell populations tested, memory B cells are equally VLRB N8-reactive yet their *TPST2* expression is equivalent to that of VLRB N8-non-reactive naïve and GC B cells (**Fig. 3.9f**). Our findings suggest that *TPST2* expression is necessary but not sufficient for activity, and that tyrosine sulfation is governed post-transcriptionally in VLRB N8$^+$ antigen-experienced B cells, potentially via regulation of enzymatic activity (**Fig. 4.1a**).

Although very little is known about the regulation of TPST activity, it has been demonstrated that TPST2 activity is potentially dependent on pH and divalent cation concentration of the Golgi apparatus - *in vitro* enzymatic activity assays demonstrated that TPST2 is most active at pH 6.0 and stimulated by $Mn^{2+}$, $Mg^{2+}$, but notably inhibited by $Ca^{2+}$ (136). The BCR activation stimulus used in our system is known to increase cytosolic $Ca^{2+}$ concentration whether sourced extracellularly or from the ER compartment. Like the ER, the Golgi apparatus $Ca^{2+}$ concentration is also regulated by ligand-gated $Ca^{2+}$ channels that can be opened by the $IP_3$ produced by phospholipase C (144). Lowering the concentration of $Ca^{2+}$ in the Golgi apparatus is responsible for accelerating protein egress (145) but perhaps it also activates TPST2 by expelling its

cationic inhibitor. However, this is an oversimplification because the Golgi subcompartments are heterogeneous. Lissandron et al. demonstrated that the *trans*-Golgi (the subcellular location of TPST enzymes) in the HeLa cell line moderately takes up $Ca^{2+}$ in response to $IP_3$ (146). Additional disparity with the ER includes a prolonged rather than rapid release of $Ca^{2+}$ by the *trans*-Golgi compartment in response to the ionomycin ionophore. Other differences likely exist for the other metal cofactors.

To associate any of these phenomena to TPST2 activity, VLRB $N8^-$ cell lines can be treated with calcium channel agonists or $Ca^{2+}$-chelating agents to support induction of VLRB N8 reactivity. Conversely, as a potential means of inhibiting sulfotransferase activity, $Mg^{2+}$ chelation or cell culture with medium selectively depleted of cofactors is expected to mimic $NaClO_3$ treatment in experimental readout (**Fig. 3.9a**). Such experiments can be combined with anti-Ig cell stimulation as this proposed mechanism of TPST2 activation may not be sufficient for nor be the sole contributor to meeting a threshold of activity. The tyrosine sulfation of HLA class I appears tunable by stimulation. Thus, the specific conditions are of interest to delineate cell populations meeting the criteria and to enable further study of any affected HLA class I functions.

Since VLRB N8 reactivity is associated with tyrosine sulfation activity, we posit that TPST2 activity is also a correlate of B cell differentiation (**Fig. 4.1a)**. If TPST2 activity is (up)regulated in primary cells, the TPST pathway may be targetable for therapy and B cell-specific forms of receptors or products, such as CD19 and TNFα respectively, may exist – both are predicted to harbor modified tyrosine residues (147) and our preliminary data suggests that CD19 but not CD20 is tyrosine-sulfated (**Fig. 4.1b**). If CD19 on antigen-experienced B cells can be distinguished from all other CD19 (much like tyrosine-sulfated HLA class I), it may be a therapeutic target for the specific depletion of memory B cells (148). Although anti-CD20 B cell depletion therapy has been successful in treating relapsing-remitting MS, another approach targeting the B cell compartment with atacicept exacerbates disease (149). These conflicting results suggest that memory B cells are mediators of disease rather than plasma cells because the latter include $CD20^-$ populations that are spared by rituximab and

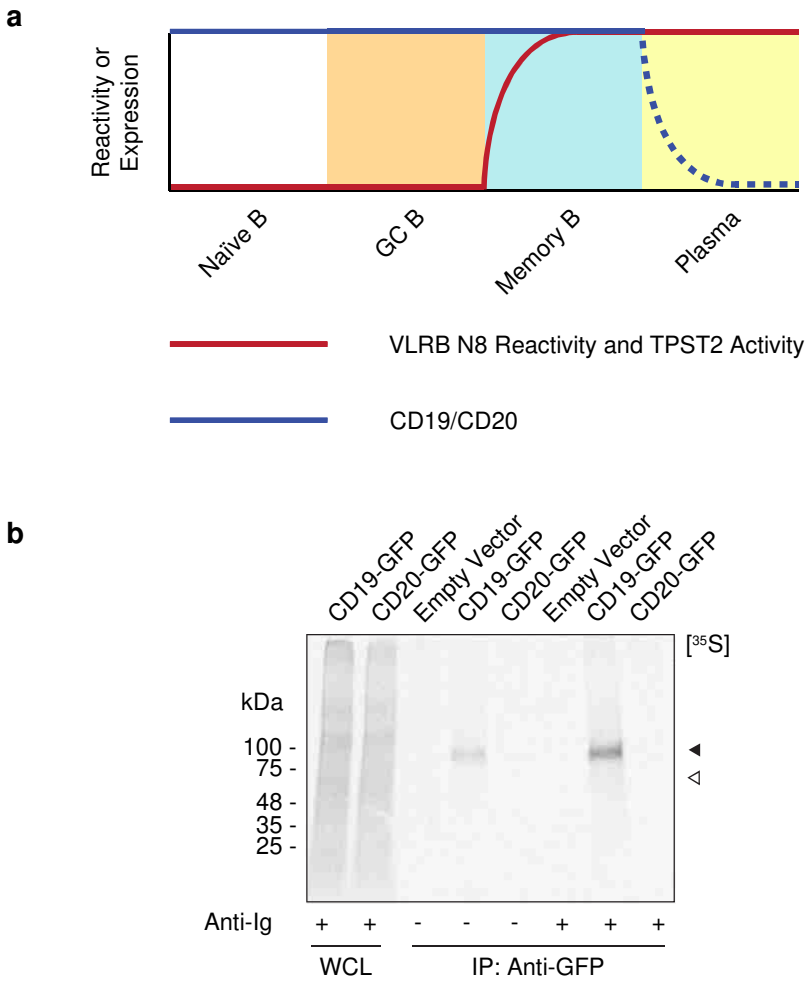


**Figure 4.1 | Current model of the relationship between VLRB N8 reactivity, tyrosylprotein sulfotransferase (TPST) activity and B cell differentiation. a** | Our results suggest that VLRB N8 reactivity (maroon) follows antigen encounter by and differentiation of naïve B cells into memory B cells and plasma cells. Does TPST2 activity also correlate with reactivity of VLRB N8? If so, TPST pathways may be targetable for therapy. CD19 and CD20 expression (blue) are absent in certain plasma cell populations. Perhaps CD19 and/or CD20 follow the same pattern of differential tyrosine sulfation as HLA class I. If TPST activity and CD19/CD20 expression coalesce uniquely at the memory B cell stage, they may serve as therapeutic targets for the selective depletion of memory B cells in autoimmune diseases such as multiple sclerosis. **b** | Using the metabolic labeling system described in **Fig. 3.9** but instead targeting exogenously introduced CD19 and CD20 fusion proteins, our preliminary data demonstrates that CD19 is tyrosine-sulfated and suggests that it is also induced by B cell receptor stimulation in the BJAB cell line. The filled arrowhead depicts the expected molecular weight of CD19-GFP whereas that of CD20-GFP is depicted by a hollow arrowhead. Whole cell lysate (WCL). Immunoprecipitation (IP).

the former are relatively resistant to antagonism of tumor necrosis factor receptor superfamily member 13B (**Fig. 4.1a**). Therefore, patients suffering from B cell-mediated diseases can benefit from therapy in which on-target effects are limited to a specific stage of differentiation such as the memory B cell stage (150, 151). Soluble factors are also subject to modification: Hortin et al. have demonstrated that complement C4 is tyrosine-sulfated (152) but there is no information on what functions are enabled. Are inflammatory markers such as TNFα also modified and is a distinct functional form produced by memory B cells?

## *4.3 Which tyrosine residues in HLA class I are subject to sulfation?*

Each MHC molecule's protein sequence determines restriction and peptide repertoire, demonstrating that function follows form (153). Although we have shown that HLA class I is differentially sulfated in antigen-experienced B cells by TPST2, the location of the modified residue(s) remain(s) to be determined and it is also unknown whether all HLA alleles are subject to modification – both are variables in potential interactions mediated by sulfo-tyrosine-HLA class I.

We rationalize that all HLA class I alleles have an equal opportunity to be modified and that these molecules share a modification site. VLRB N8 was able to segregate antigen-experienced B cells from allogeneic healthy blood and tonsil donors (**Fig. 3.6**). The chance of these 26 individuals carrying the same HLA haplotype is miniscule. Although our measurements showed that certain donor memory B and plasma cells react lowly, these are likely differences intrinsic to VLRB N8 – without crystal structure solution of a VLRB N8-HLA class I complex, we cannot conclude the degree to which the VLR antibody is affected by HLA polymorphism and whether VLRB N8 interacts directly with the sulfo-tyrosine. Furthermore, our mass spectrometry analysis identified members of all three genes with comparable spectrum counts (**Table 3.1**). Although HLA A*24-associated spectral counts were the highest among HLA class I alleles, this ranking likely reflected the KMS-11 genotype which is homozygous for HLA A*24:02 and heterozygous for HLA B and HLA C genes. HLA A*24:02 is the only shared allele between two naturally VLRB N8$^+$ cell lines (KMS-11 and OCI-My5) and neither cell line shares a common allele with BJAB cells (that is inducible

for VLRB N8 reactivity). Thus, a conserved modification site is likely shared between allelic lineages.

VLRB N8 recognition of memory B, plasma cells, and cell lines of discordant HLA haplotypes indicates that modification sites are widely conserved. HLA A, HLA B, and HLA C are highly polymorphic, with over 12,000 unique alleles documented and approximately 9,000 unique proteins (154, 155). In addition to the lone glycosylated Asn86 residue that is necessary for proper HLA class I association with ER chaperones, folding and peptide loading (156), not studied are several conserved tyrosine residues. These are tyrosines present at three different sites that face the peptide loading groove (**Figure 4.2)** (157). Tyr59 is present in all but approximately 20 non-null alleles and is located in a tyrosine sulfation consensus sequence (147). Additionally, only about 70 non-null alleles lack one or both of Tyr84 and Tyr85 in full-length HLA class I and ongoing studies indicate that one of these residues is likely sulfated (Dr. Christopher W. Cairo, personal communication) despite not being predicted to be lodged in a consensus tyrosine sulfation motif. It is noteworthy that only 53 proteins are indexed as sulfated in the UniProt database (as of July 2018) (1) and this list is not comprehensive as evidenced by the omission of molecules such as HLA class II (158).

Through the knockdown of *TPST2* and the matching reduced $^{35}S$ incorporation, we have demonstrated that at least one tyrosine residue of HLA class I is decorated with sulfation. However, proteins with multiple sulfated tyrosines exist as exemplified by PSGL-1 and CCR5. We must consider that every additional tyrosine doubles the number of possible HLA class I sulfoform permutations, each potentially unique in specificity/role. Tyrosines at positions 84 and 85 are near-universally conserved based on frequency distribution but are in violation of the consensus sequence. Most overt is their linear position next to N-glycosylated Asn86. However, an O-glycan is not only proximal to a sulfo-tyrosine on CCR5 but is complimentary in determining ligand specificity (139) suggesting that tyrosine-proximal glycans may not be an obstruction for modification. Additionally, alternative tyrosine residues must be considered that do not necessarily have to be shared by all three HLA genes.

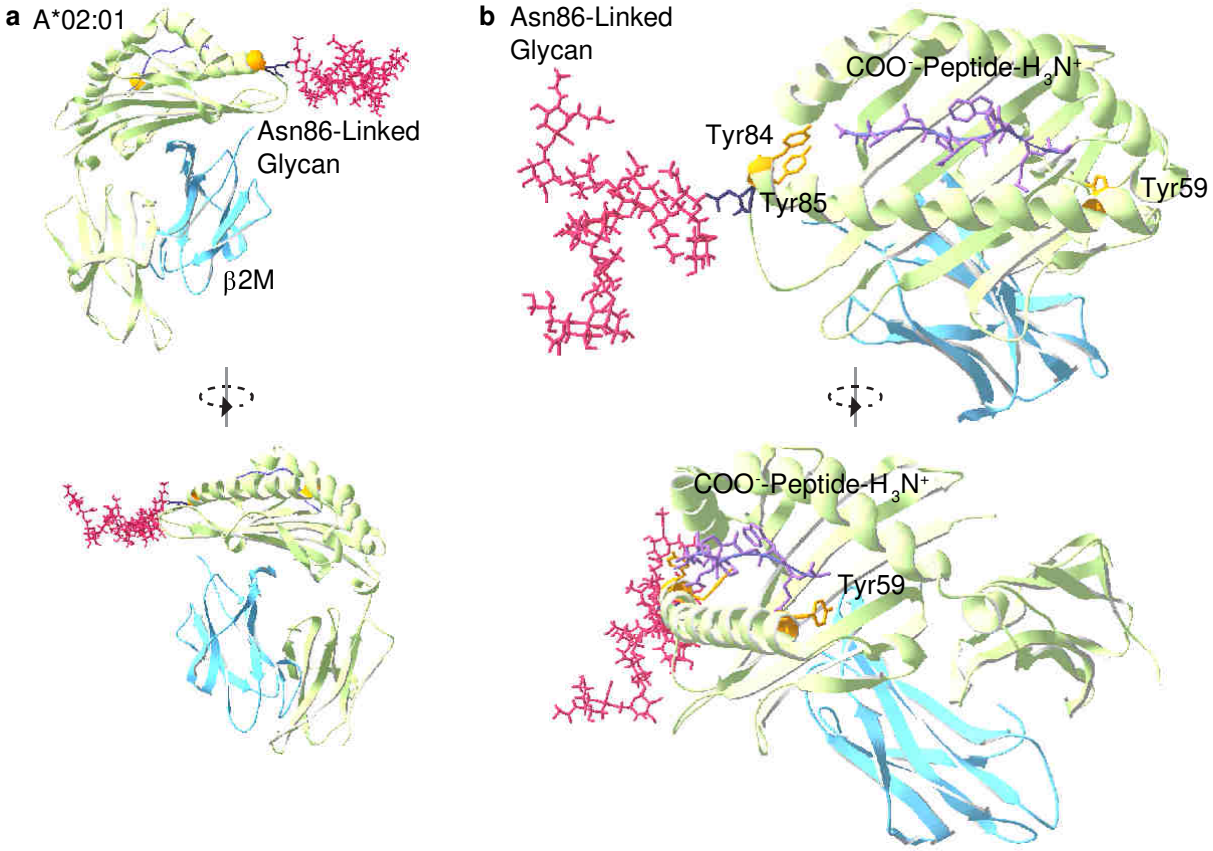


**Figure 4.2 | Tyrosines 59, 84, and 85 of HLA class I appear poised to interact with loaded peptide.** The structure of a representative HLA class I complex is depicted to facilitate visualization of the hypothesized interactions between sulfo-tyrosine-HLA class I and peptide. **a** | We show the HLA A*02:01 heavy chain (lime ribbon) modified at residue Asn86 (purple backbone and sidechains shown) with the 'oligosaccharide B' (magenta) that was determined by Barber et al. to be the most abundant variant amongst EBV-transformed B cell lines (157). HLA class I is depicted associated with the β2M light chain (cyan) and presenting peptide (light purple backbone). **b** | A magnified view of the groove of HLA A*02:01 and peptide docked within. The abnormally conserved tyrosine residues implicit in **a** are now labeled, and colored cantaloupe with the sulfation-modifiable aromatic side chains facing within the peptide loading groove. Tyr84 and Tyr85 face the C-terminus ($COO^-$) of loaded peptide opposite to Tyr59 [positioned facing the N-terminus ($H_3N^+$) of loaded peptide]. The HLA complex (PDB ID: 5C0D) was joined to a physiological glycan using the Glycosciences.de GlyProt *in silico* glycosylation service (N-glycan entry 8624).

To elucidate the identity of modified tyrosine residues, we propose that site-directed mutagenesis of potential sulfated tyrosines of HLA class I can be performed to measure changes in constitutive or inducible VLRB N8 reactivity. To avoid conflict with endogenous alleles, such studies must be conducted in an HLA class I-negative context such as that of HLA class I-null human B cell 721.221 (159), human K562 erythroleukemia or murine cell lines which are expected to be VLRB N8-non-reactive.

It is incumbent upon us to determine the location of modified residues to gain structural insight and elucidate interactions. The existence of several near-universally conserved tyrosine residues satisfy one of the requirements of a consensus motif that serves a specific and universal biological function.

## *4.4 What are the functional and biological consequences of HLA class I tyrosine sulfation?*

Classically, peptide-MHC class I complexes engage the TCR to enable $CD8^+$ T cell activation (160). Despite this, cytotoxic T cell activation has been demonstrated to be acutely sensitive, requiring as little as three cognate peptide-MHC complexes for T cell activation (161). This suggests that modified HLA is for a purpose other than enhancing TCR ligation. The multifaceted HLA class I has been implicated in HLA *cis* interactions through terminal cysteine residues and oxidative stress (162, 163); infection-induced redistribution of HLA class I into membrane microdomains (164); peculiar signaling capacity of crosslinked HLA class I molecules (165-167); and binding to non-classical receptors such as inhibitory NK cell receptors (168-172). However, the most congruent with our observations is the appreciation that a T cell response is determined by not only TCR affinity for MHC-peptide but is positively correlated with affinity between MHC for its peptide (173).

The exceptional trait common to VLRB N8-reactive memory B and plasma cells is cellular longevity and this may guide us toward deducing the function of tyrosine-sulfated HLA class I. In addition to requiring extrinsic pro-survival cues provided by the microenvironment of the bone marrow for instance (174), like all cells, differentiated B lymphocytes are also under constant immune surveillance. To escape T cell-

mediated cytotoxicity, we hypothesize that one intrinsic mechanism is tyrosine sulfation of HLA class I which alters its affinity for peptide and thus the TCR. The implications of destabilizing the ternary complex are perhaps necessary for antigen-experienced B cells because they have the inherent potential to present somatically-mutated altered self peptide borne by hypermutated Ig. Investigation into Ig-derived peptides as tumor-specific neoantigens in lymphoma has demonstrated that idiotypic peptides are indeed presented by MHC class I (175-177). Thus, we propose that raising the threshold of T cell activation is one factor permitting long-lived B cells to persist despite presenting altered self peptides.

To elucidate a mechanism behind any effect on peptide loading, the spatiotemporal location of modification must be considered since tyrosine sulfation takes place in the *trans*-Golgi compartment. Only mature, TAP-dependent, quality-controlled MHC-peptide complexes (178-180) would be subject to TPST modification and it is therefore unlikely that tyrosine-sulfated HLA class I pre-determines initial peptide loading. Additionally, being loaded first in the ER before the complex proceeds to the *trans*-Golgi network, peptide may sterically prevent TPST access or addition of a sulfuryl group especially considering the positions of the consensus tyrosines of interest. Nonetheless, our experiments demonstrated competition between antibodies VLRB N8 and W6/32 (**Figs. 3.2c** and **3.2d**) for HLA class I. Therefore, since W6/32 binding to HLA class I is partially dependent on β2M association and peptide presentation (181-183), we deduce that VLRB N8-reactive tyrosine-sulfated HLA class I complexes are also in this folded conformation and that peptide-loaded HLA class I is subject to tyrosine sulfation.

In the context of post-peptide loading regulation, in what capacity can tyrosine sulfation determine peptide affinity? All three of the tyrosines of interest face the HLA class I groove and appear poised to interact with peptide (**Fig. 4.2b**). However, the interaction of potential sulfo-tyrosine residues with MHC-presented peptides and any change in affinity is determined by the individuality of each peptide. Tyrosine sulfation is binary and even with multiple sites, too few permutations are possible for peptide selectivity. If both increases and decreases in MHC-peptide affinity are possible, we

cannot expect a global decrease in affinity (and concomitant decrease in TCR ligation): certain residues may become electrostatically attracted to sulfated tyrosine whereas others will be repulsed. If MHC-peptide affinity is stochastically altered, stronger complexes may result that are not negatively selected against during T cell development and may enhance TCR ligation. We reason that if global peptide affinity is decreased, it may be through interaction between invariant non-side chain constituents of amino acids: the N- or C-terminus of a peptide. Intriguingly, several consensus tyrosines are positioned at the ends of the peptide loading groove as delimiters of MHC class I peptide length [9-mers being the most frequent (184)] via interaction with peptide anchor residues (185). Unfortunately, MHC-peptide affinity prediction algorithms such as NetMHCcons (version 1.1, DTU Bioinformatics) (186) were not designed to include post-translational modifications. Unlike for phospho-serine and phospho-threonine, glutamic acid which lacks an aromatic ring is an equally poor mimetic residue for phospho-tyrosine (187) as it is for sulfo-tyrosine. Therefore, no reliable *in silico* predictions can be made although mutation of Tyr59 and Tyr84 of HLA A24 are both predicted to alter affinity to human IgG1 heavy chain-derived (UniProt Knowledgebase entry P0DOX5) peptides of the most common HLA A24-restricted peptide length whereas Tyr85 is not predicted to interact with peptide in this model. Due to the positions of conserved tyrosine residues, a negative charge upon their aromatic rings may enable electrostatic interactions with the zwitterionic protonated amino group or deprotonated carboxyl groups of peptide termini (**Fig. 4.2**).

As intriguing as alteration of peptide affinity can be, it is speculative and inconsistent. Weakening of peptide affinity can produce open conformation HLA class I molecules which are labile and not in line with the high VLRB N8 reactivity and HLA class I expression. Additionally, cells become prone to missing-self-mediated NK cell killing. Therefore, we cannot exclude that other known interactions beyond MHC-TCR are affected at the B cell-T cell synapse or at B cell-NK cell interfaces. These problems will need to be addressed by interrogating the HLA class I immunopeptidome itself, via T cell functional assays, or by application/production of tyrosine sulfated HLA tetramers (188). All methods can be applied in the comparison of related VLRB N8-reactive and -non-reactive B cells serving as antigen-presenting cells, whether in

VLRB N8-reactivity-variable primary cell populations, or cell lines before and after stimulation.

## *4.5 What are the physiological consequences provoked by tyrosine-sulfated HLA class I in antigen-experienced B cells?*

Our current model supposes that BCR activation and cytokine stimulation can elicit VLRB N8 reactivity (**Fig. 4.1**). After a naïve B cell has met this prerequisite, what are the biological consequences of modified HLA class I at the cellular level and the physiological consequences for humoral immunity?

The impetus for our study of VLRB N8 is that this antibody's reactivity is a correlate of antigen-experience and late-stage differentiation in B cells. However, it is an imperfect correlate with a portion of tonsillar lymphocytes being non-reactive to this reagent. Therefore, by either examining traits shared by VLRB N8-reactive cells or discarding traits shared between non-reactive cells, we can focus on the functional implications of VLRB N8 reactivity. The most informative comparisons will be between cells that are homogeneous with the exception of VLRB N8 reactivity. Our observations of the relative uniformity in VLRB N8 reactivity in peripheral blood are consistent with those of others who have observed that blood $IgD^+/CD27^+$ marginal zone-equivalent cells are unimodal and cannot be parsed even by expression of IgM, CD21, CD23, and CD1c (105). Therefore, given the antibody panels at our disposal, the best comparisons we can make would be between tonsillar VLRB N8-reactive memory B or plasma cells and their non-reactive counterparts that make up about 20% of these antigen-experienced B cells. We initiated such an endeavor by attempting to match the unaccounted-for tonsillar memory B cells to the $FCRL4^+$ minority. It has been observed that $FCRL4^+$ cells represent around 10% of tonsillar memory B cells (100). However, this previously defined subpopulation only partially corresponded to VLRB $N8^-$ cells (**Fig. 3.10**).

Further parsing of human antigen-experienced B cells can be performed using markers such as CD11b/c, CD19, CD20, CD138, and Ki-67 (108, 148). However, given the thus far inimitable staining pattern of our reagent, it is likely futile to seek cell

surface markers that follow or diverge from the pattern of VLRB N8 reactivity – if the specificity we obtained can be replicated by other means of cell surface immunophenotyping, VLRB N8 would not be as novel a reagent as it is. Not all changes undergone by a cell are accounted for by currently known cell surface markers. Recent studies into the FCRL4$^+$ memory B cell subpopulation demonstrated that FCRL4 expression is associated with a different gene expression profile (108), and antigen receptor repertoire (189). Likewise, perhaps surface markers indicative of antigen encounter remain to be discovered but do not accompany expression of a known surface marker or any surface determinant. Given that antigen stimulation is a necessity, perhaps VLRB N8 is a gauge that increases with activation history and fitness in the most successful B cells? Firstly, we observed that IgD$^+$ memory B cells are less reactive than their class-switched counterparts whether in health or disease (**Fig. 3.6**). Also consistent is the increased binding to autoimmune B cell populations which generally dominate non-disease-mediating clones and are oligoclonal in the case of MS. Perhaps VLRB N8 reactivity can be an indication of an IFN gene signature that is deferred to because circulating IFN itself is difficult to detect. To determine any associations between VLRB N8 reactivity and traits that cannot be immunophenotyped, comparative studies analyzing the antibody repertoire and transcriptome of VLRB N8-reactive and -non-reactive cell lines and B cell populations can be performed.

If our phenotyping of VLRB N8$^+$ antigen-experienced B cells reveals a correlation with activation history or longevity, the question becomes whether this is a mere association or if there are physiological implications for humoral immunity. Given the ubiquity of TPST orthologues throughout the animal kingdom and the conservation of Tyr59, Tyr84 and Tyr85 or analogues in mouse MHC class I, analogous sulfation motifs and functions are potentially preserved in mice, permitting study on any outcomes of tyrosine sulfation of MHC class I. Individually deleting either TPST paralogues in mice leads to reduced body weight (190), and infertility in TPST2 knockout animals (191). Absence of both TPSTs leads to early postnatal death and/or pulmonary and thyroid dysfunction (192). However, none of these studies have characterized the resultant immune compartment after genome editing. If tyrosine sulfation of HLA class I diminishes TCR ligation, targeted B cell deletion of *TPST2* may reveal differences in

recall responses compared to WT animals as measurable by analyzing antibody titers in response to immunization and perhaps deficiency in the memory B and plasma cell compartments.

## *4.6 VLR antibodies in clinical applications*

The application of VLR antibodies need not be limited to basic research but can be translated for clinical applications. The use of VLRB antibodies for detection of circulating diagnostic or prognostic biomarkers has been discussed in **Chapter 2**. However, diagnosis or prognosis can be realized by means other than ELISA: an anti-idiotype VLRB (VLR39) was used to track chronic lymphocytic leukemia by flow cytometry staining of peripheral blood (44); and an anti-Thomsen-Friedenreich α VLRB was successfully tested for immunohistochemistry (43). Likewise, such methods are available to us depending on the nature of a breast cancer biomarker and compatibility of a promising VLR for detection of circulating tumor cells or for phenotyping of *in situ* breast cancer tumors. Likewise, we envision that VLRB N8 can be applied much like VLR39 due to elevated binding to memory B and plasma cells from patients suffering from MS or SLE.

Whether in eliciting anti-tumor cytotoxicity (herceptin/trastuzumab inhibiting growth of HER2/neu-overexpressing tumours) (193) or in B cell depletion (rituximab targeting of CD20-expressing B cells) (194), antibodies are at the forefront of immunotherapeutic agents targeting malignancies and autoimmune diseases. However, existing therapeutic antibodies are composed of receptors of mammalian origin. Presently, research is focused on adapting VLR antibodies for therapy which is both more complicated and ambitious than diagnosis, given the *in vivo* nature of therapeutic strategies.

The traditional route for xenogeneic antibodies is fusion to host Fc which opens a host of actionable mechanisms such as antibody-dependent cellular cytotoxicity and complement-mediated cytotoxicity. Any Fc fusion protein can be tested *in vitro* for specificity and off-target killing. More artificial strategies involve cytotoxic drug or apoptotic protein conjugation to the VLR binding domain – Lee et al. demonstrated

this feasibility with a monomethyl auristatin F- (195) or apoptin-anti-EGFR repebody[1] conjugate (197) which significantly restricted tumor growth in a xenograft mouse model of non-small-cell lung cancer. Otherwise, cytotoxicity can be mediated by effector cells expressing a chimeric antigen receptor (CAR) in which the conventional single-chain variable fragment is exchanged for the antigen binding region of a VLR before fusion to the intracellular domains of receptors such as CD3 of the TCR complex to mimic the signals conferred by an immunological synapse. The efficacy of anti-CD5 and anti-BCR VLR CARs have been tested *in vitro* by observing activation marker CD69 in Jurkat cells or cytotoxicity mediated by the NK-92 cell line (198).

Most pertinent for anti-serum antigen VLR antibodies, antibody therapy does not need to focus solely on inducing cytotoxicity but can also be 'humoral' as demonstrated by the work of Hwang et al. whose anti-VEGF repebody was able to prevent binding of VEGF to both of its receptors: Flt-1 and KDR (199). Through crossreactivity with mouse VEGF, this antibody was also able to lower *de novo* vasculature formation and leakage in a mouse model of choroidal neovascularization. On a similar note, Lee et al. successfully used an anti-IL-6 repebody to neutralize soluble IL-6 in a xenograft model of non-small-cell lung cancer (200).

In therapy, antibody specificity must be counterbalanced by mending the reagent itself in the event it is a target of the host immune system. Both alloantigens and mouse monoclonal antibodies can elicit human host responses. The evolutionary distance and largely foreign structure of a VLR can prove to be its weakness as much as its strength in therapy. This potential problem can be addressed by the process of humanization which exchanges backbone residues that exhibit minimal variability and are not essential to binding (18, 196). One candidate of a tolerogenic substitution partner would be human GP1bα (**Fig. 1.2b**). As demonstrated by Rogozin et al., this glycoprotein receptor on platelets has been omnipresent throughout jawless vertebrate evolution with orthologues in all vertebrates and beyond (18). Being the likely predecessor to modern VLRs, GP1bα is uncannily similar in modular composition with 24

[1]Repebody A VLRB-based artificial scaffold and consensus sequence determined from the alignment of 1,400 VLRB LRRV modules (196). Random mutagenesis and selection culminated in several antigen-specific repebody antibodies described herein.

aa-residue LRRVs and includes a unique insert in its LRRCT, together allowing for facile exchange of residues. Other LRR alternatives exist such as SLIT2, a signaling molecule in nervous system development. However, it is possible that such corrections will not be necessary owing to the structure of VLRs: residues with the most immunogenic potential are likely the hypervariable antigen-contact residues which are sheltered within the concave surface of the structure whereas homology is expected between the plethora of LRR proteins in order to maintain the parallel β-pleated sheet structure. Supporting this hypothesis, no modification was necessary for both anti-VEGF (199) and anti-IL-6 VLR-based repebodies (200). No cytotoxicity was detectable *in vitro* for the former and, for the latter, no inflammatory cytokines nor an anti-VLR humoral response in mice were elicited when compared to vehicle treatment. These non-human studies suggest a low immunogenicity of VLRB-based scaffolds and so it remains to be determined whether they are indicative for VLR antibodies themselves or their humanized forms in human hosts.

## *4.7 'Basic' biology from the study of alternate immune systems*

The value of non-human research is best exemplified by elucidation of the ontogeny of B cells and the dual nature of adaptive immunity which was propelled by characterization of the chicken bursa of Fabricius (201). Much like the discovery of the CRISPR-Cas system in bacteria, our own research focuses on alternate solutions to the conundrum of immunity and appropriating them for human clinical benefit. However, we nonetheless share some kinship and similarities with non-mammalian organisms such as fishes and their immune systems. This is exemplified by the near-universal conservation of Ig isotypes IgM; thymus and spleen in lineages as distant as cartilaginous fishes (7). Thus, there is as much to learn from our points of convergence as there are from points of divergence. Immune features we observe in other organisms may simply be more overt rather than absent in humans.

Prior to Li and colleagues' discovery in 2006 (202), it was thought that only leukocytes such as neutrophils, macrophages and dendritic cells were capable of phagocytosis. This was dispelled by the observation that an $IgM^+$ teleost B cell population was capable of BCR- and complement receptor-independent uptake of beads,

particles, and bacteria, after which the phagosome-confined material could be degraded. These B cells are superior in presentation of particulate antigen to cognate T cells than are macrophages (203) owing to a moderate number of lysosomes and protease content (204). Have human B cells evolutionarily conserved remnants of such a role? Indeed, the identification of B cell phagocytosis was expanded to amphibians and reptiles (205) before finally being observed in mammals (203). Non-human-derived 'basic' biology is not a tangent because as we look into other species, the gaze can shift back to us.

In work more akin to our own, Altman et al. compared the humoral response between the lamprey and mouse when challenged with influenza A virus (40). Surprisingly, despite over 500 million years of separation, both organisms responded predominantly to the globular domain of HA and unfortunately, without cross-strain specificity. Additionally, the epitopes targeted overlap because individual Ig antigen-binding fragments sterically competed with VLRB-containing larval plasma. Although, there is ample evidence that fish immune systems are dissimilar to that of mammals, considering both the similarities and dissimilarities can aid us in understanding antigenicity, epitope dominance, and viral evasion in vaccine design. In this case, it can be inferred that the natural response to influenza A weighs heavily on the virus itself and cannot be altered by antibody structure - some rules of antibody recognition are universal such as biased representation of aromatic residues in paratopes (40). There is value in studying alternate organisms and systems regardless of whether our hypothesis is proven correct or wrong.

Finally, philosophically, the study of non-humans can help us appreciate the ingenuity of other organisms so that we can distance ourselves from anthropocentrism and murine-centrism that can hinder scientific research. Although adaptive responses were initially observed in jawless fishes over 50 years ago, the underlying mediators and mechanisms were deciphered only 40 years later. As best articulated by Pradeu and Du Pasquier, such relative lack of success was hampered by researchers interpreting the 'same phenomenon' as the 'same mechanism' without postulating that immunity is 'multiply-realizable' (206).

## *4.8 Concluding remarks*

500 million years of vertebrate evolution is marked by evolutionarily significant events such as evolutionary radiation, the initial colonization of terrestrial habitats, mass extinction, and glacial ages. Yet, in two highly divergent vertebrate clades, the cardinal features of adaptive immunity are remarkably analogous though not always homologous. The distinct VLR-based immune system described herein illustrates an example of the grandeurs that are the myriad solutions for the age-old challenge of immunity.

Lamprey immunity is not basic and is 'far from primitive' (207). In strong opposition to any perceived *scala naturae* in biology, fitness is relative as organisms adapt to their ecological niches. Extant species can employ divergent strategies that are equally adaptive for survival. In this dissertation, our findings support that the lamprey immune system is another form of adaptive immunity with features either nonexistent or rare in gnathostome immunity. Likewise, the reverse is also true.

Knowledge and therapeutic innovations await from the study of divergent adaptive immune systems. We hope that our scientific foray into lamprey immunity has brought us closer to answers that are within our reach, but not yet within our grasp.

# References

1. The UniProt Consortium. 2017. UniProt: the universal protein knowledgebase. *Nucleic Acids Res.* 45: D158-D169.

2. Locey, K. J. and J. T. Lennon. 2016. Scaling laws predict global microbial diversity. *Proc. Natl. Acad. Sci. U. S. A.* 113: 5970-5975.

3. Aebersold, R., J. N. Agar, I. J. Amster, M. S. Baker, C. R. Bertozzi, E. S. Boja, C. E. Costello, B. F. Cravatt, C. Fenselau, B. A. Garcia, Y. Ge, J. Gunawardena, R. C. Hendrickson, P. J. Hergenrother, C. G. Huber, A. R. Ivanov, O. N. Jensen, M. C. Jewett, N. L. Kelleher, L. L. Kiessling, N. J. Krogan, M. R. Larsen, J. A. Loo, R. R. Ogorzalek Loo, E. Lundberg, M. J. MacCoss, P. Mallick, V. K. Mootha, M. Mrksich, T. W. Muir, S. M. Patrie, J. J. Pesavento, S. J. Pitteri, H. Rodriguez, A. Saghatelian, W. Sandoval, H. Schluter, S. Sechi, S. A. Slavoff, L. M. Smith, M. P. Snyder, P. M. Thomas, M. Uhlen, J. E. Van Eyk, M. Vidal, D. R. Walt, F. M. White, E. R. Williams, T. Wohlschlager, V. H. Wysocki, N. A. Yates, N. L. Young, and B. Zhang. 2018. How many human proteoforms are there? *Nat. Chem. Biol.* 14: 206-214.

4. Cannon, J. P., R. N. Haire, J. P. Rast, and G. W. Litman. 2004. The phylogenetic origins of the antigen-binding receptors and somatic diversification mechanisms. *Immunol. Rev.* 200: 12-22.

5. Kurosaki, T., K. Kometani, and W. Ise. 2015. Memory B cells. *Nat. Rev. Immunol.* 15: 149-159.

6. Horvath, P. and R. Barrangou. 2010. CRISPR/Cas, the immune system of bacteria and archaea. *Science* 327: 167-170.

7. Flajnik, M. F. 2018. A cold-blooded view of adaptive immunity. *Nat. Rev. Immunol.*

8. Kaucka, M. and I. Adameyko. 2017. Evolution and development of the cartilaginous skull: From a lancelet towards a human face. *Semin. Cell Dev. Biol.*

9. Guo, Z., D. Andreou, and J. R. Britton. 2017. Sea Lamprey Petromyzon marinus Biology and Management Across Their Native and Invasive Ranges: Promoting Conservation by Knowledge Transfer. *Rev. Fish. Sci. Aquac.* 25: 84-99.

10. Zwollo, P. 2012. Why spawning salmon return to their natal stream: the immunological imprinting hypothesis. *Dev. Comp. Immunol.* 38: 27-29.

11. Ota, T., T. A. Nguyen, E. Huang, H. W. Detrich 3rd, and C. T. Amemiya. 2003. Positive Darwinian selection operating on the immunoglobulin heavy chain of Antarctic fishes. *J. Exp. Zool. B. Mol. Dev. Evol.* 295: 45-58.

12. Janvier, P. 2006. Palaeontology: modern look for ancient lamprey. *Nature* 443: 921-924.

13. Gess, R. W., M. I. Coates, and B. S. Rubidge. 2006. A lamprey from the Devonian period of South Africa. *Nature* 443: 981-984.

14. Perey, D. Y., J. Finstad, B. Pollara, and R. A. Good. 1968. Evolution of the immune response. VI. First and second set skin homograft rejections in primitive fishes. *Lab. Invest.* 19: 591-597.

15. FINSTAD, J. and R. A. GOOD. 1964. The Evolution of the Immune Response. 3. Immunologic Responses in the Lamprey. *J. Exp. Med.* 120: 1151-1168.

16. Pancer, Z., W. E. Mayer, J. Klein, and M. D. Cooper. 2004. Prototypic T cell receptor and CD4-like coreceptor are expressed by lymphocytes in the agnathan sea lamprey. *Proc. Natl. Acad. Sci. U. S. A.* 101: 13273-13278.

17. Pancer, Z., C. T. Amemiya, G. R. Ehrhardt, J. Ceitlin, G. L. Gartland, and M. D. Cooper. 2004. Somatic diversification of variable lymphocyte receptors in the agnathan sea lamprey. *Nature* 430: 174-180.

18. Rogozin, I. B., L. M. Iyer, L. Liang, G. V. Glazko, V. G. Liston, Y. I. Pavlov, L. Aravind, and Z. Pancer. 2007. Evolution and diversification of lamprey antigen receptors: evidence for involvement of an AID-APOBEC family cytosine deaminase. *Nat. Immunol.* 8: 647-656.

19. Nagawa, F., N. Kishishita, K. Shimizu, S. Hirose, M. Miyoshi, J. Nezu, T. Nishimura, H. Nishizumi, Y. Takahashi, S. Hashimoto, M. Takeuchi, A. Miyajima, T. Takemori, A. J. Otsuka, and H. Sakano. 2007. Antigen-receptor genes of the agnathan lamprey are assembled by a process involving copy choice. *Nat. Immunol.* 8: 206-213.

20. Guo, P., M. Hirano, B. R. Herrin, J. Li, C. Yu, A. Sadlonova, and M. D. Cooper. 2009. Dual nature of the adaptive immune system in lampreys. *Nature* 459: 796-801.

21. Ratcliffe, M. J. 2006. Antibodies, immunoglobulin genes and the bursa of Fabricius in chicken B cell development. *Dev. Comp. Immunol.* 30: 101-118.

22. Boehm, T., N. McCurley, Y. Sutoh, M. Schorpp, M. Kasahara, and M. D. Cooper. 2012. VLR-based adaptive immunity. *Annu. Rev. Immunol.* 30: 203-220.

23. Li, J., S. Das, B. R. Herrin, M. Hirano, and M. D. Cooper. 2013. Definition of a third VLR gene in hagfish. *Proc. Natl. Acad. Sci. U. S. A.* 110: 15013-15018.

24. Bajoghli, B., P. Guo, N. Aghaallaei, M. Hirano, C. Strohmeier, N. McCurley, D. E. Bockman, M. Schorpp, M. D. Cooper, and T. Boehm. 2011. A thymus candidate in lampreys. *Nature* 470: 90-94.

25. Gojobori, T. and M. Nei. 1986. Relative contributions of germline gene variation and somatic mutation to immunoglobulin diversity in the mouse. *Mol. Biol. Evol.* 3: 156-167.

26. Kasamatsu, J., Y. Sutoh, K. Fugo, N. Otsuka, K. Iwabuchi, and M. Kasahara. 2010. Identification of a third variable lymphocyte receptor in the lamprey. *Proc. Natl. Acad. Sci. U. S. A.* 107: 14304-14308.

27. Hirano, M., P. Guo, N. McCurley, M. Schorpp, S. Das, T. Boehm, and M. D. Cooper. 2013. Evolutionary implications of a third lymphocyte lineage in lampreys. *Nature* 501: 435-438.

28. Das, S., J. Li, S. J. Holland, L. M. Iyer, M. Hirano, M. Schorpp, L. Aravind, M. D. Cooper, and T. Boehm. 2014. Genomic donor cassette sharing during VLRA and VLRC assembly in jawless vertebrates. *Proc. Natl. Acad. Sci. U. S. A.* 111: 14828-14833.

29. Criscitiello, M. F., Y. Ohta, M. Saltis, E. C. McKinney, and M. F. Flajnik. 2010. Evolutionarily conserved TCR binding sites, identification of T cells in primary lymphoid tissues, and surprising trans-rearrangements in nurse shark. *J. Immunol.* 184: 6950-6960.

30. Chien, Y. H., M. Iwashima, K. B. Kaplan, J. F. Elliott, and M. M. Davis. 1987. A new T-cell receptor gene located within the alpha locus and expressed early in T-cell differentiation. *Nature* 327: 677-682.

31. Naik, A. K., A. Hawwari, and M. S. Krangel. 2015. Specification of Vdelta and Valpha usage by Tcra/Tcrd locus V gene segment promoters. *J. Immunol.* 194: 790-794.

32. Alder, M. N., B. R. Herrin, A. Sadlonova, C. R. Stockard, W. E. Grizzle, L. A. Gartland, G. L. Gartland, J. A. Boydston, C. L. Turnbough Jr, and M. D. Cooper. 2008. Antibody responses of variable lymphocyte receptors in the lamprey. *Nat. Immunol.* 9: 319-327.

33. Litman, G. W., J. P. Rast, and S. D. Fugmann. 2010. The origins of vertebrate adaptive immunity. *Nat. Rev. Immunol.* 10: 543-553.

34. Kuraku, S. and S. Kuratani. 2006. Time scale for cyclostome evolution inferred with a phylogenetic diagnosis of hagfish and lamprey cDNA sequences. *Zoolog Sci.* 23: 1053-1064.

35. Huizinga, E. G., S. Tsuji, R. A. Romijn, M. E. Schiphorst, P. G. de Groot, J. J. Sixma, and P. Gros. 2002. Structures of glycoprotein Ibalpha and its complex with von Willebrand factor A1 domain. *Science* 297: 1176-1179.

36. Velikovsky, C. A., L. Deng, S. Tasumi, L. M. Iyer, M. C. Kerzic, L. Aravind, Z. Pancer, and R. A. Mariuzza. 2009. Structure of a lamprey variable lymphocyte receptor in complex with a protein antigen. *Nat. Struct. Mol. Biol.* 16: 725-730.

37. Collins, B. C., R. J. Gunn, T. R. McKitrick, R. D. Cummings, M. D. Cooper, B. R. Herrin, and I. A. Wilson. 2017. Structural Insights into VLR Fine Specificity for Blood Group Carbohydrates. *Structure* 25: 1667-1678.e4.

38. Boes, M. 2000. Role of natural and immune IgM antibodies in immune responses. *Mol. Immunol.* 37: 1141-1149.

39. Herrin, B. R., M. N. Alder, K. H. Roux, C. Sina, G. R. Ehrhardt, J. A. Boydston, C. L. Turnbough Jr, and M. D. Cooper. 2008. Structure and specificity of lamprey monoclonal antibodies. *Proc. Natl. Acad. Sci. U. S. A.* 105: 2040-2045.

40. Altman, M. O., J. R. Bennink, J. W. Yewdell, and B. R. Herrin. 2015. Lamprey VLRB response to influenza virus supports universal rules of immunogenicity and antigenicity. *Elife* 4: 10.7554/eLife.07467.

41. Yu, C., S. Ali, J. St-Germain, Y. Liu, X. Yu, D. L. Jaye, M. F. Moran, M. D. Cooper, and G. R. Ehrhardt. 2012. Purification and identification of cell surface antigens using lamprey monoclonal antibodies. *J. Immunol. Methods* 386: 43-49.

42. Tasumi, S., C. A. Velikovsky, G. Xu, S. A. Gai, K. D. Wittrup, M. F. Flajnik, R. A. Mariuzza, and Z. Pancer. 2009. High-affinity lamprey VLRA and VLRB monoclonal antibodies. *Proc. Natl. Acad. Sci. U. S. A.* 106: 12891-12896.

43. Hong, X., M. Z. Ma, J. C. Gildersleeve, S. Chowdhury, J. J. Barchi Jr, R. A. Mariuzza, M. B. Murphy, L. Mao, and Z. Pancer. 2013. Sugar-binding proteins from fish: selection of high affinity "lambodies" that recognize biomedically relevant glycans. *ACS Chem. Biol.* 8: 152-160.

44. Nakahara, H., B. R. Herrin, M. N. Alder, R. Catera, X. J. Yan, N. Chiorazzi, and M. D. Cooper. 2013. Chronic lymphocytic leukemia monitoring with a Lamprey idiotope-specific antibody. *Cancer. Immunol. Res.* 1: 223-228.

45. Han, B. W., B. R. Herrin, M. D. Cooper, and I. A. Wilson. 2008. Antigen recognition by variable lymphocyte receptors. *Science* 321: 1834-1837.

46. Stanfield, R. L., H. Dooley, M. F. Flajnik, and I. A. Wilson. 2004. Crystal structure of a shark single-domain antibody V region in complex with lysozyme. *Science* 305: 1770-1773.

47. Desmyter, A., T. R. Transue, M. A. Ghahroudi, M. H. Thi, F. Poortmans, R. Hamers, S. Muyldermans, and L. Wyns. 1996. Crystal structure of a camel single-domain VH antibody fragment in complex with lysozyme. *Nat. Struct. Biol.* 3: 803-811.

48. Doria-Rose, N. A., R. M. Klein, M. G. Daniels, S. O'Dell, M. Nason, A. Lapedes, T. Bhattacharya, S. A. Migueles, R. T. Wyatt, B. T. Korber, J. R. Mascola, and M. Connors. 2010. Breadth of human immunodeficiency virus-specific neutralizing activity in sera: clustering analysis and association with clinical variables. *J. Virol.* 84: 1631-1636.

49. Doores, K. J., L. Kong, S. A. Krumm, K. M. Le, D. Sok, U. Laserson, F. Garces, P. Poignard, I. A. Wilson, and D. R. Burton. 2015. Two classes of broadly neutralizing antibodies within a single lineage directed to the high-mannose patch of HIV envelope. *J. Virol.* 89: 1105-1118.

50. Scanlan, C. N., J. Offer, N. Zitzmann, and R. A. Dwek. 2007. Exploiting the defensive sugars of HIV-1 for drug and vaccine design. *Nature* 446: 1038-1045.

51. Walker, L. M., M. Huber, K. J. Doores, E. Falkowska, R. Pejchal, J. P. Julien, S. K. Wang, A. Ramos, P. Y. Chan-Hui, M. Moyle, J. L. Mitcham, P. W. Hammond, O. A. Olsen, P. Phung, S. Fling, C. H. Wong, S. Phogat, T. Wrin, M. D. Simek, Protocol G Principal Investigators, W. C. Koff, I. A. Wilson, D. R. Burton, and P. Poignard. 2011. Broad neutralization coverage of HIV by multiple highly potent antibodies. *Nature* 477: 466-470.

52. Simek, M. D., W. Rida, F. H. Priddy, P. Pung, E. Carrow, D. S. Laufer, J. K. Lehrman, M. Boaz, T. Tarragona-Fiol, G. Miiro, J. Birungi, A. Pozniak, D. A. McPhee, O. Manigart, E. Karita, A. Inwoley, W. Jaoko, J. Dehovitz, L. G. Bekker, P. Pitisuttithum, R. Paris, L. M. Walker, P. Poignard, T. Wrin, P. E. Fast, D. R. Burton, and W. C. Koff. 2009. Human immunodeficiency virus type 1 elite neutralizers: individuals with broad and potent neutralizing activity identified by using a high-throughput neutralization assay together with an analytical selection algorithm. *J. Virol.* 83: 7337-7348.

53. Moore, P. L., E. S. Gray, C. K. Wibmer, J. N. Bhiman, M. Nonyane, D. J. Sheward, T. Hermanus, S. Bajimaya, N. L. Tumba, M. R. Abrahams, B. E. Lambson, N. Ranchobe, L. Ping, N. Ngandu, Q. Abdool Karim, S. S. Abdool Karim, R. I. Swanstrom, M. S. Seaman, C. Williamson, and L. Morris. 2012. Evolution of an HIV glycan-dependent broadly neutralizing antibody epitope through immune escape. *Nat. Med.* 18: 1688-1692.

54. Williams, L. D., G. Ofek, S. Schatzle, J. R. McDaniel, X. Lu, N. I. Nicely, L. Wu, C. S. Lougheed, T. Bradley, M. K. Louder, K. McKee, R. T. Bailer, S. O'Dell, I. S. Georgiev, M. S. Seaman, R. J. Parks, D. J. Marshall, K. Anasti, G. Yang, X. Nie, N. L. Tumba, K. Wiehe, K. Wagh, B. Korber, T. B. Kepler, S. Munir Alam, L. Morris, G. Kamanga, M. S. Cohen, M. Bonsignori, S. M. Xia, D. C. Montefiori, G. Kelsoe, F. Gao, J. R. Mascola, M. A. Moody, K. O. Saunders, H. X. Liao, G. D. Tomaras, G. Georgiou,

and B. F. Haynes. 2017. Potent and broad HIV-neutralizing antibodies in memory B cells and plasma. *Sci. Immunol.* 2: 10.1126/sciimmunol.aal2200.

55. Kwong, P. D. and J. R. Mascola. 2012. Human antibodies that neutralize HIV-1: identification, structures, and B cell ontogenies. *Immunity* 37: 412-425.

56. Doria-Rose, N. A., C. A. Schramm, J. Gorman, P. L. Moore, J. N. Bhiman, B. J. DeKosky, M. J. Ernandes, I. S. Georgiev, H. J. Kim, M. Pancera, R. P. Staupe, H. R. Altae-Tran, R. T. Bailer, E. T. Crooks, A. Cupo, A. Druz, N. J. Garrett, K. H. Hoi, R. Kong, M. K. Louder, N. S. Longo, K. McKee, M. Nonyane, S. O'Dell, R. S. Roark, R. S. Rudicell, S. D. Schmidt, D. J. Sheward, C. Soto, C. K. Wibmer, Y. Yang, Z. Zhang, NISC Comparative Sequencing Program, J. C. Mullikin, J. M. Binley, R. W. Sanders, I. A. Wilson, J. P. Moore, A. B. Ward, G. Georgiou, C. Williamson, S. S. Abdool Karim, L. Morris, P. D. Kwong, L. Shapiro, and J. R. Mascola. 2014. Developmental pathway for potent V1V2-directed HIV-neutralizing antibodies. *Nature* 509: 55-62.

57. Klein, F., R. Diskin, J. F. Scheid, C. Gaebler, H. Mouquet, I. S. Georgiev, M. Pancera, T. Zhou, R. B. Incesu, B. Z. Fu, P. N. Gnanapragasam, T. Y. Oliveira, M. S. Seaman, P. D. Kwong, P. J. Bjorkman, and M. C. Nussenzweig. 2013. Somatic mutations of the immunoglobulin framework are generally required for broad and potent HIV-1 neutralization. *Cell* 153: 126-138.

58. Yu, C., Y. Liu, J. T. Chan, J. Tong, Z. Li, M. Shi, D. Davani, M. Parsons, S. Khan, W. Zhan, S. Kyu, E. Grunebaum, P. Campisi, E. J. Propst, D. L. Jaye, S. Trudel, M. F. Moran, M. Ostrowski, B. R. Herrin, F. E. Lee, I. Sanz, M. D. Cooper, and G. R. Ehrhardt. 2016. Identification of human plasma cells with a lamprey monoclonal antibody. *JCI Insight* 1: 10.1172/jci.insight.84738. Epub 2016 Mar 17.

59. Dolman, C. E. 1973. The Donald T. Fraser Memorial Lecture, 1973. Landmarks and pioneers in the control of diphtheria. *Can. J. Public Health* 64: 317-336.

60. Magnadottir, B., S. Gudmundsdottir, B. K. Gudmundsdottir, and S. Helgason. 2009. Natural antibodies of cod (Gadus morhua L.): specificity, activity and affinity. *Comp. Biochem. Physiol. B. Biochem. Mol. Biol.* 154: 309-316.

61. Canadian Cancer Society's Advisory Committee on Cancer Statistics. 2017. Canadian Cancer Statistics 2017. Canadian Cancer Society, Toronto, ON.

62. Kazarian, A., O. Blyuss, G. Metodieva, A. Gentry-Maharaj, A. Ryan, E. M. Kiseleva, O. M. Prytomanova, I. J. Jacobs, M. Widschwendter, U. Menon, and J. F. Timms. 2017. Testing breast cancer serum biomarkers for early detection and prognosis in pre-diagnosis samples. *Br. J. Cancer* 116: 501-508.

63. Bellan, C., L. Stefano, F. Giulia de, E. A. Rogena, and L. Lorenzo. 2009. Burkitt lymphoma versus diffuse large B-cell lymphoma: a practical approach. *Hematol. Oncol.* 27: 182-185.

64. Vohra, P., B. Buelow, Y. Y. Chen, M. Serrano, M. S. Vohra, A. Berry, and B. M. Ljung. 2016. Estrogen receptor, progesterone receptor, and human epidermal growth factor receptor 2 expression in breast cancer FNA cell blocks and paired histologic specimens: A large retrospective study. *Cancer. Cytopathol.* 124: 828-835.

65. Molina, R., J. M. Auge, J. M. Escudero, X. Filella, G. Zanon, J. Pahisa, B. Farrus, M. Munoz, and M. Velasco. 2010. Evaluation of tumor markers (HER-2/neu oncoprotein, CEA, and CA 15.3) in patients with locoregional breast cancer: prognostic value. *Tumour Biol.* 31: 171-180.

66. Greipp, P. R., J. San Miguel, B. G. Durie, J. J. Crowley, B. Barlogie, J. Blade, M. Boccadoro, J. A. Child, H. Avet-Loiseau, R. A. Kyle, J. J. Lahuerta, H. Ludwig, G. Morgan, R. Powles, K. Shimizu, C. Shustik, P. Sonneveld, P. Tosi, I. Turesson, and J. Westin. 2005. International staging system for multiple myeloma. *J. Clin. Oncol.* 23: 3412-3420.

67. Li, J., R. Orlandi, C. N. White, J. Rosenzweig, J. Zhao, E. Seregni, D. Morelli, Y. Yu, X. Y. Meng, Z. Zhang, N. E. Davidson, E. T. Fung, and D. W. Chan. 2005. Independent validation of candidate breast cancer serum biomarkers identified by mass spectrometry. *Clin. Chem.* 51: 2229-2235.

68. Blixt, O., D. Bueti, B. Burford, D. Allen, S. Julien, M. Hollingsworth, A. Gammerman, I. Fentiman, J. Taylor-Papadimitriou, and J. M. Burchell. 2011. Autoantibodies to aberrantly glycosylated MUC1 in early stage breast cancer are associated with a better prognosis. *Breast Cancer Res.* 13: R25.

69. Brandle, S. M., B. Obermeier, M. Senel, J. Bruder, R. Mentele, M. Khademi, T. Olsson, H. Tumani, W. Kristoferitsch, F. Lottspeich, H. Wekerle, R. Hohlfeld, and K. Dornmair. 2016. Distinct oligoclonal band antibodies in multiple sclerosis recognize ubiquitous self-proteins. *Proc. Natl. Acad. Sci. U. S. A.* 113: 7864-7869.

70. Pavlou, M. P., V. Kulasingam, E. R. Sauter, B. Kliethermes, and E. P. Diamandis. 2010. Nipple aspirate fluid proteome of healthy females and patients with breast cancer. *Clin. Chem.* 56: 848-855.

71. Misek, D. E. and E. H. Kim. 2011. Protein biomarkers for the early detection of breast cancer. *Int. J. Proteomics* 2011: 343582.

72. Berg, W. A., L. Gutierrez, M. S. NessAiver, W. B. Carter, M. Bhargavan, R. S. Lewis, and O. B. Ioffe. 2004. Diagnostic accuracy of mammography, clinical examination, US, and MR imaging in preoperative assessment of breast cancer. *Radiology* 233: 830-849.

73. Siegel, R. L., K. D. Miller, and A. Jemal. 2017. Cancer Statistics, 2017. *CA Cancer. J. Clin.* 67: 7-30.

74. van 't Veer, L. J., H. Dai, M. J. van de Vijver, Y. D. He, A. A. Hart, M. Mao, H. L. Peterse, K. van der Kooy, M. J. Marton, A. T. Witteveen, G. J. Schreiber, R. M. Kerkhoven, C. Roberts, P. S. Linsley, R. Bernards, and S. H. Friend. 2002. Gene expression profiling predicts clinical outcome of breast cancer. *Nature* 415: 530-536.

75. van Winden, A. W., M. C. Gast, J. H. Beijnen, E. J. Rutgers, D. E. Grobbee, P. H. Peeters, and C. H. van Gils. 2009. Validation of previously identified serum biomarkers for breast cancer with SELDI-TOF MS: a case control study. *BMC Med. Genomics* 2: 4-8794-2-4.

76. Li, Y., Y. Li, T. Chen, A. S. Kuklina, P. Bernard, F. J. Esteva, H. Shen, M. Ferrari, and Y. Hu. 2014. Circulating proteolytic products of carboxypeptidase N for early detection of breast cancer. *Clin. Chem.* 60: 233-242.

77. Le Naour, F., D. E. Misek, M. C. Krause, L. Deneux, T. J. Giordano, S. Scholl, and S. M. Hanash. 2001. Proteomics-based identification of RS/DJ-1 as a novel circulating tumor antigen in breast cancer. *Clin. Cancer Res.* 7: 3328-3335.

78. Dube, D. H. and C. R. Bertozzi. 2005. Glycans in cancer and inflammation--potential for therapeutics and diagnostics. *Nat. Rev. Drug Discov.* 4: 477-488.

79. Peracaula, R., G. Tabares, L. Royle, D. J. Harvey, R. A. Dwek, P. M. Rudd, and R. de Llorens. 2003. Altered glycosylation pattern allows the distinction between prostate-specific antigen (PSA) from normal and tumor origins. *Glycobiology* 13: 457-470.

80. Fernandes, B., U. Sagman, M. Auger, M. Demetrio, and J. W. Dennis. 1991. Beta 1-6 branched oligosaccharides as a marker of tumor progression in human breast and colon neoplasia. *Cancer Res.* 51: 718-723.

81. Abbott, K. L., K. Aoki, J. M. Lim, M. Porterfield, R. Johnson, R. M. O'Regan, L. Wells, M. Tiemeyer, and M. Pierce. 2008. Targeted glycoproteomic identification of biomarkers for human breast carcinoma. *J. Proteome Res.* 7: 1470-1480.

82. Neve, R. M., K. Chin, J. Fridlyand, J. Yeh, F. L. Baehner, T. Fevr, L. Clark, N. Bayani, J. P. Coppe, F. Tong, T. Speed, P. T. Spellman, S. DeVries, A. Lapuk, N. J. Wang, W. L. Kuo, J. L. Stilwell, D. Pinkel, D. G. Albertson, F. M. Waldman, F. McCormick, R. B. Dickson, M. D. Johnson, M. Lippman, S. Ethier, A. Gazdar, and J. W. Gray. 2006. A collection of breast cancer cell lines for the study of functionally distinct cancer subtypes. *Cancer. Cell.* 10: 515-527.

83. Chao, G., W. L. Lau, B. J. Hackel, S. L. Sazinsky, S. M. Lippow, and K. D. Wittrup. 2006. Isolating and engineering human antibodies using yeast surface display. *Nat. Protoc.* 1: 755-768.

84. Nanjappa, V., J. K. Thomas, A. Marimuthu, B. Muthusamy, A. Radhakrishnan, R. Sharma, A. Ahmad Khan, L. Balakrishnan, N. A. Sahasrabuddhe, S. Kumar, B. N.

Jhaveri, K. V. Sheth, R. Kumar Khatana, P. G. Shaw, S. M. Srikanth, P. P. Mathur, S. Shankar, D. Nagaraja, R. Christopher, S. Mathivanan, R. Raju, R. Sirdeshmukh, A. Chatterjee, R. J. Simpson, H. C. Harsha, A. Pandey, and T. S. Prasad. 2014. Plasma Proteome Database as a resource for proteomics research: 2014 update. *Nucleic Acids Res.* 42: D959-65.

85. Walz, S., J. S. Stickel, D. J. Kowalewski, H. Schuster, K. Weisel, L. Backert, S. Kahn, A. Nelde, T. Stroh, M. Handel, O. Kohlbacher, L. Kanz, H. R. Salih, H. G. Rammensee, and S. Stevanovic. 2015. The antigenic landscape of multiple myeloma: mass spectrometry (re)defines targets for T-cell-based immunotherapy. *Blood* 126: 1203-1213.

86. Kieke, M. C., E. V. Shusta, E. T. Boder, L. Teyton, K. D. Wittrup, and D. M. Kranz. 1999. Selection of functional T cell receptor mutants from a yeast surface-display library. *Proc. Natl. Acad. Sci. U. S. A.* 96: 5651-5656.

87. Babyak, M. A. 2004. What you see may not be what you get: a brief, nontechnical introduction to overfitting in regression-type models. *Psychosom. Med.* 66: 411-421.

88. Ali, E. M., M. Sheta, and M. A. E. Mohsen. 2011. Elevated serum and tissue VEGF associated with poor outcome in breast cancer patients. *Alexandria Journal of Medicine* 47: 217-224.

89. Boder, E. T. and K. D. Wittrup. 1997. Yeast surface display for screening combinatorial polypeptide libraries. *Nat. Biotechnol.* 15: 553-557.

90. Saeed, A. I., V. Sharov, J. White, J. Li, W. Liang, N. Bhagabati, J. Braisted, M. Klapa, T. Currier, M. Thiagarajan, A. Sturn, M. Snuffin, A. Rezantsev, D. Popov, A. Ryltsov, E. Kostukovich, I. Borisovsky, Z. Liu, A. Vinsavich, V. Trush, and J. Quackenbush. 2003. TM4: a free, open-source system for microarray data management and analysis. *BioTechniques* 34: 374-378.

91. Yu, X., T. Tsibane, P. A. McGraw, F. S. House, C. J. Keefer, M. D. Hicar, T. M. Tumpey, C. Pappas, L. A. Perrone, O. Martinez, J. Stevens, I. A. Wilson, P. V. Aguilar, E. L. Altschuler, C. F. Basler, and J. E. Crowe Jr. 2008. Neutralizing antibodies derived from the B cells of 1918 influenza pandemic survivors. *Nature* 455: 532-536.

92. Hammarlund, E., M. W. Lewis, S. G. Hansen, L. I. Strelow, J. A. Nelson, G. J. Sexton, J. M. Hanifin, and M. K. Slifka. 2003. Duration of antiviral immunity after smallpox vaccination. *Nat. Med.* 9: 1131-1137.

93. Tangye, S. G., Y. J. Liu, G. Aversa, J. H. Phillips, and J. E. de Vries. 1998. Identification of functional human splenic memory B cells by expression of CD148 and CD27. *J. Exp. Med.* 188: 1691-1703.

94. Klein, U., K. Rajewsky, and R. Kuppers. 1998. Human immunoglobulin (Ig)M+IgD+ peripheral blood B cells expressing the CD27 cell surface antigen carry somatically mutated variable region genes: CD27 as a general marker for somatically mutated (memory) B cells. *J. Exp. Med.* 188: 1679-1689.

95. Pascual, V., Y. J. Liu, A. Magalski, O. de Bouteiller, J. Banchereau, and J. D. Capra. 1994. Analysis of somatic mutation in five B cell subsets of human tonsil. *J. Exp. Med.* 180: 329-339.

96. Bohnhorst, J. O., M. B. Bjorgan, J. E. Thoen, J. B. Natvig, and K. M. Thompson. 2001. Bm1-Bm5 classification of peripheral blood B cells reveals circulating germinal center founder cells in healthy individuals and disturbance in the B cell subpopulations in patients with primary Sjogren's syndrome. *J. Immunol.* 167: 3610-3618.

97. Denoeud, J. and M. Moser. 2011. Role of CD27/CD70 pathway of activation in immunity and tolerance. *J. Leukoc. Biol.* 89: 195-203.

98. Jung, J., J. Choe, L. Li, and Y. S. Choi. 2000. Regulation of CD27 expression in the course of germinal center B cell differentiation: the pivotal role of IL-10. *Eur. J. Immunol.* 30: 2437-2443.

99. Fecteau, J. F., G. Cote, and S. Neron. 2006. A new memory CD27-IgG+ B cell population in peripheral blood expressing VH genes with low frequency of somatic mutation. *J. Immunol.* 177: 3728-3736.

100. Ehrhardt, G. R., J. T. Hsu, L. Gartland, C. M. Leu, S. Zhang, R. S. Davis, and M. D. Cooper. 2005. Expression of the immunoregulatory molecule FcRH4 defines a distinctive tissue-based population of memory B cells. *J. Exp. Med.* 202: 783-791.

101. Wei, C., J. Anolik, A. Cappione, B. Zheng, A. Pugh-Bernard, J. Brooks, E. H. Lee, E. C. Milner, and I. Sanz. 2007. A new population of cells lacking expression of CD27 represents a notable component of the B cell memory compartment in systemic lupus erythematosus. *J. Immunol.* 178: 6624-6633.

102. Linthicum, D. S. and W. H. Hildemann. 1970. Immunologic responses of Pacific hagfish. 3. Serum antibodies to cellular antigens. *J. Immunol.* 105: 912-918.

103. Alder, M. N., I. B. Rogozin, L. M. Iyer, G. V. Glazko, M. D. Cooper, and Z. Pancer. 2005. Diversity and function of adaptive immune receptors in a jawless vertebrate. *Science* 310: 1970-1973.

104. Kirchdoerfer, R. N., B. R. Herrin, B. W. Han, C. L. Turnbough Jr, M. D. Cooper, and I. A. Wilson. 2012. Variable lymphocyte receptor recognition of the immunodominant glycoprotein of Bacillus anthracis spores. *Structure* 20: 479-486.

105. Weller, S., M. C. Braun, B. K. Tan, A. Rosenwald, C. Cordier, M. E. Conley, A. Plebani, D. S. Kumararatne, D. Bonnet, O. Tournilhac, G. Tchernia, B. Steiniger, L. M. Staudt, J. L. Casanova, C. A. Reynaud, and J. C. Weill. 2004. Human blood IgM "memory" B cells are circulating splenic marginal zone B cells harboring a prediversified immunoglobulin repertoire. *Blood* 104: 3647-3654.

106. Dunn-Walters, D. K., P. G. Isaacson, and J. Spencer. 1995. Analysis of mutations in immunoglobulin heavy chain variable region genes of microdissected marginal zone (MGZ) B cells suggests that the MGZ of human spleen is a reservoir of memory B cells. *J. Exp. Med.* 182: 559-566.

107. McGuffin, L. J., J. D. Atkins, B. R. Salehe, A. N. Shuid, and D. B. Roche. 2015. IntFOLD: an integrated server for modelling protein structures and functions from amino acid sequences. *Nucleic Acids Res.* 43: W169-73.

108. Ehrhardt, G. R., A. Hijikata, H. Kitamura, O. Ohara, J. Y. Wang, and M. D. Cooper. 2008. Discriminating gene expression profiles of memory B cell subpopulations. *J. Exp. Med.* 205: 1807-1817.

109. Lebron, J. A. and P. J. Bjorkman. 1999. The transferrin receptor binding site on HFE, the class I MHC-related protein mutated in hereditary hemochromatosis. *J. Mol. Biol.* 289: 1109-1118.

110. Jenei, A., S. Varga, L. Bene, L. Matyus, A. Bodnar, Z. Bacso, C. Pieri, R. Gaspar Jr, T. Farkas, and S. Damjanovich. 1997. HLA class I and II antigens are partially coclustered in the plasma membrane of human lymphoblastoid cells. *Proc. Natl. Acad. Sci. U. S. A.* 94: 7269-7274.

111. Ploegh, H. L., L. E. Cannon, and J. L. Strominger. 1979. Cell-free translation of the mRNAs for the heavy and light chains of HLA-A and HLA-B antigens. *Proc. Natl. Acad. Sci. U. S. A.* 76: 2273-2277.

112. Perosa, F., G. Luccarelli, M. Prete, E. Favoino, S. Ferrone, and F. Dammacco. 2003. Beta 2-microglobulin-free HLA class I heavy chain epitope mimicry by monoclonal antibody HC-10-specific peptide. *J. Immunol.* 171: 1918-1926.

113. Palanichamy, A., L. Apeltsin, T. C. Kuo, M. Sirota, S. Wang, S. J. Pitts, P. D. Sundar, D. Telman, L. Z. Zhao, M. Derstine, A. Abounasr, S. L. Hauser, and H. C. von Budingen. 2014. Immunoglobulin class-switched B cells form an active immune axis between CNS and periphery in multiple sclerosis. *Sci. Transl. Med.* 6: 248ra106.

114. Bennett, L., A. K. Palucka, E. Arce, V. Cantrell, J. Borvak, J. Banchereau, and V. Pascual. 2003. Interferon and granulopoiesis signatures in systemic lupus erythematosus blood. *J. Exp. Med.* 197: 711-723.

115. Baechler, E. C., F. M. Batliwalla, G. Karypis, P. M. Gaffney, W. A. Ortmann, K. J. Espe, K. B. Shark, W. J. Grande, K. M. Hughes, V. Kapur, P. K. Gregersen, and T. W. Behrens. 2003. Interferon-inducible gene expression signature in peripheral blood cells of patients with severe lupus. *Proc. Natl. Acad. Sci. U. S. A.* 100: 2610-2615.

116. van Baarsen, L. G., T. C. van der Pouw Kraan, J. J. Kragt, J. M. Baggen, F. Rustenburg, T. Hooper, J. F. Meilof, M. J. Fero, C. D. Dijkstra, C. H. Polman, and C. L. Verweij. 2006. A subtype of multiple sclerosis defined by an activated immune defense program. *Genes Immun.* 7: 522-531.

117. Yamaguchi, K. D., D. L. Ruderman, E. Croze, T. C. Wagner, S. Velichko, A. T. Reder, and H. Salamon. 2008. IFN-beta-regulated genes show abnormal expression in therapy-naive relapsing-remitting MS mononuclear cells: gene expression analysis employing all reported protein-protein interactions. *J. Neuroimmunol.* 195: 116-120.

118. Stone, M. J., S. Chuang, X. Hou, M. Shoham, and J. Z. Zhu. 2009. Tyrosine sulfation: an increasingly recognised post-translational modification of secreted proteins. *N. Biotechnol.* 25: 299-317.

119. Baeuerle, P. A. and W. B. Huttner. 1986. Chlorate--a potent inhibitor of protein sulfation in intact cells. *Biochem. Biophys. Res. Commun.* 141: 870-877.

120. Ploegh, H. L., H. T. Orr, and J. L. Stominger. 1981. Biosynthesis and cell surface localization of nonglycosylated human histocompatibility antigens. *J. Immunol.* 126: 270-275.

121. Jourdan, M., A. Caraux, G. Caron, N. Robert, G. Fiol, T. Reme, K. Bollore, J. P. Vendrell, S. Le Gallou, F. Mourcin, J. De Vos, A. Kassambara, C. Duperray, D. Hose, T. Fest, K. Tarte, and B. Klein. 2011. Characterization of a transitional preplasmablast population in the process of human B cell to plasma cell differentiation. *J. Immunol.* 187: 3931-3941.

122. Farzan, M., T. Mirzabekov, P. Kolchinsky, R. Wyatt, M. Cayabyab, N. P. Gerard, C. Gerard, J. Sodroski, and H. Choe. 1999. Tyrosine sulfation of the amino terminus of CCR5 facilitates HIV-1 entry. *Cell* 96: 667-676.

123. Pouyani, T. and B. Seed. 1995. PSGL-1 recognition of P-selectin is controlled by a tyrosine sulfation consensus at the PSGL-1 amino terminus. *Cell* 83: 333-343.

124. Ludeman, J. P. and M. J. Stone. 2014. The structural role of receptor tyrosine sulfation in chemokine recognition. *Br. J. Pharmacol.* 171: 1167-1179.

125. Kamal, A. and M. Khamashta. 2014. The efficacy of novel B cell biologics as the future of SLE treatment: a review. *Autoimmun. Rev.* 13: 1094-1101.

126. Kinzel, S. and M. S. Weber. 2016. B Cell-Directed Therapeutics in Multiple Sclerosis: Rationale and Clinical Evidence. *CNS Drugs* 30: 1137-1148.

127. Duddy, M., M. Niino, F. Adatia, S. Hebert, M. Freedman, H. Atkins, H. J. Kim, and A. Bar-Or. 2007. Distinct effector cytokine profiles of memory and naive human B cell subsets and implication in multiple sclerosis. *J. Immunol.* 178: 6092-6099.

128. Spiro, R. G. 2002. Protein glycosylation: nature, distribution, enzymatic formation, and disease implications of glycopeptide bonds. *Glycobiology* 12: 43R-56R.

129. Godbey, W. T., K. K. Wu, and A. G. Mikos. 1999. Poly(ethylenimine) and its role in gene delivery. *J. Control. Release* 60: 149-160.

130. Keller, A., A. I. Nesvizhskii, E. Kolker, and R. Aebersold. 2002. Empirical statistical model to estimate the accuracy of peptide identifications made by MS/MS and database search. *Anal. Chem.* 74: 5383-5392.

131. Wilkins, P. P., K. L. Moore, R. P. McEver, and R. D. Cummings. 1995. Tyrosine sulfation of P-selectin glycoprotein ligand-1 is required for high affinity binding to P-selectin. *J. Biol. Chem.* 270: 22677-22680.

132. Pluckthun, A. 2015. Designed ankyrin repeat proteins (DARPins): binding proteins for research, diagnostics, and therapy. *Annu. Rev. Pharmacol. Toxicol.* 55: 489-511.

133. Venkatachalam, K. V. 2003. Human 3'-phosphoadenosine 5'-phosphosulfate (PAPS) synthase: biochemistry, molecular biology and genetic deficiency. *IUBMB Life* 55: 1-11.

134. Baeuerle, P. A. and W. B. Huttner. 1984. Inhibition of N-glycosylation induces tyrosine sulphation of hybridoma immunoglobulin G. *Embo J.* 3: 2209-2215.

135. Monigatti, F., B. Hekking, and H. Steen. 2006. Protein sulfation analysis--A primer. *Biochim. Biophys. Acta* 1764: 1904-1913.

136. Mishiro, E., Y. Sakakibara, M. C. Liu, and M. Suiko. 2006. Differential enzymatic characteristics and tissue-specific expression of human TPST-1 and TPST-2. *J. Biochem.* 140: 731-737.

137. Duma, L., D. Haussinger, M. Rogowski, P. Lusso, and S. Grzesiek. 2007. Recognition of RANTES by extracellular parts of the CCR5 receptor. *J. Mol. Biol.* 365: 1063-1075.

138. Somers, W. S., J. Tang, G. D. Shaw, and R. T. Camphausen. 2000. Insights into the molecular basis of leukocyte tethering and rolling revealed by structures of P- and E-selectin bound to SLe(X) and PSGL-1. *Cell* 103: 467-479.

139. Carlow, D. A., K. Gossens, S. Naus, K. M. Veerman, W. Seo, and H. J. Ziltener. 2009. PSGL-1 function in immunity and steady state homeostasis. *Immunol. Rev.* 230: 75-96.

140. Seibert, C., M. Cadene, A. Sanfiz, B. T. Chait, and T. P. Sakmar. 2002. Tyrosine sulfation of CCR5 N-terminal peptide by tyrosylprotein sulfotransferases 1 and 2 follows a discrete pattern and temporal sequence. *Proc. Natl. Acad. Sci. U. S. A.* 99: 11031-11036.

141. Snapp, K. R., H. Ding, K. Atkins, R. Warnke, F. W. Luscinskas, and G. S. Kansas. 1998. A novel P-selectin glycoprotein ligand-1 monoclonal antibody recognizes an epitope within the tyrosine sulfate motif of human PSGL-1 and blocks recognition of both P- and L-selectin. *Blood* 91: 154-164.

142. Park, R. J., T. Wang, D. Koundakjian, J. F. Hultquist, P. Lamothe-Molina, B. Monel, K. Schumann, H. Yu, K. M. Krupzcak, W. Garcia-Beltran, A. Piechocka-Trocha, N. J. Krogan, A. Marson, D. M. Sabatini, E. S. Lander, N. Hacohen, and B. D. Walker. 2017. A genome-wide CRISPR screen identifies a restricted set of HIV host dependency factors. *Nat. Genet.* 49: 193-203.

143. Choe, H., W. Li, P. L. Wright, N. Vasilieva, M. Venturi, C. C. Huang, C. Grundner, T. Dorfman, M. B. Zwick, L. Wang, E. S. Rosenberg, P. D. Kwong, D. R. Burton, J. E. Robinson, J. G. Sodroski, and M. Farzan. 2003. Tyrosine sulfation of human antibodies contributes to recognition of the CCR5 binding region of HIV-1 gp120. *Cell* 114: 161-170.

144. Pinton, P., T. Pozzan, and R. Rizzuto. 1998. The Golgi apparatus is an inositol 1,4,5-trisphosphate-sensitive Ca2+ store, with functional properties distinct from those of the endoplasmic reticulum. *Embo J.* 17: 5298-5308.

145. Porat, A. and Z. Elazar. 2000. Regulation of intra-Golgi membrane transport by calcium. *J. Biol. Chem.* 275: 29233-29237.

146. Lissandron, V., P. Podini, P. Pizzo, and T. Pozzan. 2010. Unique characteristics of Ca2+ homeostasis of the trans-Golgi compartment. *Proc. Natl. Acad. Sci. U. S. A.* 107: 9198-9203.

147. Monigatti, F., E. Gasteiger, A. Bairoch, and E. Jung. 2002. The Sulfinator: predicting tyrosine sulfation sites in protein sequences. *Bioinformatics* 18: 769-770.

148. Halliley, J. L., C. M. Tipton, J. Liesveld, A. F. Rosenberg, J. Darce, I. V. Gregoretti, L. Popova, D. Kaminiski, C. F. Fucile, I. Albizua, S. Kyu, K. Y. Chiang, K. T. Bradley, R. Burack, M. Slifka, E. Hammarlund, H. Wu, L. Zhao, E. E. Walsh, A. R. Falsey, T. D. Randall, W. C. Cheung, I. Sanz, and F. E. Lee. 2015. Long-Lived Plasma Cells Are Contained within the CD19(-)CD38(hi)CD138(+) Subset in Human Bone Marrow. *Immunity* 43: 132-145.

149. Bar-Or, A., R. A. Grove, D. J. Austin, J. M. Tolson, S. A. VanMeter, E. W. Lewis, F. J. Derosier, M. C. Lopez, S. T. Kavanagh, A. E. Miller, and P. S. Sorensen. 2018. Subcutaneous ofatumumab in patients with relapsing-remitting multiple sclerosis: The MIRROR study. *Neurology* 90: e1805-e1814.

150. Li, R., K. R. Patterson, and A. Bar-Or. 2018. Reassessing B cell contributions in multiple sclerosis. *Nat. Immunol.*

151. Hartung, H. P. and B. C. Kieseier. 2010. Atacicept: targeting B cells in multiple sclerosis. *Ther. Adv. Neurol. Disord.* 3: 205-216.

152. Hortin, G., H. Sims, and A. W. Strauss. 1986. Identification of the site of sulfation of the fourth component of human complement. *J. Biol. Chem.* 261: 1786-1793.

153. Paul, S., D. Weiskopf, M. A. Angelo, J. Sidney, B. Peters, and A. Sette. 2013. HLA class I alleles are associated with peptide-binding repertoires of different size, affinity, and immunogenicity. *J. Immunol.* 191: 5831-5839.

154. Robinson, J., M. J. Waller, P. Parham, J. G. Bodmer, and S. G. Marsh. 2001. IMGT/HLA Database--a sequence database for the human major histocompatibility complex. *Nucleic Acids Res.* 29: 210-213.

155. Robinson, J., J. A. Halliwell, J. D. Hayhurst, P. Flicek, P. Parham, and S. G. Marsh. 2015. The IPD and IMGT/HLA database: allele variant databases. *Nucleic Acids Res.* 43: D423-31.

156. Rudd, P. M., T. Elliott, P. Cresswell, I. A. Wilson, and R. A. Dwek. 2001. Glycosylation and the immune system. *Science* 291: 2370-2376.

157. Barber, L. D., T. P. Patel, L. Percival, J. E. Gumperz, L. L. Lanier, J. H. Phillips, J. C. Bigge, M. R. Wormwald, R. B. Parekh, and P. Parham. 1996. Unusual uniformity of the N-linked oligosaccharides of HLA-A, -B, and -C glycoproteins. *J. Immunol.* 156: 3275-3284.

158. Sant, A. J., M. Zacheis, T. Rumbarger, K. S. Giacoletto, and B. D. Schwartz. 1988. Human Ia alpha- and beta-chains are sulfated. *J. Immunol.* 140: 155-160.

159. Lisovsky, I., G. Isitman, J. Bruneau, and N. F. Bernard. 2015. Functional analysis of NK cell subsets activated by 721.221 and K562 HLA-null cells. *J. Leukoc. Biol.* 97: 761-767.

160. Apps, R., Y. Qi, J. M. Carlson, H. Chen, X. Gao, R. Thomas, Y. Yuki, G. Q. Del Prete, P. Goulder, Z. L. Brumme, C. J. Brumme, M. John, S. Mallal, G. Nelson, R. Bosch, D. Heckerman, J. L. Stein, K. A. Soderberg, M. A. Moody, T. N. Denny, X. Zeng, J. Fang, A. Moffett, J. D. Lifson, J. J. Goedert, S. Buchbinder, G. D. Kirk, J. Fellay, P. McLaren, S. G. Deeks, F. Pereyra, B. Walker, N. L. Michael, A. Weintrob,

S. Wolinsky, W. Liao, and M. Carrington. 2013. Influence of HLA-C expression level on HIV control. *Science* 340: 87-91.

161. Purbhoo, M. A., D. J. Irvine, J. B. Huppa, and M. M. Davis. 2004. T cell killing does not require the formation of a stable mature immunological synapse. *Nat. Immunol.* 5: 524-530.

162. Makhadiyeva, D., L. Lam, M. Moatari, J. Vallance, Y. Zheng, E. C. Campbell, and S. J. Powis. 2012. MHC class I dimer formation by alteration of the cellular redox environment and induction of apoptosis. *Immunology* 135: 133-139.

163. Lynch, S., S. G. Santos, E. C. Campbell, A. M. Nimmo, C. Botting, A. Prescott, A. N. Antoniou, and S. J. Powis. 2009. Novel MHC class I structures on exosomes. *J. Immunol.* 183: 1884-1891.

164. Achdout, H., I. Manaster, and O. Mandelboim. 2008. Influenza virus infection augments NK cell inhibition through reorganization of major histocompatibility complex class I proteins. *J. Virol.* 82: 8030-8037.

165. Zilian, E., H. Saragih, V. Vijayan, O. Hiller, C. Figueiredo, A. Aljabri, R. Blasczyk, G. Theilmeier, J. U. Becker, J. Larmann, and S. Immenschuh. 2015. Heme Oxygenase-1 Inhibits HLA Class I Antibody-Dependent Endothelial Cell Activation. *PLoS One* 10: e0145306.

166. Zhang, X., E. Rozengurt, and E. F. Reed. 2010. HLA class I molecules partner with integrin beta4 to stimulate endothelial cell proliferation and migration. *Sci. Signal.* 3: ra85.

167. Tsai, E. W. and E. F. Reed. 2014. MHC class I signaling: new functional perspectives for an old molecule. *Tissue Antigens* 83: 375-381.

168. Poon, K., D. Montamat-Sicotte, N. Cumberbatch, A. J. McMichael, and M. F. Callan. 2005. Expression of leukocyte immunoglobulin-like receptors and natural killer receptors on virus-specific CD8+ T cells during the evolution of Epstein-Barr virus-specific immune responses in vivo. *Viral Immunol.* 18: 513-522.

169. Held, W. and R. A. Mariuzza. 2008. Cis interactions of immunoreceptors with MHC and non-MHC ligands. *Nat. Rev. Immunol.* 8: 269-278.

170. Ugolini, S., C. Arpin, N. Anfossi, T. Walzer, A. Cambiaggi, R. Forster, M. Lipp, R. E. Toes, C. J. Melief, J. Marvel, and E. Vivier. 2001. Involvement of inhibitory NKRs in the survival of a subset of memory-phenotype CD8+ T cells. *Nat. Immunol.* 2: 430-435.

171. Uhrberg, M., N. M. Valiante, N. T. Young, L. L. Lanier, J. H. Phillips, and P. Parham. 2001. The repertoire of killer cell Ig-like receptor and CD94:NKG2A receptors in

T cells: clones sharing identical alpha beta TCR rearrangement express highly diverse killer cell Ig-like receptor patterns. *J. Immunol.* 166: 3923-3932.

172. Jones, D. C., V. Kosmoliaptsis, R. Apps, N. Lapaque, I. Smith, A. Kono, C. Chang, L. H. Boyle, C. J. Taylor, J. Trowsdale, and R. L. Allen. 2011. HLA class I allelic sequence and conformation regulate leukocyte Ig-like receptor binding. *J. Immunol.* 186: 2990-2997.

173. Engels, B., V. H. Engelhard, J. Sidney, A. Sette, D. C. Binder, R. B. Liu, D. M. Kranz, S. C. Meredith, D. A. Rowley, and H. Schreiber. 2013. Relapse or eradication of cancer is predicted by peptide-major histocompatibility complex affinity. *Cancer. Cell.* 23: 516-526.

174. Chang, H. D., K. Tokoyoda, and A. Radbruch. 2018. Immunological memories of the bone marrow. *Immunol. Rev.* 283: 86-98.

175. Gricks, C. S., E. Rawlings, L. Foroni, J. A. Madrigal, and P. L. Amlot. 2001. Somatically mutated regions of immunoglobulin on human B-cell lymphomas code for peptides that bind to autologous major histocompatibility complex class I, providing a potential target for cytotoxic T cells. *Cancer Res.* 61: 5145-5152.

176. Strothmeyer, A. M., D. Papaioannou, M. Duhren-von Minden, M. Navarrete, K. Zirlik, K. Heining-Mikesch, and H. Veelken. 2010. Comparative analysis of predicted HLA binding of immunoglobulin idiotype sequences indicates T cell-mediated immunosurveillance in follicular lymphoma. *Blood* 116: 1734-1736.

177. Khodadoust, M. S., N. Olsson, L. E. Wagar, O. A. Haabeth, B. Chen, K. Swaminathan, K. Rawson, C. L. Liu, D. Steiner, P. Lund, S. Rao, L. Zhang, C. Marceau, H. Stehr, A. M. Newman, D. K. Czerwinski, V. E. Carlton, M. Moorhead, M. Faham, H. E. Kohrt, J. Carette, M. R. Green, M. M. Davis, R. Levy, J. E. Elias, and A. A. Alizadeh. 2017. Antigen presentation profiling reveals recognition of lymphoma immunoglobulin neoantigens. *Nature* 543: 723-727.

178. Geng, J., A. J. Zaitouna, and M. Raghavan. 2018. Selected HLA-B allotypes are resistant to inhibition or deficiency of the transporter associated with antigen processing (TAP). *PLoS Pathog.* 14: e1007171.

179. Yewdell, J. W., E. Reits, and J. Neefjes. 2003. Making sense of mass destruction: quantitating MHC class I antigen presentation. *Nat. Rev. Immunol.* 3: 952-961.

180. Neisig, A., J. Roelse, A. J. Sijts, F. Ossendorp, M. C. Feltkamp, W. M. Kast, C. J. Melief, and J. J. Neefjes. 1995. Major differences in transporter associated with antigen presentation (TAP)-dependent translocation of MHC class I-presentable peptides and the effect of flanking sequences. *J. Immunol.* 154: 1273-1279.

181. Tran, T. M., P. Ivanyi, I. Hilgert, T. Brdicka, M. Pla, B. Breur, M. Flieger, E. Ivaskova, and V. Horejsi. 2001. The epitope recognized by pan-HLA class I-reactive monoclonal antibody W6/32 and its relationship to unusual stability of the HLA-B27/beta2-microglobulin complex. *Immunogenetics* 53: 440-446.

182. Shields, M. J. and R. K. Ribaudo. 1998. Mapping of the monoclonal antibody W6/32: sensitivity to the amino terminus of beta2-microglobulin. *Tissue Antigens* 51: 567-570.

183. Ladasky, J. J., B. P. Shum, F. Canavez, H. N. Seuanez, and P. Parham. 1999. Residue 3 of beta2-microglobulin affects binding of class I MHC molecules by the W6/32 antibody. *Immunogenetics* 49: 312-320.

184. Trolle, T., C. P. McMurtrey, J. Sidney, W. Bardet, S. C. Osborn, T. Kaever, A. Sette, W. H. Hildebrand, M. Nielsen, and B. Peters. 2016. The Length Distribution of Class I-Restricted T Cell Epitopes Is Determined by Both Peptide Supply and MHC Allele-Specific Binding Preference. *J. Immunol.* 196: 1480-1487.

185. Bouvier, M. and D. C. Wiley. 1994. Importance of peptide amino and carboxyl termini to the stability of MHC class I molecules. *Science* 265: 398-402.

186. Karosiene, E., C. Lundegaard, O. Lund, and M. Nielsen. 2012. NetMHCcons: a consensus method for the major histocompatibility complex class I predictions. *Immunogenetics* 64: 177-186.

187. Anthis, N. J., J. R. Haling, C. L. Oxley, M. Memo, K. L. Wegener, C. J. Lim, M. H. Ginsberg, and I. D. Campbell. 2009. Beta integrin tyrosine phosphorylation is a conserved mechanism for regulating talin-induced integrin activation. *J. Biol. Chem.* 284: 36700-36710.

188. Kawana-Tachikawa, A., M. Tomizawa, J. Nunoya, T. Shioda, A. Kato, E. E. Nakayama, T. Nakamura, Y. Nagai, and A. Iwamoto. 2002. An efficient and versatile mammalian viral vector system for major histocompatibility complex class I/peptide complexes. *J. Virol.* 76: 11982-11988.

189. Liu, Y., J. R. McDaniel, S. Khan, P. Campisi, E. J. Propst, T. Holler, E. Grunebaum, G. Georgiou, G. C. Ippolito, and G. R. A. Ehrhardt. 2018. Antibodies Encoded by FCRL4-Bearing Memory B Cells Preferentially Recognize Commensal Microbial Antigens. *J. Immunol.* 200: 3962-3969.

190. Ouyang, Y. B., J. T. Crawley, C. E. Aston, and K. L. Moore. 2002. Reduced body weight and increased postimplantation fetal death in tyrosylprotein sulfotransferase-1-deficient mice. *J. Biol. Chem.* 277: 23781-23787.

191. Borghei, A., Y. B. Ouyang, A. D. Westmuckett, M. R. Marcello, C. P. Landel, J. P. Evans, and K. L. Moore. 2006. Targeted disruption of tyrosylprotein sulfotransferase-2, an enzyme that catalyzes post-translational protein tyrosine O-sulfation, causes male infertility. *J. Biol. Chem.* 281: 9423-9431.

192. Westmuckett, A. D., A. J. Hoffhines, A. Borghei, and K. L. Moore. 2008. Early postnatal pulmonary failure and primary hypothyroidism in mice with combined TPST-1 and TPST-2 deficiency. *Gen. Comp. Endocrinol.* 156: 145-153.

193. Vu, T. and F. X. Claret. 2012. Trastuzumab: updated mechanisms of action and resistance in breast cancer. *Front. Oncol.* 2: 62.

194. Hauser, S. L., E. Waubant, D. L. Arnold, T. Vollmer, J. Antel, R. J. Fox, A. Bar-Or, M. Panzara, N. Sarkar, S. Agarwal, A. Langer-Gould, C. H. Smith, and HERMES Trial Group. 2008. B-cell depletion with rituximab in relapsing-remitting multiple sclerosis. *N. Engl. J. Med.* 358: 676-688.

195. Lee, J. J., H. J. Choi, M. Yun, Y. Kang, J. E. Jung, Y. Ryu, T. Y. Kim, Y. J. Cha, H. S. Cho, J. J. Min, C. W. Chung, and H. S. Kim. 2015. Enzymatic prenylation and oxime ligation for the synthesis of stable and homogeneous protein-drug conjugates for targeted therapy. *Angew. Chem. Int. Ed Engl.* 54: 12020-12024.

196. Lee, S. C., K. Park, J. Han, J. J. Lee, H. J. Kim, S. Hong, W. Heu, Y. J. Kim, J. S. Ha, S. G. Lee, H. K. Cheong, Y. H. Jeon, D. Kim, and H. S. Kim. 2012. Design of a binding scaffold based on variable lymphocyte receptors of jawless vertebrates by module engineering. *Proc. Natl. Acad. Sci. U. S. A.* 109: 3299-3304.

197. Lee, J. J., J. A. Kang, Y. Ryu, S. S. Han, Y. R. Nam, J. K. Rho, D. S. Choi, S. W. Kang, D. E. Lee, and H. S. Kim. 2017. Genetically engineered and self-assembled oncolytic protein nanoparticles for targeted cancer therapy. *Biomaterials* 120: 22-31.

198. Moot, R., S. S. Raikar, L. Fleischer, M. Querrey, D. E. Tylawsky, H. Nakahara, C. B. Doering, and H. T. Spencer. 2016. Genetic engineering of chimeric antigen receptors using lamprey derived variable lymphocyte receptors. *Mol. Ther. Oncolytics* 3: 16026.

199. Hwang, D. E., J. H. Ryou, J. R. Oh, J. W. Han, T. K. Park, and H. S. Kim. 2016. Anti-Human VEGF Repebody Effectively Suppresses Choroidal Neovascularization and Vascular Leakage. *PLoS One* 11: e0152522.

200. Lee, J. J., H. J. Kim, C. S. Yang, H. H. Kyeong, J. M. Choi, D. E. Hwang, J. M. Yuk, K. Park, Y. J. Kim, S. G. Lee, D. Kim, E. K. Jo, H. K. Cheong, and H. S. Kim. 2014. A high-affinity protein binder that blocks the IL-6/STAT3 signaling pathway effectively suppresses non-small cell lung cancer. *Mol. Ther.* 22: 1254-1265.

201. Cooper, M. D., D. A. Raymond, R. D. Peterson, M. A. South, and R. A. Good. 1966. The functions of the thymus system and the bursa system in the chicken. *J. Exp. Med.* 123: 75-102.

202. Li, J., D. R. Barreda, Y. A. Zhang, H. Boshra, A. E. Gelman, S. Lapatra, L. Tort, and J. O. Sunyer. 2006. B lymphocytes from early vertebrates have potent phagocytic and microbicidal abilities. *Nat. Immunol.* 7: 1116-1124.

203. Parra, D., A. M. Rieger, J. Li, Y. A. Zhang, L. M. Randall, C. A. Hunter, D. R. Barreda, and J. O. Sunyer. 2012. Pivotal advance: peritoneal cavity B-1 B cells have phagocytic and microbicidal capacities and present phagocytosed antigen to CD4+ T cells. *J. Leukoc. Biol.* 91: 525-536.

204. Delamarre, L., M. Pack, H. Chang, I. Mellman, and E. S. Trombetta. 2005. Differential lysosomal proteolysis in antigen-presenting cells determines antigen fate. *Science* 307: 1630-1634.

205. Zimmerman, L. M., L. A. Vogel, K. A. Edwards, and R. M. Bowden. 2010. Phagocytic B cells in a reptile. *Biol. Lett.* 6: 270-273.

206. Pradeu, T. and L. Du Pasquier. 2018. Immunological memory: What's in a name? *Immunol. Rev.* 283: 7-20.

207. Rast, J. P. and K. M. Buckley. 2013. Lamprey immunity is far from primitive. *Proc. Natl. Acad. Sci. U. S. A.* 110: 5746-5747.